NASA Contractor Report 3091

Position Paper on the Potential of Inadvertent Weather Modification of the Florida Peninsula Resulting From Neutralization of Space Shuttle Solid Rocket Booster Exhaust Clouds

Eugene Bollay, Lance Bosart, Earl Droessler,
James Jiusto, G. Garland Lala, Volker Mohnen,
Vincent Schaefer, and Patrick Squires

CONTRACT NAS1-14965
NOVEMBER 1979

NASA

NASA Contractor Report 3091

Position Paper on the Potential of Inadvertent Weather Modification of the Florida Peninsula Resulting From Neutralization of Space Shuttle Solid Rocket Booster Exhaust Clouds

Eugene Bollay, Lance Bosart, Earl Droessler,
James Jiusto, G. Garland Lala, Volker Mohnen,
Vincent Schaefer, and Patrick Squires
Institute on Man and Science
Rensselaerville, New York

Prepared for
Langley Research Center
under Contract NAS1-14965

NASA
National Aeronautics
and Space Administration

Scientific and Technical
Information Branch

1979

TABLE OF CONTENTS

Summary

Commencing in the early 1980's, NASA plans regular Space Shuttle launches employing solid propellant rockets that liberate primarily HCl and Al_2O_3. To neutralize the acidic nature of the low-level stabilized ground cloud (SGC) that often results, a concept of injecting compounds into the exhaust cloud was proposed. This position paper on Inadvertent Weather Modification is based on data characterizing the physical, chemical and dispersion state of the neutralized ground cloud within the first three hours after launch, supplied by NASA-Langley Research Center. From this government-supplied information, we have estimated the exhaust cloud characteristics beyond three hours and up to seven days. We then discussed in detail the involvement of the neutralized SGC in warm and cold cloud precipitation processes. Based on the climatology of the Florida Peninsula, we assessed the risk for weather modification. Certain weather situations warrant launch rescheduling because of the risk of

- intensification or diminution of rainfall
- thunderstorm activity
- strong wind development
- haze and fog intensification
- possible impact on hurricanes

The effect of cloud neutralization, while minimizing the possibility of acid rain, may well generate more nuclei conducive to cloud modification. In any event, some degree of microphysical changes to natural clouds would appear inevitable and careful launch scheduling to minimize such possibilities are enumerated. Cloud microphysics changes leading to significant

and/or statistically detectable weather modification are considerably more difficult to establish - as is generally the case on planned weather modification programs under optimum circumstances. While some degree of weather modification might occur in individual cases, the cumulative effects of 40 projected launches per year (appropriately spaced) at Cape Canaveral capable of producing significant and deleterious inadvertent weather modification is estimated to be of low probability.

It must be emphasized that the projections in this report are based on limited data available on NASA rocket-plume aerosol characteristics. Knowledge of complex aerosol chemistry and nucleation properties is based considerably on relatively few laboratory studies. In situ rocket plume measurements of cloud physics properties are even more scarce, thereby necessitating certain assumptions and deductive reasoning to perform this analysis. The need for more research and reliable field measurements is recommended in several sections of this report.

Chapter I. Preface and Limitations of Study

We have investigated the possible impact of the neutralized, stabilized space shuttle exhaust cloud on the weather of the Florida Peninsula for a time period of three hours after launch up to seven days after launch. This position paper is based on information supplied by NASA-Langley Research Center (all data on the S.G.C.) and on information extracted from pertinent literature. An assessment team was formed consisting of the following members who have complementary research experience in vital areas of inadvertent weather modification:

Dr. Volker A. Mohnen, Director Atmospheric Sciences Research Center The University at Albany	Scientific Project Director and Chairman of the Assessment Team. Discussant of Chapter I entitled "Preface and Limitations of Study," and Chapter VII entitled "Risk Assessment and Synthesis."
Dr. Vincent J. Schaefer, Leading Professor, Atmospheric Sciences Research Center, The University at Albany	Discussant of Chapter VII entitled "Risk Assessment and Synthesis."
Mr. Eugene Bollay, Former Chief, Office of Weather Modification, NOAA	Contributor to Chapter I, "Preface and Limitations of Study," and discussant of Chapter VII entitled "Risk Assessment and Synthesis."
Dr. G. Garland Lala, Research Associate, Atmospheric Sciences Research Center, The University at Albany	Principal discussant of Chapter III entitled "Assumptions and Numerical Values," and discussant of Chapter VII entitled "Risk Assessment and Synthesis."
Dr. Patrick Squires, National Hail Project, National Center for Atmospheric Research	Principal discussant of Chapter V entitled "Warm Clouds," and discussant of Chapter VII entitled "Risk Assessment and Synthesis."
Dr. James E. Jiusto, Head Atmospheric Physics, Atmospheric Sciences Research Center, The University at Albany	Principal discussant of Chapter II entitled "Historical Weather Modification Programs and Comparisons with Neutralized Rocket Clouds," Chapter IV entitled "Cold Cloud Processes and the Neutralized Cloud," and discussant of Chapter VII entitled "Risk Assessment and Synthesis."
Dr. Lance Bosart, Associate Professor, Dept. of Atmospheric Science, The University at Albany	Principal discussant of Chapter VI entitled "Florida Synoptic Climatology," and discussant of Chapter VII entitled "Risk Assessment and Synthesis."
Dr. Earl Droessler, Dean for Research, North Carolina State University	Project Reviewer

The assessment team met twice for three days each at the NASA-Langley Research Center, Hampton, Virginia and the Institute on Man and Science, Rensselaerville, New York. In the interim period, the members of the team have been in regular contact through individual and conference calls. The problem was approached as outlined in the block diagram.

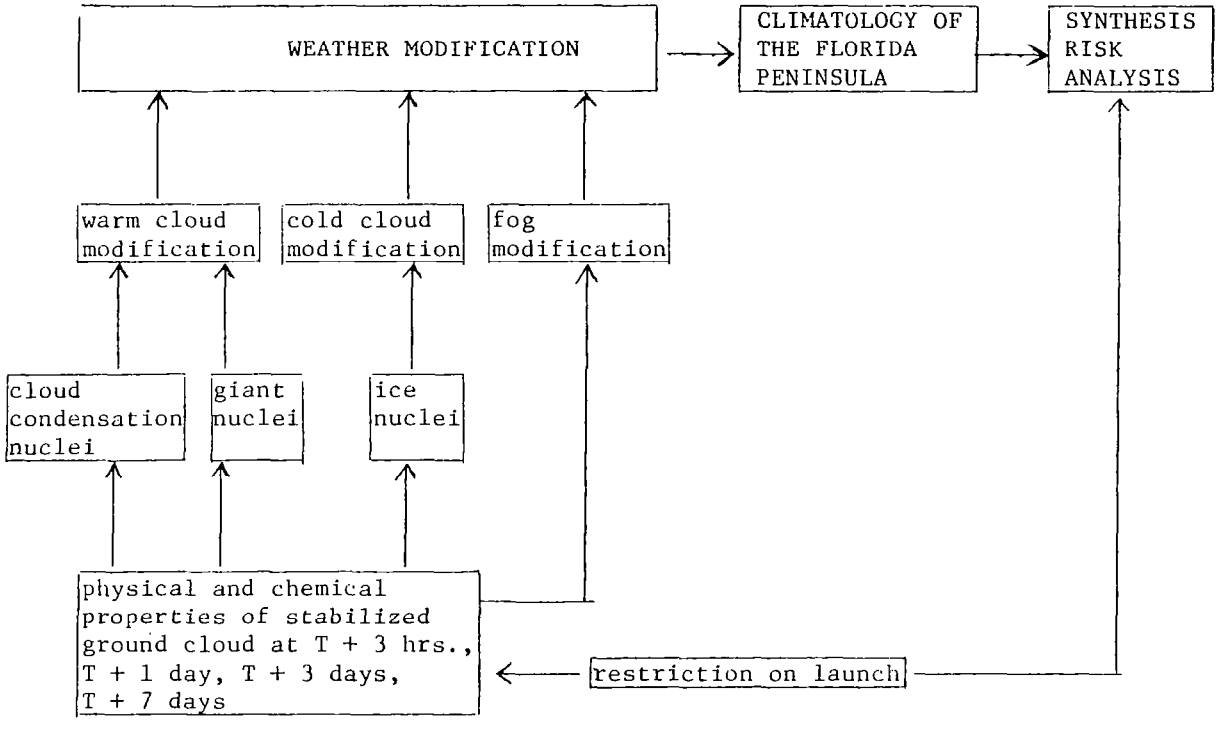

Limitations and Assumptions:

- Restricted to the Florida Peninsula.
- Principal consideration of the neutralized S.G.C. starting at 3 hours after launch.
- Neutralization of the S.G.C. will be accompanied by spraying ammonia into the cloud from aircraft and towers.
- Assessment made with time after launch as parameter, such as T + 3 hours, T + 1 day, T + 3 days and T + 7 days. The physical and chemical parameters of the neutralized S.C.C. have been estimated for these times. However, the determining factor for weather modification are the concentrations of cloud and ice nuclei within the neutralized S.G.C. Once these two vital parameters have been directly measured, a comparison with the values estimated in this position paper will determine the appropriate time after launch for impact assessment.

Assessment primarily based upon the effect of the neutralized S.G.C. on the microphysics of clouds. Possible dynamical effects on cloud systems not directly affected by the neutralized S.G.C. aerosol have not been considered.

Modification of cloud microphysics, while of considerable importance in determining weather modification effects, does not in itself assure that detectable or significant alteration of the weather will occur. Choosing cloud microphysics alone for the assessment of weather modification impact tends to exaggerate the effect because this approach assumes that the ideal conditions for modification prevail at the time the exhaust cloud encounters a cloud cell or system. Detectable weather modification at the scale of a precipitation network requires that a sizable number of clouds or a substantial fraction of a cloud system must be modified in a systematic way over a selected time interval. Therefore, a meaningful assessment of weather modification by the exhaust cloud at the larger scale requires that knowledge of the possible modification of cloud microphysics must be combined with a detailed study of the large scale weather patterns of the area of interest.

To fully assess the possible impact of the acid-neutralized cloud, a research program requiring cloud physics measurements would be necessary. The cumulative effect on rainfall in the immediate launch area might be substantial. The following intuitive projections about inadvertent weather modification prompted NASA to initiate this assessment.

The output of aerosol acting as freezing and cloud forming nuclei from as many as 40 launches per year could (depending on aerosol nucleation characteristics) be roughly comparable to that of many weather modification programs (Chapter II) and analagous in some respects to the aerosol output of a city like St. Louis. The impact of that city on the local climate has been studied and reported in the literature.

Depending on the precise nucleation characteristics and number of condensation nuclei and freezing nuclei released and formed by the acid-neutralized cloud, there could well be an initial significant decrease in precipitation along the plume trajectory, and at some distance downwind along the trajectory increases in precipitation might be expected. In strong convection situations, increases in precipitation might occur at close proximity to the launch site.

Because of the variability of meteorological conditions, one would not expect the increases in precipitation to necessarily occur in the same area each time. It must be pointed out that the importance of this problem depends directly on the number of launches per year. Generally it would not be easy to detect the precipitation effect from one launch because of the natural variability of precipitation patterns without some supporting cloud physics measurements.

To understand and fully assess the importance of this problem, a research program should be initiated in the following areas:

1. Activity spectra of CCN and IN in the neutralized exhaust cloud
2. Fallout analysis of neutralized exhaust cloud
3. Trajectory study and diffusion of plume to determine both regions of possible precipitation decreases and regions of possible increases (also severe storm effects - hail, winds)
4. Cloud physics characteristics of the cloud systems in vicinity of the launch site

Activity spectrum of the neutralized exhaust cloud

It is essential to know the number and size distribution of SGC particles. In addition, we need to know the size and number of particles that can serve as cloud-forming nuclei and which particles can serve as freezing nuclei, and their activation temperatures.

Fallout analysis

The fallout pattern of the exhaust cloud downwind from the launch site under various wind speeds and atmospheric stability conditions must be established. This will permit the establishment of a residual budget of nucleation material by size distribution for specified time periods. From these analyses and measurements, one can determine where downwind, in terms of time and concentration of nucleation material, the increase in precipitation should be detected.

Trajectory and diffusion

In addition to simple fallout due to gravity, the plume also undergoes vertical and lateral diffusion and sometimes, in the presence of convective clouds, enhanced vertical mixing, all of which tends to dilute the concentration of particles. These mixing and diffusion processes take place along the trajectory dominated by the wind flow. It is therefore important that a detailed trajectory measurement program be initiated after each launch in order to know, not predict, where and in what concentrations the nucleation material is located.

Cloud physics characteristics of the clouds in the vicinity of the launch area

It is now generally accepted that precipitation from clouds is generated by at least two processes: the Bergeron-Findeisen process, which involves

ice crystals, and the collision-coalescence process where condensation nuclei form the initial large drops to start the rain process (see Chapter V). There is now also general agreement that in continental air masses there are many condensation nuclei which are competing for the available moisture, thereby inhibiting the formation of precipitation by the coalescence process and thereby favoring the Bergeron process as the rain initiator. In maritime air masses, the coalescence process may be the initiating mechanism.

It is important to know the cloud physics characteristics in order to assess which mechanism, and therefore which particles, are most important in assessing the inadvertent precipitation potential. Such surveys should be made for at least a year because the air mass characteristics affecting the Florida Peninsula, quite obviously, vary significantly with the seasons.

The cloud physics measurements, the fallout measurements, and the trajectory and diffusion observations are all possible with established and available instrumentation. Some of these measurements have already been undertaken by NASA. A final assessment of the detailed inadvertent weather modification effects must await the availability of such measurements.

In the interim, we have based this assessment on limited data available to date regarding:

a. cloud (SGC) volume and expansion measurements provided by NASA for several Titan rocket launches over one hour

b. chemistry of the reaction products as presently known or estimated

c. preliminary cloud microphysics and laboratory measurements

This information has been analyzed in the light of certain cloud physics principles of nucleation and natural cloud evolution, known synoptic characteristics of the Florida area, and against the backdrop of a still evolving weather modification science. The results, while lacking the benefit of the detailed measurement program outlined above, are considered to constitute a rational appraisal of the problem and risk factors involved.

Chapter II Historical Weather Modification Programs and Comparisons with Neutralized Rocket Clouds

OUTLINE

Tables

Chapter II Historical Weather Modification Programs and Comparisons with Neutralized Rocket Clouds

A. Neutralized Rocket Cloud Mass Concentrations

In order to gain a perspective on the potential impact of cloud modification agents in the neutralized shuttle exhaust cloud, one can compare the particulate masses (and concentrations) involved with the amount of seeding material used on planned weather modification programs. As a frame of reference, the two principal exhaust constituents are listed in Table II-1 in terms of total mass in the ground (trench) and column clouds combined. Also shown are estimated mass concentrations at times of 20 min, 3 hr, and 3 days when cloud volumes are projected to be approximately 10 km^3, 300 km^3, and 7,200 km^3, respectively.

Table II-1 Neutralized Shuttle Exhaust-Cloud (Mass Components)*

Constituent	Mass	Cloud Conc. (t = 20 min)	Cloud Conc. (t = 3 hr)	Cloud Conc. (t = 3 days)
Al_2O_3	67.6×10^3 kg	6760 $\mu g\ m^{-3}$*	225 $\mu g\ m^{-3}$*	9.39 $\mu g\ m^{-3}$*
NH_4Cl	67.9×10^3	6790	226	9.43

*1 $\mu g\ m^{-3}$ = 1 $kg\ km^{-3}$

While cloud effects at $T \geq 3$ hr are the primary concern of this analysis, the values of aerosol mass concentration in the neutralized cloud at t = 20 min are of interest for several reasons:

a. Shuttle cloud volumes are more accurately known at this time.

b. Planned cloud-seeding treatments often apply over a similarly short time interval.

* See Chapter III.

c. The potential inadvertent weather modification effects may be more pronounced shortly after rocket launch under most circumstances

In essence Al_2O_3 can act as an ice nucleating (IN) agent in supercooled clouds, while NH_4Cl particles can serve as effective cloud condensation nuclei (CCN). (Other neutralization agents have been considered that produce $CaCl_2$ or NaCl; such salts are quite similar in their droplet forming characteristics to NH_4Cl.) In short, at T = 20 min the neutralized cloud will contain approximately 6760 μg m^{-3} of Al_2O_3 (potential IN) and 6960 μg m^{-3} of NH_4Cl (effective CCN); three hours later the concentrations will have reduced to respective values of 225 and 232 μg m^{-3}.

B. Cold Cloud Seeding

NOAA has been charged with keeping records of all weather modification activities in the United States. During 1975 their report (Charack, 1976) shows that 88 activities under 72 separate weather modification programs were conducted. The specific seeding objectives are shown in Table II-2.

Table II-2 1975 Seeding Activities in the U.S.A.

Precipitation Augmentation	44
Fog Dissipation	15
Hail Reduction	14
Research	15
Total	88

Of these activities, over 75% involved the seeding of supercooled clouds with ice nuclei from silver iodide, dry ice, and AgI admixtures. Table II-3 presents a summary of activities and seeding agents employed.

Programs were planned in 25 states, preponderently west of the Mississippi River, with a total target area of 422,656 km^2 (163,194 mi^2). Two programs were conducted in Florida involving a target area of 12,634 km^2 (4,878 mi^2).

Table II-3 Summary of 1976 Weather Modification Activities - U.S.A. (after Charack, 1976)

		Federal	Nonfederal	Total
(a)	Modification days (cumulative)	129	1,654	1,783
(b)	Modification days (stratiform clouds)	36	186	222
(c)	Modification days (isolated clouds)	17	866	883
(d)	Modification days (organized clouds)	50	510	560
(e)	Modification days (fog)	31	57	88
(f)	Modification missions	135	2,173	2,308
(g)	Airborne apparatus operation, hours	400	1,262	1,662
(h)	Ground-based apparatus operation, hours	2,499	44,527	47,026
(i)	Dry ice (kg)	0	20,662	20,662
(j)	Polyelectrolyte (kg)	0	1,265	1,265
(k)	Silver iodide dispensed from ground (kg)	63	897	960
(l)	Silver iodide dispensed by airborne means (kg)	35	592	627
(m)	Liquid propane (gal)	5,614	0	5,614
(n)	Charged H_2O (gal)	14,630	0	14,630
(o)	Lithium chloride solution (gal)	15	0	15

Silver iodide was the most commonly used seeding agent in cold clouds, being involved in 50 modification activities versus only 11 for dry ice. As indicated in Table II-3, the total amount of AgI dispensed over the entire year at various locations was 1.587×10^3 kg. From Table II-1 it is evident that the total amount of Al_2O_3 (40 projected launches) released at a single Florida location (over the altitude of reference) would amount to 2700×10^3 kg. As is discussed in Chapter IV, however, the number of ice nuclei per given mass of material is estimated to be some 4-5 orders of magnitude greater for AgI than for Al_2O_3. Allowing for this difference, but recognizing the concentrated nature of the repetitive Florida releases, it becomes

apparent that the mass of Al_2O_3 involved may not be insignificant. Closer analysis is necessary.

The number concentration of effective IN per given volume of air and temperature is more fundamental to cloud modification. As a general statement, many rain (snow)-making programs are based on adding 1-10 l^{-1} effective ice nuclei at supercooled cloud temperatures of approximately -10 to -15 C. Hail modification supposedly requires of order a few 100 l^{-1} to reduce the size of damaging hail; while calculations suggest that if hurricane winds can be diminished at all, IN seeding concentrations of up to 100 l^{-1} might be needed.

Seeding rates with AgI to accomplish the above objectives vary roughly from a few kg day^{-1} (winter snowpack enhancement) to a few kg hr^{-1} (intense storm modification). Note that the Al_2O_3 rocket exhaust release amounts to approximately 68.5 x 10^3 kg in only 24 sec over the first 1.6 km altitude of prime interest (Table II-4, NASA JPL Tech. Memo 33-712). Again one must temper this seemingly extreme output rate by the lesser nucleation activity of Al_2O_3 versus AgI.

A few selected weather modification programs will serve to illustrate both the seeding rates and IN concentrations customarily achieved.

1. Snowpack Enhancement

The Climax (Colorado) I and II programs represent one of the longest experiments (10 years) and more definitive examinations of increasing snowfall from orographic supercooled clouds. Snowfall increases of 15-20% were obtained by seeding with silver iodide ground generators in orographic clouds no colder than about -21° C; at colder cloud top temperatures, natural ice nuclei were sufficient such that added ice nuclei had no effect or a negative effect--snowfall decrease (Grant et al., 1971). It

Table II-4 Exhaust Products released into Atmosphere by Space Shuttle SRMs (Partial list: Mission 3B)*

Altitude band, km	Δaltitude, km	Time,	Δtime,	Average mass flow, 10^3 kg/s	Mass, 10^3 kg	Exhaust products[a] Al_2O_3	HCl	CO	CO_2
						0.302028	0.200315	0.241719	0.0343946
								Exit	Exit
0-0.0095	0.0095	0-2	2	9.444	18.88	5.704	3.953	4.565	0.6495
0.0095-0.039	0.0295	2-4	↕	9.446	18.89	5.704	3.953	4.565	0.6496
0.039-0.087	0.048	4-6	↕	9.446	↕	5.705	3.954	4.566	0.6496
0.087-0.160	0.073	6-8	↕	9.447	↕	5.705	3.954	4.566	0.6497
0.16-0.25	0.090	8-10	2	9.448	18.89	5.706	3.953	4.566	0.6498
0.25-0.50	0.250	10-14	4	9.449	37.79	11.41	7.912	9.134	1.300
			↕						↕
0.50-0.85	0.35	14-18	↕	9.451	37.79	11.41	7.911	9.136	
0.85-1.3	0.45	18-22	↕	9.451	37.80	11.42	7.912	9.137	
1.3-1.9	0.60	22-26	4	9.454	37.81	11.42	7.914	9.139	1.300
1.9-2.2	0.30	26-28	2	9.445	18.89	5.704	3.953	4.565	0.6496
2.2-2.5	0.30	28-30	2	9.292	18.58	5.612	3.889	4.491	0.6390
2.5-3.3	0.80	30-34	4	8.859	35.43	10.70	7.416	8.564	1.219
			↕						
3.3-4.2	0.90	34-38	↕	8.282	33.12	10.00	6.933	8.006	1.133
4.2-5.1	0.90	38-42	4	7.705	30.81	9.307	6.450	7.448	1.060
5.1-6.0	0.90	42-45.44	3.44	7.123	24.50	7.399	5.128	5.921	0.8426
6-9	3	45.44-56.06	10.62	6.526	69.29	20.93	14.50	16.75	2.383
9-12	↕	56.06-65.52	9.46	6.630	62.70	18.94	13.12	15.16	2.157
12-15	↕	65.52-74.01	8.49	6.925	58.78	17.75	12.30	14.21	2.021
15-18	↕	74.01-81.64	7.63	7.147	54.52	16.47	11.41	13.18	1.875
18-21	↕	81.64-88.70	7.06	7.270	51.32	15.50	10.74	12.40	1.765
21-24	↕	88.70-94.90	6.20	7.320	45.37	13.70	9.497	10.97	1.561
24-27	↕	94.90-100.8	5.90	7.298	43.05	13.00	9.011	10.41	1.481
27-30	↕	100.8 -106.2	5.40	7.227	39.02	11.78	8.167	9.431	1.342
30-33	↕	106.2 -111.2	5.00	7.089	35.44	10.70	7.417	8.565	1.219
33-36	↕	111.2 -116.08	4.88	6.230	30.40	9.180	6.362	7.347	1.045
36-39	3	116.08-120.80	4.72	3.227	15.24	4.602	3.189	3.680	0.5241
39-41.6	2.6	120.80-124.85	4.05	0.8686	3.519	1.063	0.7366	0.8506	0.1210
			TOTAL		915.6	276.5	191.6	221.3	31.49

[a]The mass is indicated below the symbol for each specie.

*NASA JPL Technical Memorandum 33-712.

should be emphasized that this critical minimum temperature will vary considerably with geographic location, type of cloud cells involved, season, and particularly updraft strength. In short cumuliform, summer clouds with strong updrafts would require greater concentrations of IN to reach any "over-seeding" level.

Based on the above results, the San Juan, Colorado program of the Bureau of Reclamation was instituted (Grant and Kahan, 1974). It employed 33 AgI ground generators and a snowfall target area of 3,367 km^2 (1,300 mi^2). Seeding characteristics were as follows:

a. seeding rate - 0.5 to 3.4 kg day^{-1}, depending on cloud temperature

b. IN activity - about 1.5 to 2 x 10^{16} IN hr^{-1} (10^{14}-10^{15} g^{-1}, -15 to -20 C)

c. seeding concentration - estimated 1-10 l^{-1}

2. Snowfall Distribution

The NOAA Great Lakes Seeding Experiment (1967-71) had as its principal objective the overseeding of winter storms to create smaller crystals that would advect further inland (Weickmann, 1974). At least one experiment provided perhaps the first clear-cut physical example of overseeding. The seeding parameters (aircraft AgI flares) were as follows:

a. seed rate - 2.4 kg over 27 min or ∿5 kg/hr

b. active IN - 10^{15} to 10^{16} g^{-1} at cloud T of -9 to -24 C

c. seed concentration - calculated estimate of 2,000 l^{-1}

Measurements at the ground (Holroyd and Jiusto, 1970) confirmed that approximately 1,000 crystals/liter resulted in the overseeded clouds. This led to dramatic changes in size (reduced) and type of falling snow crystals

from the rapidly glaciated cloud. This extreme concentration of seeded crystals, higher than anything accurately reported to date, represents perhaps a limiting value for analyzing possible seeding effects by NASA rockets.

3. Hail Suppression

Two hail suppression concepts have been advanced: (1) rapid and total cloud glaciation (as in the Great Lakes experiment above) to prevent formation of large hail and (2) moderate seeding to create competition for water vapor amongst the introduced ice embryos and hence smaller hail. The first concept is considered impractical in that it requires about 10^3-10^4 IN l^{-1} over substantial times and volumes in space. The second concept, generally accepted but not always realized in practice, is to produce IN concentrations of order 10^2 l^{-1}.

The Russians (Sulakvelidze et al., 1974) have claimed the most success--up to 90% or more--in diminishing damage due to hail. Their seeding aims are 100 IN l^{-1} concentrations, approximately 1 kg AgI per storm cell during its rapid development stage at roughly 20-40 min, and rocket seeding doses of 100 g every 2 minutes. This translates into a typical seeding rate of 1-3 kg hr^{-1}.

In this country, the National Hail Research Experiment (NHRE) conducted in NE Colorado has failed to achieve such positive results. In fact, indications are that seeding may have increased total hail mass by an average of 60% though the results were not considered statistically significant (Long et al., 1976). While geographic differences apparently account for some of the differences in the two experiments (Atlas, 1976), NHRE may have lacked the capability of the Russian approach in terms of rapid timely delivery of large concentrations of seeding material.

While the stated goal has been to achieve comparable seeding rates and concentrations, it is not evident from the literature that such has been achieved (Young and Atlas, 1974; NHRE Project Plan 1975-80; Long et al., 1976).

Schleusener (1968) has suggested that AgI seeding rates >2 kg hr^{-1} will suppress hail activity, while lesser rates may well stimulate storm intensity. Local storm conditions would undoubtedly alter any such critical seeding value, but it seems reasonably plausible that seeding can result in either hail diminution or enhancement.

4. Hurricane Modification

Too few hurricanes have been seeded to verify or negate the more plausible modification concepts or numerical models proposed (Simpson, 1970; Rosenthal, 1971). These models suggest that heavy seeding with AgI beyond the radius of the intense eye wall clouds could release sufficient latent heat to set up a secondary circulation. The net effect could be a relaxation in the strength of the primary wind vortex, with even a small percentage reduction considered capable of substantially reducing hurricane damage.

Hurricane Debbie was seeded on two consecutive days in August 1969 with corresponding suggested wind reductions of about 30% and 15%, respectively (Gentry, 1974). Pyrotechnics (200), each containing 190 g of AgI, were dropped into the hurricane along a 30-40 km track in about 10 min; 5 such seeding runs were made on each day. The pyrotechnics were designed to burn for 6 km of fall and produce an estimated 10^{12}-10^{14} nuclei g^{-1} at the characteristic temperatures involved. Thus on each run, the AgI seeding would amount to:

a. rates of 38 kg per 10 min

b. IN numbers of $3.8 \times 10^{16-18}$ (10 min)

c. a highly variable IN concentration which one can roughly estimate to be of order several 100 l^{-1} initially, followed by rapid dilution in the strong vortex winds involved

5. Florida Area Cumulus Experiment (FACE)

The FACE program of NOAA (1970-76) was designed to stimulate rainfall over the Florida peninsula. The concept involved heavy seeding to merge isolated cumuli into large organized systems of greater duration and intensity. As in the hurricane seeding, but on a more modest scale, cloud stimulation by latent heat release is predicated.

Successful results (25-60% enhancement) have been reported (Woodley et al., 1976; Simpson and Dennis, 1974). This so-called "dynamic seeding" has been accompanied by AgI seeding from aircraft to the tune of:

a. 100 g to 1 kg per cloud

b. about 10^{13} active IN g^{-1} at T = -10C

c. seeding rates of 15 kg day^{-1} (a few hours of seeding presumably)

On some occasions, particularly with relatively stationary echoes, rainfall decreases from seeding were indicated.

This seeding program is particularly relevant because it was conducted over the south-central Florida peninsula during the summer season. As indicated previously (Mohnen et al., 1976), this is the time of year when Al_2O_3 particle seeding from NASA rockets should be most significant.

C. Warm Cloud Seeding

The seeding of warm clouds (i.e., warmer than 0^{o} C) with hygroscopic particles to stimulate rain is predicated on a natural deficiency of giant nuclei in such clouds. Early salt-seeding concepts and experiments (Bowen,

1952; Davies, 1954; Fournier d'Albe, 1955) were based on the assumption that the addition of 1 giant nucleus of 10-20 μm dia. (10^{-9} to 10^{-8} g) of NaCl per liter of air would enhance droplet coalescence and subsequent rainfall. Sodium chloride was and still is the most common type of seeding material used.

Most of the recent salt seeding of warm clouds has been conducted in India, with only limited experiments in this country (South Dakota School of Mines and Technology Project Cloud Catcher; Pennsylvania State University studies in the Virgin Islands). However, the basic seeding concepts have not changed substantially from those indicated above. Kapoor et al. (1976) dispersed NaCl with a particle mode diameter of 10 μm in clouds in India. Their seeding rate was 12-15 kg per 3 km of flight path, with a total salt consumption of 1975 kg. Fournier d'Albe (1976) has suggested global regions where salt seeding to enhance rainfall might be feasible, assuming still the particle sizes and concentrations mentioned (namely about 1 l^{-1} $\geq$10 μm dia.).

One particle per liter of NaCl (10^{-9} to 10^{-8} g) amounts to a mass concentration of 1-10 kg km^{-3} (or 1-10 μg m^{-3}). Referring to Table II-1, it is evident that the neutralized-cloud salt component (NH_4Cl) substantially exceeds this mass concentration at t = 3 hr and is still comparable with it at t = 3 days. However, the particle sizes, drop competition and solubility ratios (NH_4Cl to attached Al_2O_3) must be evaluated to determine cloud modification potential (Chapter V).

In terms of promoting droplet growth on hygroscopic nuclei, the exact chemical nature of the soluble particle is not as critical as with ice nucleants (e.g., AgI vs. Al_2O_3). As mentioned NH_4Cl and $CaCl_2$ (as well as a variety of salts) are quite comparable to NaCl in droplet growth characteristics -

at least to a factor of 2 in contrast to orders of magnitude differences in effectiveness of various ice nucleants. As is discussed in Chapter III, most particles in the exhaust cloud will be "mixed" nuclei. Such nuclei consist of both insoluble and soluble components, in this case Al_2O_3 plus the soluble chloride. Mixed nuclei behave rather similarly to pure hygroscopic particles in initial droplet formation, provided the insoluble component is not greater than 90% of the total mass (Junge and McLaren, 1971).

Again it is essential to examine the number concentration of neutralized-exhaust products that can serve as effective cloud condensation nuclei. From the normalized particle size distributions and total aerosol number concentrations versus time in the cloud (Fig. III-4 and Table III-4 of Chapter III), one can obtain the concentration of mixed-nuclei greater than any given size. Table II-5 presents such values.

Table II-5 Concentration of Aerosols in Neutralized Cloud Greater than Indicated Sizes vs. Time

Dia.	Approximate Aerosol Concentration T + 3 hr	T + 1 day	T + 3 days
0.2 μm	9.2×10^{6} l^{-1}	1.1×10^{6} l^{-1}	3.9×10^{5} l^{-1}
1	1.0×10^{4}	1.2×10^{3}	4.3×10^{2}
2	7.7×10^{2}	9.4×10^{1}	3.3×10^{1}
5	1.2×10^{2}	1.4×10^{1}	5.0×10^{0}
10	1.3×10^{1}	1.6×10^{0}	5.5×10^{-1}
20	5.6×10^{-1}	6.8×10^{-2}	2.4×10^{-2}
50	2.1×10^{-3}	2.5×10^{-4}	8.8×10^{-5}

It is evident, solubility and competition considerations permitting, that giant nuclei (10 μm dia.) potentially suitable for warm cloud seeding are still present after 1 day in sufficient number (1 l^{-1}) to possibly

influence precipitation. There is also a rather sizeable concentration of "large" nuclei (0.2 - 1 μm dia.) to produce smaller cloud droplets that can compete with the larger saline drops (Chapter V).

D. Warm Fog Modification

One of the first, if not the first, scientific efforts to modify weather was that of Houghton and Radford (1938). They attempted to dissipate fogs by spraying into them sufficient $CaCl_2$ solution drops to lower the relative humidity to about 90%; the natural fog drops would thus evaporate and re-condense on the large sedimenting spray drops. Marginal success over limited clearing volumes was achieved, but the seeding agent amounts required were prohibitive - approximately 2.5 g m^{-3} or 2.5×10^3 kg for an airspace of 10^6 m^3.

In recent attempts to clear fogs at airports, the above concept was revived and improved by NASA (Calspan contractor) and then the Air Force (convenient summary by Silverman and Weinstein, 1974). Basically dry salt particles of carefully prescribed sizes were injected into fogs to only slightly reduce relative humidity. While the end result was theoretically the same, the salt seeding requirement decreased by 2-3 orders of magnitude. Calculations and lab experiments (Jiusto et al., 1970), essentially confirmed by subsequent field experiments, suggested the NaCl seeding requirements of Table II-6.

Table II-6 Calculated Salt (NaCl) Seeding to Clear Warm Fogs (Fog Thickness = 100 m; Volume = 10^8 m^3)

Salt Dia.	Number Conc.	Mass Conc.	Mass-Single Treatment	Mass 3 m sec^{-1} Winds
10 μm	900 l^{-1}	$9x10^2$ μg m^{-3}	90 kg	450 kg hr^{-1}
20	330	$3.3x10^3$	325	1625
45	110	$11x10^3$	1120	5600

Other model computations (Silverman and Weinstein, 1974), involving urea seeds and somewhat different conditions resulted in still larger mass seeding requirements.

Assuming that 20 μm dia. particles are near optimum, it is evident from Tables II-5 and 6 that warm fog seeding involves much higher salt concentrations than those in the neutralized exhaust cloud. At T + 3 hr, the rocket cloud particles of $\geq$20 μm are only about 0.5 l^{-1} (vs. 330 l^{-1} required - Table II-6); even at T + 20 min, the rocket cloud concentration of such giant nuclei is at least an order of magnitude below the fog seeding level.

Thus warm fog modification with hygroscopic material does involve much larger concentrations of giant nuclei than that in the rocket cloud. However, two caveats are noted:

1. Such warm fog seeding has virtually been abandoned, partially because of marginal clearing results but also because of ecological concerns regarding the high doses of seeding material.

2. The concentration of "large" exhaust particles (0.2 - 2.0 μm) surpasses that proposed in any fog or cloud modification work. These can generate undesirable haze conditions to be discussed elsewhere.

E. Summary

Comparisons of the amounts and concentrations of seeding material used on weather modification programs with potential nucleants in the neutralized rocket cloud indicate the following:

1. While the ice nucleating capability of Al_2O_3 is some 4-6 orders of magnitude less than AgI, the enormous quantities quickly released suggest that certain cold-cloud seeding effects may well be realized. (Much depends on the ice activation characteristics of Al_2O_3-NH_4Cl complex particles in the neutralized cloud - Chapter IV.)

2. At this point, possible Florida inadvertent weather effects due to Al_2O_3 in changing precipitation (increase or decrease); in altering hail storms; or in hurricane modification, cannot be excluded (in that order of decreasing probability). Not all inadvertent weather modification should be construed as necessarily detrimental.

3. The mixed nuclei (condensation) in the rocket cloud exceed in mass and in number concentration the minimum values considered necessary to influence warm rain. (Critical solubility and growth competition factors must be considered as well - Chapter V.) Such concentrations of giant nuclei persist for perhaps a day after launch.

4. Only warm fog seeding requirements with giant (>10 μ dia.) hygroscopic particles clearly exceed the concentration found in the rocket cloud. However, large nuclei (0.2 - 2.0 μm) favorable for haze formation would be generated in abundance.

References

Atlas, D., 1976: The present and future of hail suppression. Second WMO Scientific Conf. on Weather Mod., Boulder, Colo., WMO No. 443, 207.

Bowen, E., 1952: A new method of stimulating convective clouds to produce rain and hail. Quart. J. R. Met. Soc., 78, 37.

Charack, M., 1976: Weather modification activities for calendar year 1975. NOAA Report, Environ. Mod. Office, Rockville, Md.

Davies, M., 1954: Experiments on artificial stimulation of rain in East Africa. Nature, 174, 256.

Fournier d'Albe, E., Lateef, A., Rassool, S., and I. Zaidi, 1955: The cloud seeding trials in the central Punjab. Quart. J. R. Met. Soc., 81, 574.

Fournier d'Albe, E., 1976: Climatic zones favorable for cloud seeding with hygroscopic nuclei. Second WMO Conf. on Weather Mod., Boulder, Colo., WMO No. 443, 3.

Gentry, C., 1970: Modification experiments on Hurricane Debbie. Proc. 2nd Nat. Conf. Wea. Mod., AMS, 205-208.

Grant, L., Chappell, C., and P. Mielke, 1971: The Climax Experiment for seeding cold orographic clouds. Intl. Conf. Weather Mod., Canberra, Australia, AMS, 78.

Grant, L. and A. Kahan, 1974: Weather modification for augmenting orographic precipitation. In Weather and Climate Modification (W. Hess, ed.), Wiley & Sons, 282.

Holroyd, E. and J. Jiusto, 1971: Snowfall from a heavily seeded cloud. J. Appl. Meteor., 10, 266.

Houghton, H. and W. Radford, 1938: On the local dissipation of natural fog. M.I.T. Papers in Phys. Oceanog. Met., 6, No. 3.

Jiusto, J., Pilie, R., and W. Kocmond, 1970: Fog modification with giant hygroscopic nuclei. J. Appl. Meteor., 7, 860-869.

Junge, C. and E. McLaren, 1971: Relationship of cloud nuclei spectra to aerosol size distribution and composition. J. Atmos. Sci., 28, 382.

Kapoor, R., et al., 1976: An operational rain stimulation experiment using warm technique over Rihand Catchment in Northeast India. Second WMO Conf. Weather Mod., Boulder, Colo., WMO No. 443, 15.

Long, A., Crow, E., and A. Huggins, 1976: Analysis of the hailfall during 1972-74 in the National Hail Research Experiment. Second WMO Conf. Weather Mod., Boulder, Colo., WMO No. 443. 265.

Mohnen, V. et al., 1976: Position paper on the potential of inadvertent weather modification of the Florida peninsula resulting from the stabilized ground cloud. Final Report for period March-August, 1976, under NASA Grant NAS9-14940 000-001, NASA CR-151199, 1976, 201 pp.

National Hail Research Experiment - Staff Project Plan, 1975-80: Nat. Center for Atmos. Research, Boulder, Colo., Aug., 1974, 285 pp.

Rosenthal, S., 1971: On search for hurricane modification tactics through numerical simulation. 52nd AGU Meeting, Washington, D. C.

Schleusener, R., 1968: Hailfall damage suppression by cloud seeding. Proc. 1st Nat. Conf. Weather Mod., AMS, 484-493.

Silverman, B. and A. Weinstein, 1974: Fog. In Weather and Climate Modification (W. Hess, ed.), Wiley & Sons, 355.

Simpson, J., 1970: Cumulus cloud modification: progress and prospects. A Century of Weather Progress, AMS, 143-155.

Simpson, J. and A. Dennis, 1974: Cumulus clouds and their modification. In Weather and Climate Modification (W. Hess, ed.), Wiley & Sons, 229.

Sulakvelidze, G., Biblashvili, N., and V. Lapcheva, 1967: Formation of Precipitation and Modification of Hail Processes. Israel Program for Scientific Translations (NSF), 208 pp.

Weickmann, H., 1974: The mitigation of Great Lakes storms. In Weather and Climate Modification (W. Hess, Ed.), Wiley & Sons, 318.

Woodley, W., Simpson, J., Biondini, R., and G. Sambataro, 1976: On NOAA's Florida Area Cumulus Experiment (FACE). Main rainfall results 1970-75. Second WMO Conf. Weather Mod., WMO No. 443, 151.

Young, K. and D. Atlas, 1974: NHRE microphysics: an overview with emphasis on hail growth and suppression. Fourth Conf. Weather Mod., Fort Lauderdale, AMS, 119.

Chapter III Assumptions and Numerical Values

OUTLINE

A. Introduction

In any attempt to assess the weather modification effect of an aerosol cloud, one of the most important aspects is the particle size distribution and number concentration. The distribution and concentration are important in determining whether entrainment of the aerosol into a cloud will inhibit or promote precipitation and will also determine the dominant precipitation mechanism. Equally important is the background aerosol character and its concentration relative to the aerosol being introduced. Knowing the distribution and concentration of the two aerosols allows one to estimate whether there will be any weather modification impact and the magnitude of the effect.

B. Background Aerosols

From a warm-cloud weather modification perspective, specification of the aerosol in terms of a supersaturation spectrum is more meaningful. A supersaturation spectrum gives the total number of particles (cloud condensation nuclei) activated at a given supersaturation. Typical supersaturations used are in the range of less than 0.1% to 2% which covers the range of supersaturation occurring naturally in clouds and fog. Supersaturation spectra follow a power law of the form

$$N = CS^k$$

where S is the supersaturation, C is the concentration at 1% supersaturation and k is the slope of the spectrum. Measurements of the supersaturate spectra over the Florida peninsula have been carried out by Fitzgerald (1972) for aerosols of both maritime and continental origins. The results of these measurements are summarized below.

Over Land $N = 515\ S_c^{0.53}$

Over Water $N = 291\ S_c^{0.46}$

(S_c in percent)

Cloud condensation nucleus concentrations are substantially less than condensation or Aitken nucleus concentrations because condensation nuclei typically are measured at a supersaturation of approximately 100-300% and represents the total aerosol population in contrast with cloud condensation nuclei which are measured at a few percent supersaturation or less.

Background levels of ice nuclei for evaluating the potential weather modification impact on cold clouds are given in Chapter IV.

C. Volume of the Neutralized Ground Cloud and Aerosol Mass Concentration

1. Cloud Volume as a Function of Time

The specification of the cloud volume as a function of time for long periods is a very difficult problem. The dispersion of the cloud will be influenced by the meteorological conditions prevailing at the time, as well as the trajectory of the cloud. Estimation of the cloud volume from turbulent diffusion alone can be expected to produce large errors as the dimensions of the cloud become greater than the scale of turbulent mixing. Pasquill(1962) summarizes several studies of diffusion at large scales which show the dispersion to be nearly a linear function of the distance from the source. Considering the limited information available on dispersion at large scales and the need to determine the cloud volume as a function of time in a general manner for a variety of conditions, we have chosen to assume the cloud volume increases linearly with time from a measured volume. This approximation in its simplicity is probably representative of our knowledge of how the cloud will disperse

over a time period of several days. Because the analysis done in this study relates primarily to concentrations of particles, it would be very easy to apply these results to other dispersion models through the matching of predicted concentration values.

The cloud volumes used here are one half of the values used in a previous study (Mohnen et al., 1976) based on more recent measurements of exhaust cloud volumes from Titan rocket launches. Table III-1 gives the estimated cloud volume at various times after launch on a linear increase in volume with time.

Table III-1 Estimated Cloud Volumes vs. Time

Time	Cloud Volume
T + 3 hrs.	3×10^2 km^3
T + 1 day	2.4×10^3 km^3
T + 3 days	7.2×10^3 km^3
T + 5 days	1.2×10^4 km^3
T + 7 days	1.7×10^4 km^3

2. Aerosol Mass Concentration in the Neutralized Ground Cloud

The specifications of the mass concentration in the cloud are based on the total emissions of the solid rocket booster in the lower atmosphere. Further it is assumed that all of the HCl emitted by the rocket engine is converted to a solid aerosol by the particular neutralization agent used. Values for the amounts of material in the lower trench cloud and the elevated column cloud are taken from the neutralization study of VanderArend et al. (1976). Table III-2 below summarizes the emission of Al_2O_3 and HCl for the total cloud and its components.

Table III-2 Exhaust Products Summary

Component	Total Cloud (Metric Tons)
Al_2O_3	67.6 MT
HCl	46.9 MT

The neutralization study by VanderArend (1976) recommends neutralization of the trench cloud by the spraying of a solution of $(Na)_2\ CO_3$ into the flame trench during the first 8 seconds of the launch. When considering the large quantity of liquid to be delivered, the small droplet size required, and the technology available for producing fine sprays, one must conclude that this is not a feasible approach.

Considering recent evidence that the ground level concentrations of hydrogen chloride will be at an acceptable low level, the need to neutralize the trench cloud in the flame trench is not as great as originally presumed. A more feasible solution to the neutralization of the trench cloud would be through the introduction of ammonia at a time when the exhaust cloud has cooled enough to remove any hazard of the burning of ammonia. Conceivably, this could be accomplished by spraying from aircraft or by spraying from fixed towers. The use of ammonia for neutralizing the column cloud has been considered in detail by VanderArend (1976). The neutralization reaction in the cloud will occur in accordance with the equation

$$NH_3 + HCl \rightarrow NH_4Cl \qquad (1)$$

Table III-3 summarizes the masses of solid material in the cloud after the neutralization of the hydrogen chloride by ammonia.

Table III-3 Mass of Solid Material in the Exhaust Cloud after Neutralization

Al_2O_3	67.6 MT
NH_4Cl	68.9 MT
Total	136.5 MT

Mass concentration in the neutralized cloud can be calculated from the mass of material given in Table III-3 and the cloud volumes given in Table III-1. Table III-4 summarizes the mass concentrations in the neutralized cloud as a function of time.

Table III-4 Mass Concentration vs. Time

Time	Mass Concentration ($\mu g\ m^{-3}$)
T + 3 hrs.	4.5×10^2
T + 1 day	5.6×10^1
T + 3 days	1.9×10^1
T + 5 days	1.1×10^1
T + 7 days	8.2×10^0

D. Aerosol Size Distribution

1. Size Distribution of the Al_2O_3 Aerosol

The starting point for the analysis of the size distribution was the data of Varsi (1976) on the sizes of the aluminum oxide aerosol as measured with impactors and an electrical mobility analyzer. In a previous study by Mohnen et al. (1976), it was found that for sizes larger than 0.07 micron diameter the data were well described by a power law of the form

$$dN = N_1 D^{-3.5} dD \quad (0.07\ \mu m<D<50\ \mu m). \tag{2}$$

For sizes below 0.07 micron, equation (2) departed substantially from the data, and it was necessary to introduce a second power law function of the form

$$dN = No\ D^{-1.75}\ dD\ (0.02<D<0.07\ \mu m) \qquad (3)$$

to describe the data at smaller sizes.

In an attempt to refine the previous size distribution analysis, a log normal size distribution function of the form

$$dN = \frac{N}{\sqrt{2\pi}\ \ln^2\sigma g}\ EXP[-0.5\ (\ln D-\ln Dg)^2/\ln^2\sigma g]d\ \ln\ D \qquad (4)$$

was fitted to the electrical aerosol analyzer data presented by Varsi. In the above expression, σg is the geometric standard deviation and Dg is the geometric mean diameter. (All references in this report to the geometric mean diameter refer to the number distribution.) The best values of σg and Dg derived from a least squares fit to the data are given in Table III-5 below. The case identifications are the same as those used in the original report by Varsi.

Table III-5 Least Squares Values for a Log Normal Distribution Fit to Electrical Aerosol Analyzer Data

Case	Dg	σg
ETR (T + 7)	7.9×10^{-6} cm	1.6
ETR (T + 13)	9.1×10^{-6} cm	1.6
WTR (T + 6:30)	7.1×10^{-6} cm	1.6
WTR (T + 13:30)	5.5×10^{-6} cm	2.2

The log normal function was found to provide an excellent description of the electrical analyzer data. In the first two cases, the results seem reasonable with the increase in the geometric mean diameter attributable to coagulation processes. In the second pair of cases, the decrease in the geometric mean diameter is not consistent with what one would expect from the physical situation and must have been caused by either measurement error or sampling a different part of the cloud at the later time. Based on four measurements, it is difficult to arrive at a set of parameters for the distribution with a high degree of confidence.

When the log normal functions fit to the electrical aerosol analyzer are compared with the impactor data, it is found that they underestimate the large particle concentrations by several orders of magnitude. Based on this observation one must conclude that the size distribution is too complicated to be described by a single function, but rather must be described by some combination of functions.

For the atmospheric aerosol, the distribution of mass as a function of diameter quite often exhibits two or three distinct modes (Whitby, 1973). The mode occurring at the smallest size, the fine particle mode ($d_g \tilde{\sim} 0.01$ μm), is thought to be the result of combustion processes. This mode contains the largest number of particles, but rapidly decays through the processes of condensation or coagulation with a time scale of a few hours to a day. The mode occurring in the intermediate size range ($d_g \tilde{\sim} 0.1$ μm), called the accumulation mode, is the final size range of submicron size particles before they are removed from the atmosphere. This mode has a lifetime of the order of a few days. A third mode, the coarse particle mode ($d_g \tilde{\sim} 2$ μm), is the result of mechanically produced aerosols modified by the process of sedimentation and removal processes associated with impaction. Thus, it is not uncommon for observed aerosol size distributions to be made up of several components when the full range of aerosol interaction and sources are considered.

The multimodal nature of the atmospheric aerosol distribution and the analysis of the aluminum oxide aerosol spectrum suggests that an appropriate model for the particle distribution in the ground cloud should be described by a multimodal function. Because this study is concerned with the aerosol distribution at long times from the generation,

the model chosen consists of two modes corresponding to the accumulation and coarse particle modes. The fine particle mode can be neglected because of its short lifetime. Each of the modes is described by a log normal distribution function resulting in a distribution function of the form

$$dN = \sum_{i=1}^{2} \frac{N_i}{\sqrt{2\pi}\ \ln^2\sigma gi} \text{EXP}[-0.5\ (\ln D - \ln Dgi)^2/\ln^2\sigma gi]d\ln D \qquad (5)$$

where the subscript i is used to designate the individual mode. A close fit to the measured data can be obtained by choosing Dg1 equal to 0.1 μm and Dg2 equal to 2 μm with both modes having a geometric standard deviation of 2. The amplitudes of the function (N_i) were chosen such that the two modes contain equal masses of material, resulting in the number of particles in the smaller mode being 8000 times the number in the larger mode. The resultant distribution function normalized to a concentration of one particle per unit volume is presented in Figures III-1 and III-2 in differential and cumulative forms.

2. Aerosol Number Concentration

Having specified the aerosol size distribution, the number concentration can be derived from the total mass of aluminum oxide in the cloud and the total mass in the distribution.(5) By integrating the mass distribution, assuming a density of 2.5 g cm^{-3} for the aluminum oxide, and equating this to the total mass in the cloud, the amplitudes (N_i) of the distribution were determined. The number concentrations for the aerosol referred to the total cloud volume derived in this manner are given in Table III-6.*

*All particle distributions presented here will be in normalized form, enabling the reader to determine concentrations as a function of size by multiplying the distribution by the concentrations in Table III-6.

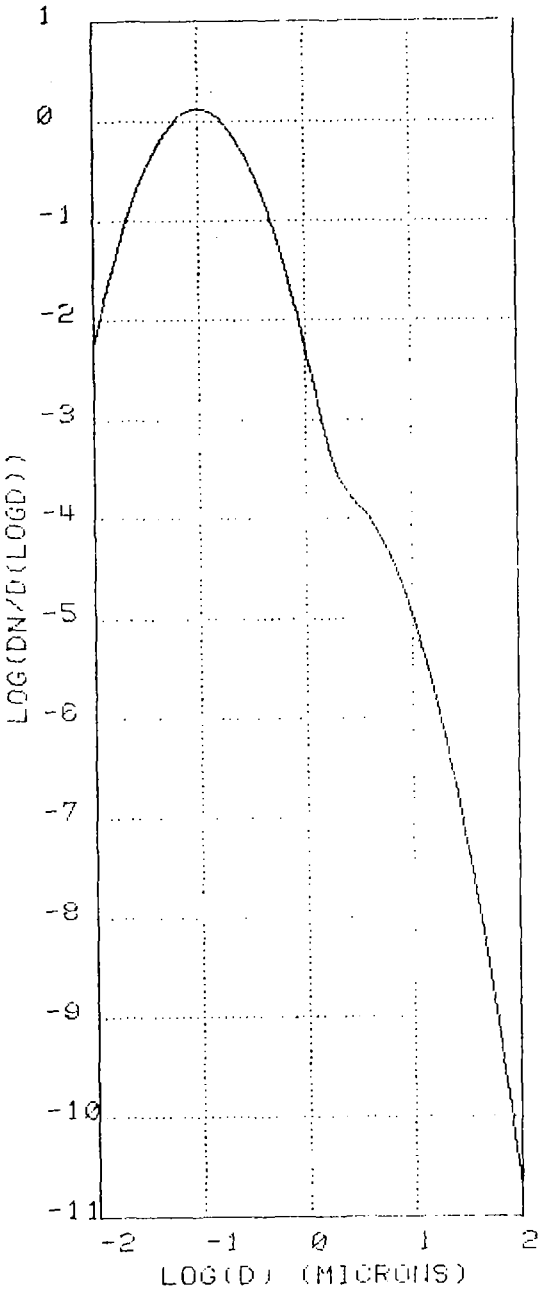

Figure III-1 The size distribution of the aluminum oxide aerosol presented as the normalized differential concentration versus particle diameter.

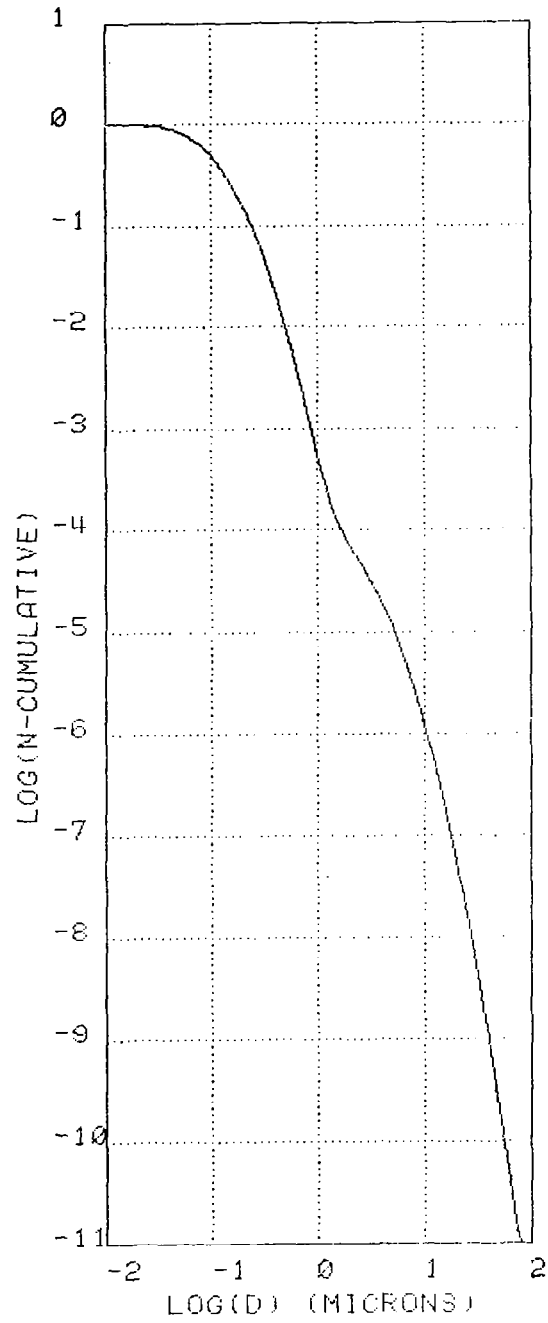

Figure III-2 The size distribution of the aluminum oxide aerosol presented as the normalized cumulative concentration (number of particles greater than indicated diameter) versus particle diameter.

Table III-6 Aluminum Oxide Aerosol Number Concentration vs. Time

Time	Total Cloud
T + 3 hrs.	9.9×10^{9} m^{-3}
T + 1 day	1.2×10^{9} m^{-3}
T + 3 days	4.2×10^{8} m^{-3}
T + 5 days	2.5×10^{8} m^{-3}
T + 7 days	1.8×10^{8} m^{-3}

For purposes of this study, the total mass of material in the cloud at 3 hours is assumed conserved at later times.

3. Distribution of the Neutralization Product

In both the trench cloud and the column cloud the neutralization process will result in the attachment of the reaction product to the Al_2O_3 aerosol through either condensation or coagulation. Independent of whether the attachment process is condensation or coagulation, the physical mechanism controlling the process is diffusion of material to the aluminum oxide aerosol. Therefore, for either process the growth law for the aluminum oxide particles will have the same form

$$\frac{dD}{dt} = \frac{4\kappa C}{(D+2\ell)} \tag{6}$$

where D is the particle diameter, t the time, κ a rate coefficient, C the concentration of material, and ℓ is a length determined by the balance of the kinetic flux of material with the diffusive flux ($\ell \tilde{\approx} 1.5 \times 10^{-4}$). Equation (6) can be integrated to give the particle size as a function of time resulting in the equation

$$D = -2\ell + ((Do + 2\ell)^2 + 8\kappa ct)^{\frac{1}{2}} \tag{7}$$

where D is the size at time t and Do is the initial size.

If one neglects the effects of curvature and the formation of new particles, it can be shown that a unique distribution function results from the attachment of the neutralization product onto the existing

aerosol. The final distribution function will be determined only by the initial size distribution of aluminum oxide particles and the mass of material available for attachment to these particles. In approaching the problem as one of redistribution of an amount of material, one avoids the very complex problem of predicting concentration and rates of reaction as a function of time. Even if one were to undertake such an ambitious modeling program, there are insufficient data available to accurately prescribe conditions in the cloud. Thus we are able to arrive at a reasonable final result without having to model the characteristics of the cloud in detail.

Assuming that all particles follow this growth equation, the equation for the time rate of change of the distribution function is as follows

$$\frac{\partial f}{\partial t} + \frac{\partial}{\partial D}\left(f\frac{dD}{dt}\right) = 0 \tag{8}$$

where f is the distribution function which is a function of particle size and time.

Using the growth equation (6), equation (8) can be solved for the distribution function as a function of time resulting in the equation

$$f(D,t) = (D+2\ell)\ No\left[-2\ell+((D+2\ell)^2-\alpha)^{\frac{1}{2}}\right]/((D+2\ell)^2-\alpha)^{\frac{1}{2}} \tag{9}$$

$$\alpha = 8\kappa ct$$

where No is the initial distribution, equation (5). Assuming that some fraction or all of the neutralization product becomes attached to the aluminum oxide allows the calculation of the final particle distribution from knowledge of the masses of aluminum oxide and the neutralization product.

This is accomplished by determining the value of the parameter α such that the total mass in the final distribution is equal to the sum of the masses of aluminum oxide and ammonium chloride. The parameter α contains the product of the concentration, the rate coefficient and time, but in this simple analysis it is not necessary to specify any of these factors, but only that a certain mass of material is transported by the physical process described in the growth equation. It has been assumed that the time available for neutralization is sufficiently long to provide for complete neutralization of the hydrogen chloride which is probably unrealistic, but leads to a solution representing a worst case in terms of the cloud physics impact of the neutralized cloud.

The assumed value for the diffusion length ℓ is dependent on the process assumed to be dominant. For molecular transport a value on the order of one micron is appropriate, but for coagulation processes it is of the order of one-tenth micron. The choice of a value for α has little effect on the large end of the final distribution where most of the mass is deposited. At the small particle end, the value determines the smallest size particle present and the slope of the distribution function. The value used here was chosen because it produces a realistic distribution function at small sizes and is a reasonable value if one assumes molecular transport processes to be dominant. Under the assumed conditions for the masses of the components, the initial distribution function and the value of the diffusion length, the value of α corresponding to total neutralization of the cloud is 1.1×10^{-8} cm^2.

Figures III-3 and III-4 are plots of the resulting distribution for the cloud after the attachment process. Figure III-3 is the differential distribution, and Figure III-4 is the cumulative distribution. The numbers of particles in each of the component clouds are the same as given in Table III-6 because it was assumed that the attachment process changed only the particle size and composition and not the number.

4. Aerosol Composition and Supersaturation Spectra

Particles containing hygroscopic material, such as those created by the neutralization of the exhaust cloud, will begin to condense water and will form solution droplets at relative humidities below water saturation. For humidities less than a certain critical supersaturation, these solution droplets grow to a size where the vapor pressure over the droplet is in equilibrium with the ambient humidity. If the humidity exceeds the critical supersaturation of the particle, the droplet will no longer be able to remain in equilibrium with its environment, and it will grow to an ever increasing size. Thus, the important property of a nucleus with regard to cloud formation is its critical supersaturation.

Two competing processes are responsible for this behavior of hygroscopic nuclei. The curvature effect acts to increase the humidity over the droplet, while the solution effect, due to the presence of dissolved salts, acts to reduce the humidity. The saturation ratio (ratio of the actual vapor pressure to the saturation value) over a solution droplet is given by

$$\frac{e}{eo} = \text{EXP}\ \left(\frac{4\sigma Mw}{\rho RTD}\right)\ \left(\frac{\nu\omega}{\nu\omega+\nu s}\right) \qquad (10)$$

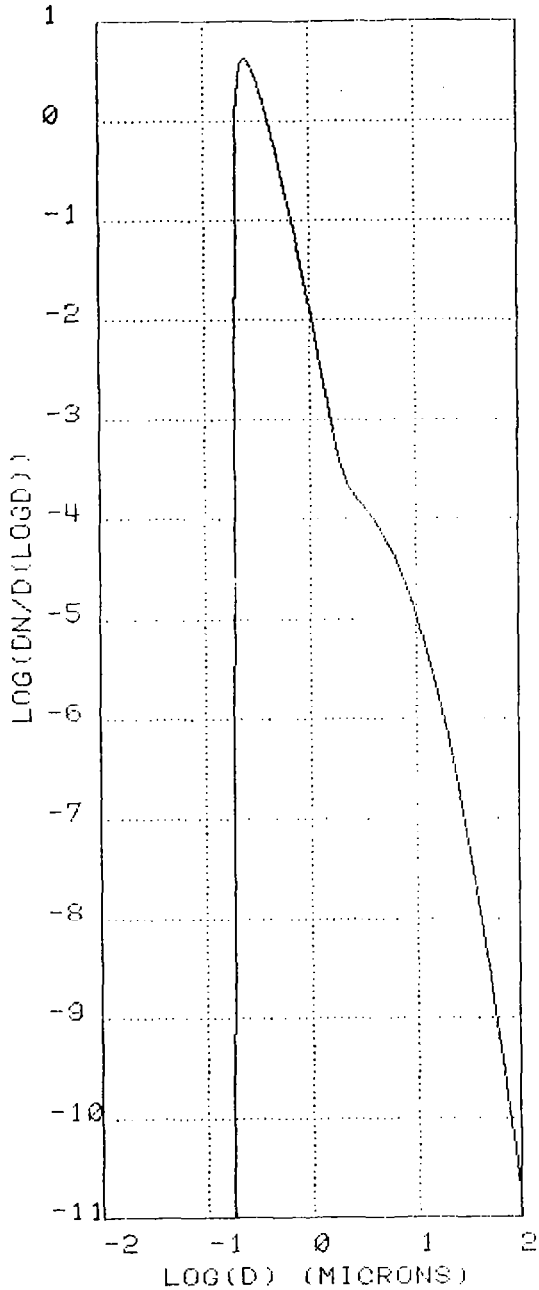

Figure III-3 The size distribution of the neutralized exhaust aerosol composed of ammonium chloride deposited onto the initial aluminum oxide aerosol presented as the normalized differential concentration versus particle size.

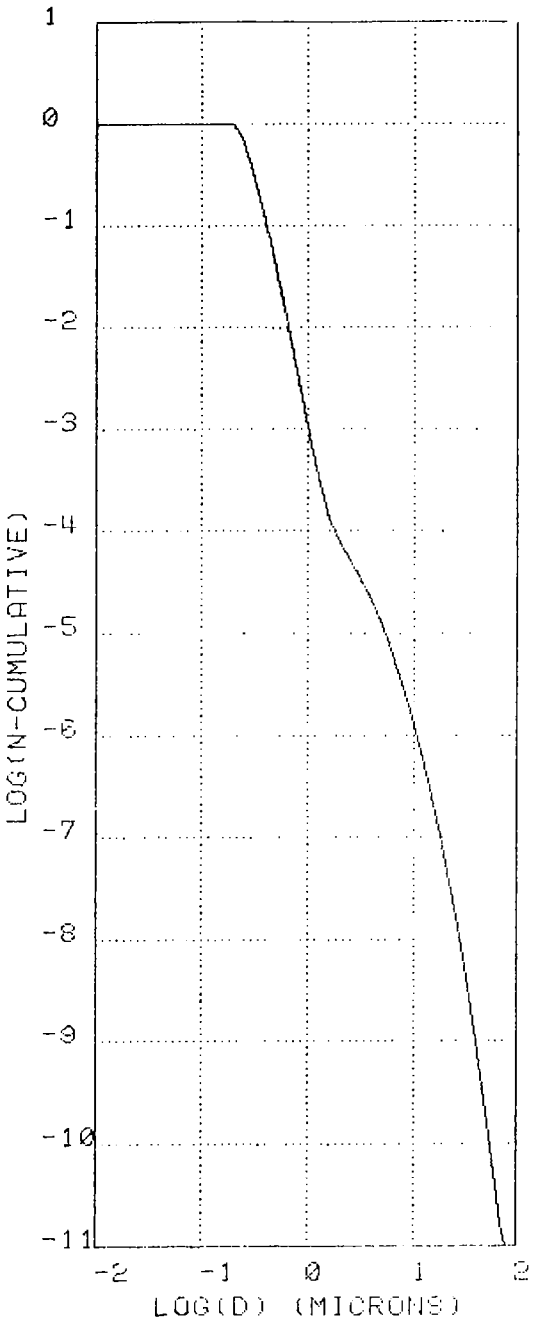

Figure III-4 The size distribution of the neutralized exhaust aerosol composed of ammonium chloride deposited onto the initial aluminum oxide aerosol presented as the normalized cumulative concentration (number greater than the indicated size) versus particle diameter.

which is just the product of the exponential curvature term and the solution term. The solution term is the ratio of the number of moles of water to the total number of moles of water and dissolved salt. Taking into account that the particles are only partially soluble, equation (10) can be written as

$$\frac{e}{eo} = EXP\left[\frac{a}{D}\right]\left[\frac{D^3+Co}{D^3+Cl}\right] \qquad (11)$$

$$a = \frac{4\sigma Mw}{\rho\omega RT}$$

$$Co = -Do^3\rho o - \rho s\ (Dp^3-Do^3)$$

$$Cl = Co + i\ \rho s\ Mw\ (Dp^3-Do^3)/Ms$$

where Do is the diameter of the insoluble particles, ρo its density, Dp the diameter of the mixed particle, D the diameter of the droplet, ρs the density of the hygroscopic salt, and i a factor introduced to account for the non-ideal nature of the solution. Mw and Ms are the molecular weights of water and the dissolved salt, respectively.

At the critical supersaturation for the particle, the saturation ratio over the droplet is a maximum. The droplet diameter corresponding to the critical supersaturation can be determined by taking the first derivative of equation (11) with respect to D and setting the result equal to zero. Following this procedure results in the following polynomial equation for the critical diameter Dc.

$$Dc^6 + Dc^4\ 3(Co-Cl)/a + Dc^3(Cl+Co) + CoCl = 0 \qquad (12)$$

Thus, to find the critical supersaturation for a particle of given size and composition, one must solve equation (12) for the root corresponding to the critical diameter and evaluate equation (10) at the critical size, Dc.

The composition of the nuclei resulting from the neutralization of the exhaust cloud is not uniform because of the size dependence of the particle growth rate. Utilizing the equation for the final size of the particle (7) and the value of alpha ($\alpha = 1.1 \times 10^{-8}$ cm^2), ratios of the volume of soluble of soluble material to the total volume of the particle were computed. Figure III-5 is a plot of the volume ratio as a function of final particle size for the neutralized cloud. The smallest particles in either cloud are completely soluble with the fraction of soluble material decreasing with increasing particle size.

The supersaturation spectrum of the aerosol was computed from knowledge of the particle size and composition using equations (11) and (12) with number concentrations computed from equations (5) and (9). A supersaturation spectrum gives the number of particles active at all supersaturations less than a given value. Figure III-6 shows the spectra derived for the component clouds using this procedure. Because all of the particles are active condensation nuclei, the spectra are presented in normalized form and are related to the number concentrations given in Table III-6.

The least active particle in either cloud has a critical supersaturation of 6.5×10^{-2} percent which is considerably less than the values of 0.1 to 1 percent which occur in fog or cloud forming processes. Thus one can conclude that all of the particles resulting from the neutralization of the exhaust cloud will form droplets in a cloud or fog forming process. Because of the large size of some of the particles, they may not be able to reach their critical diameter and therefore will grow as large haze droplets.

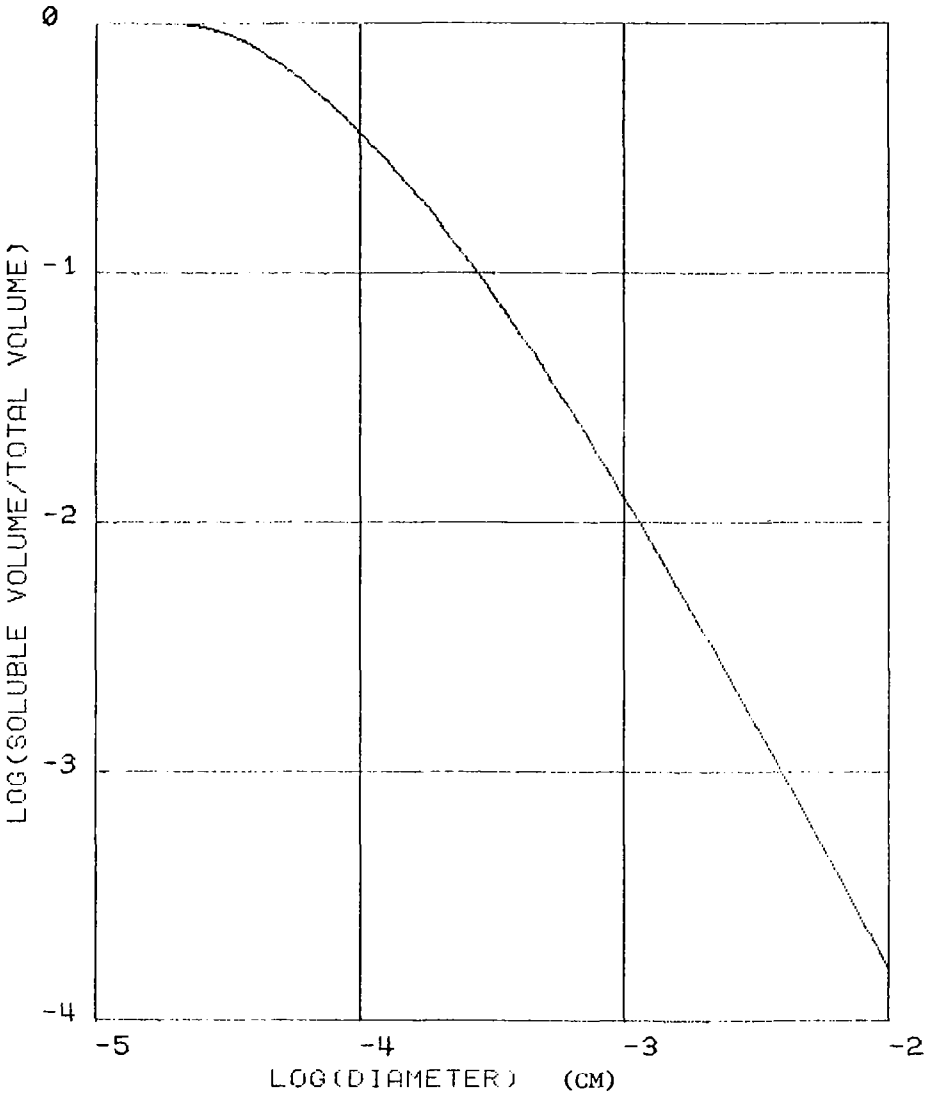

Figure III-5 The ratio of the volume of soluble material (ammonium chloride) to the total particle colume as a function of particle size for the neutralized exhaust aerosol.

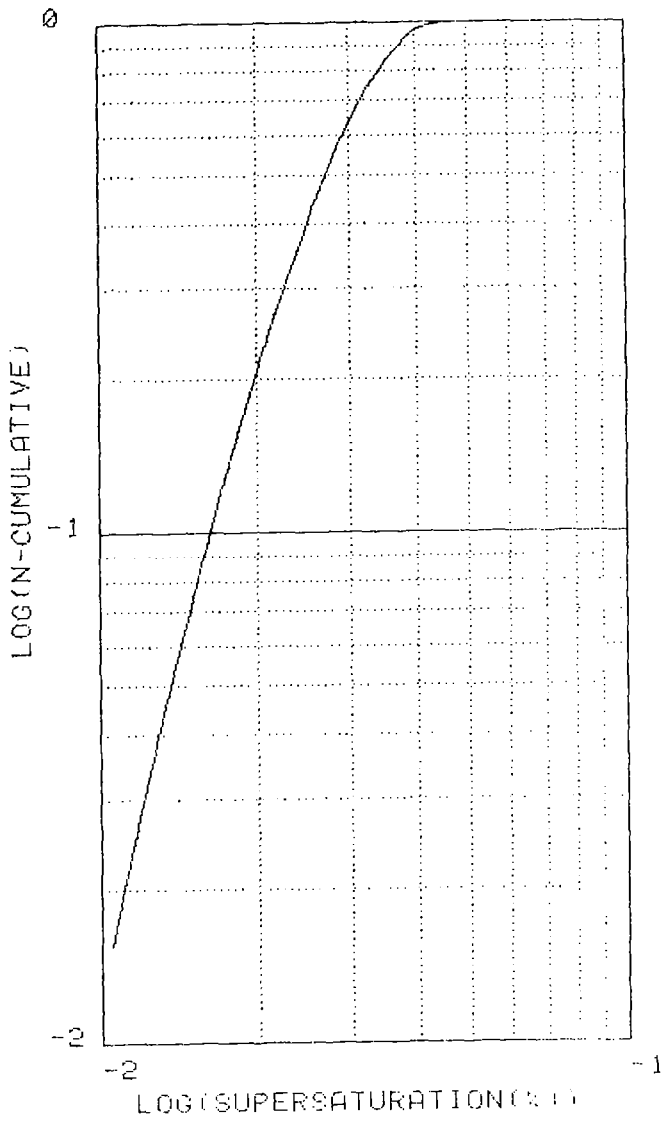

Figure III-6 The cloud condensation spectrum for the neutralized exhaust aerosol presented as the normalized cumulative concentration of particles with critical supersaturation less than the indicated value.

E. Summary and Recommendations

Specification of the neutralized rocket motor exhaust aerosol in the stabilized ground cloud has been accomplished in terms of cloud volume, average mass concentration, particle size distribution, particle composition, and cloud nucleus supersaturation spectra. These results have been derived from extrapolated cloud volume data, mass of the exhaust products, assumed neutralization with ammonia, and deposition of the neutralization product onto the aluminum oxide aerosol by a diffusion controlled process. Under the assumption that all mass present at three hours is present at later times and the size distribution remains constant in form, the resulting set of specifications are consistent with mass conservation. The effects of non-linear cloud expansion and particle sedimentation have been excluded but may be incorporated easily because all subsequent analysis is based solely on the concentration of particles.

Future measurements of the aerosol in the stabilized ground cloud should be concerned with the mass balance, as well as the volume history of the cloud. Direct measurement of total particle concentrations, as well as cloud nucleus and ice nucleus concentrations, are desirable. Laboratory and experimental work on the details of the neutralization process are desirable for better definition of the size and composition of the neutralized aerosol. A complete set of data on the aerosol properties, as well as activity of the aerosol as cloud nuclei and ice nuclei for both neutralized and unneutralized exhaust clouds, is of the greatest importance in correctly assessing the inadvertent weather modification impact of shuttle exhaust products.

F. References

1. Fitzgerald, J. N., 1972: "A Study of the Initial Phase of Cloud Droplet Growth by Condensation: Comparison Between Theory and Observation," University of Chicago Cloud Physics Lab., Tech. Note 44, 144 pp.

2. Mohnen, V., et al., 1976: Position paper on the potential of inadvertant weather modification of the Florida peninsula resulting from the stabilized ground cloud. Final Report for the period March-August 1976, under NASA Grant NAS9-14940 000-001, NASA CR-151199, 1976, 201 pp.

3. Pasquill, F., 1962: Atmospheric Diffusion. D. Van Nostrand Company, 297 pp.

4. Van der Arend, P. C.; Stoy, S. T.; and Kranyecz, T. E.; 1976: Feasibility Study of Launch Vehicle Ground Cloud Neutralization. NASA CR-145000, 142 pp.

5. Varsi, G., 1976: Particulate Measurements. Presentation at Space Shuttle Environmental Assessment Workshop (Stratosphere) March 1976.

6. Whitby, K. T., 1973: On the Multimodal Nature of the Atmospheric Aerosol Size Distributions, presented at the VIII International Conference on Nucleation, Leningrad, USSR, (Sept. 24-28, 1973).

Chapter IV Cold Cloud Processes and the Neutralized Cloud

OUTLINE

Tables

Figures

Chapter IV Cold Cloud Processes and the Neutralized Cloud

A prior study (Mohnen et al., 1976) for NASA was made to estimate the effects on clouds and weather of the exhaust products from rocket launches. The products of primary concern from the solid rocket propellant involved were Al_2O_3 . HCl, and reactive byproducts. For a detailed discussion of the cloud physics processes involved and the conclusions reached, the reader is referred to that document. For clarity and comparison with the neutralized rocket cloud effects, some reference to and abstraction from the prior study (hereafter referred to as PS*) will be made.

A. Precipitation from Clouds - Ice Crystal Development and Droplet Coalescence

Only a small percentage of clouds reach the precipitation stage. The progression from minute cloud droplets (circa 1-25 μm radius) to falling hydrometeors, if it is to occur at all, involves three basic processes:

a. droplet collisions and coalescence

b. the ice crystal or Bergeron-Findeison process whereby ice crystals grow by diffusion of water vapor at the expense of evaporating supercooled drops and from cloud vapor generated in vertical updrafts

c. the ice crystal process augmented by collisions with droplets (riming) and/or other crystals (aggregation)

Warm rain or that due entirely to a droplet coalescence dominates at tropical latitudes. It may even play a role at higher latitudes with unstable clouds not extending far above the freezing level. The

*PS-V, for example, will indicate Prior Study-Chapter V (Mohnen et al., 1976)

ice crystal mechanism clearly is dominant at polar latitudes and also highly significant at mid-latitudes. In the latter zone, where the world's population and industrialized nations are concentrated, the ice phase combined with collisional mechanisms (item c) prevail. It is well recognized that the heavier mid-latitude precipitation (rain or snow) can only be explained by this combination of mechanisms (Houghton, 1950).

Florida, while a sub-tropical region, can experience rainfall by either mechanism (a) or (c) above. However, deep cloud systems and the ice phase undoubtedly are instrumental in the major production of rainfall on the peninsula. As described in Chapter VI, the summer rainy season extends from roughly May to September or October. During this time, rainfall is likely every day (50% probability) vs. 1-2 days per week in winter; half the rainfall comes from local showers and thundershowers (Bradley, 1972).

Clearly in these deep convection systems, ice nuclei and crystals are the initial building blocks for subsequent riming, snowflake aggregation, latent heat release, and heavy rainfall. The Florida Area Cumulus Experiment (FACE), conducted by NOAA from 1970-1975, is predicated on the belief that cloud seeding with additional ice nuclei in summer can merge clouds and enhance rainfall (Woodley and Sax, 1976). As mentioned in the last chapter, FACE seeding has led to both reported increases and decreases in precipitation at reasonable levels of statistical significance. Thus, the recognized role of the ice phase in Florida precipitation and the comparison between ice nuclei seeding concentrations and that inadvertently released in NASA space shuttle launches -- regular and neutralized -- are highly relevant.

B. Ice Nuclei in the Atmosphere

1. Ice Nucleation Mechanisms

Particles that promote the formation of ice in clouds do so via:

a. condensation-freezing

b. adsorption ("sorption")

c. immersion within a supercooled drop and subsequent freezing

d. surface contact with a supercooled drop

e. sublimation (or direct deposition of vapor onto a solid nucleant)

While some uncertainty remains, the condensation-freezing process is a principal mode of nucleation in the atmosphere. In short, mixed ice nuclei, consisting of mainly hydrophobic composition with some hygroscopic sites are effective in attracting a water film and then initiating freezing. Adsorption nuclei differ in degree of water affinity, usually developing patches of water rather slowly. Immersion nuclei, which trigger the freezing of drops at particular supercooled temperatures, represent another common type of freezing nuclei. Dry contact nuclei, necessarily very small and hydrophobic to avoid building up a water film, appear capable of freezing contacting droplets at relatively warm temperatures. Sublimation nuclei generally are considered to be relatively rare in natural cloud processes, although artificial seeding agents such as silver iodide can act in this manner.

Note that the neutralized cloud particles will be mainly mixed nuclei, consisting of insoluble (Al_2O_3) and soluble (NH_4Cl) components. Thus they have the potential for serving as either condensation-freezing or immersion-freezing IN.

2. Characteristics of an Effective Ice Nucleus

While exceptions can always be cited, a "good" ice nucleus for initiating freezing at a relatively warm supercooled temperature will generally possess most of the following characteristics:

a. a crystal lattice structure somewhat similar to ice (hexagonal symmetry and lattice dimensions)

b. insoluble or only slightly soluble in water

c. a low contact angle with water (not hydrophobic) or, in other words, a strong affinity for attracting and holding water vapor molecules

d. some but not too many hydrophillic (hygroscopic) sites to help attract water vapor

e. a suitable ionic or irregular surface structure for bonding of polar water molecules

Silver iodide, the most commonly used seeding agent, has a hexagonal lattice structure very similar to that of ice (Table IV-1) and fulfills criteria a-c above. Lead iodide (PbI_2), with a reasonably good lattice structure and nucleation threshold of -6^{o} C, is slightly soluble and small particles may dissolve before they have time to nucleate. Note that the alpha form of Al_2O_3 has a reasonably effective temperature threshold of activation (discussed in subsequent section).

Table IV-1 Crystal Structure of Illustrative Compounds (a, c are the basal plane and prism plane molecular distances)

	Crystal Form	a(Å)	c(Å)	Basal Misfit	Prism Misfit	Nucleation Threshold T
Ice	Hex.	4.52	7.36	-	-	-
AgI	Hex.	4.58	7.49	1.4%	1.6%	-4 C
PbI_2	Hex.	4.52	6.86	0.5	3.6	-6
CuS	Hex.	3.80	16.43	2.8	7.1	-7
Al_2O_3 (a)	Hex.	4.76	12.99	5.0	24.2	-8 to -12 C
Fe_3O_4	Cubic					-8
Kaolin	Triclinic					-9
Gypsum	Monoclinic					-16

Conversely, certain organic substances such as metaldehyde have less favorable crystalline structure, but can nucleate at temperatures warmer than AgI. It is believed that some organic IN possess favorable ionic surface properties (item e).

The sizes of crystalline IN strongly influence the temperatures at which they nucleate. For a particle of radius r causing elastic strain E within the ice because of lattice misfit, the critical free energy of ice embryo formation is (after Fletcher, 1962):

$$G^* = \frac{16\pi\sigma ij^3\, g(M, r)}{3[-N_s kT \ln(e_i/e_s)+CE^2]^2}, \qquad (1)$$

where σij is the surface free energy between ice and vapor (sublimation) or ice and liquid (freezing), M = Cos (contact angle), e_s is saturation vapor pressure over ice, and e_i the ambient (or liquid) vapor pressure. The strong effects of particle size and contact angle M (water attracting ability) are illustrated in Figure IV-1 for liquid freezing. In short, particles $\geq$ 0.1 μm radius and with M $\gtrsim$ 0.8 should be the more

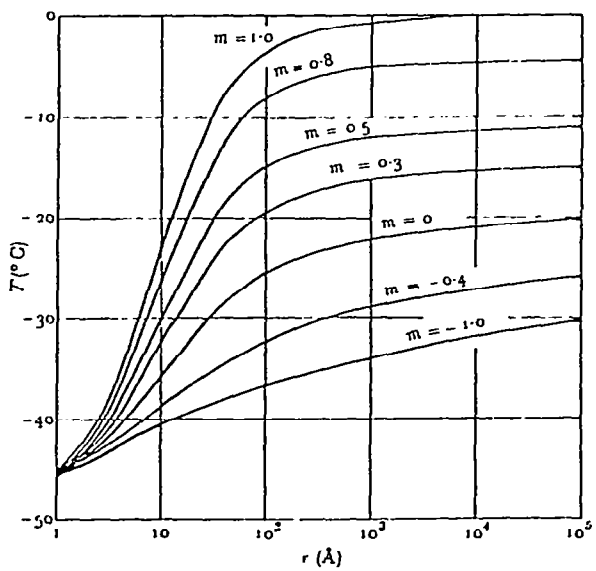

Fig. IV-1. Temperature T at which a spherical particle of radius r and surface parameter m will nucleate an ice-crystal from water in one second by freezing.

effective ice nuclei. (Note that AgI has a contact angle of about 20^{o}, M = 0.94; AgI smoke particle sizes are mainly between .01 and 0.1 μm.)

3. Natural IN Concentrations and Sources

While condensation nuclei are plentiful in the atmosphere, particularly over continents and at mid-latitudes, ice nuclei are scarce. The well-quoted global concentration of IN is 1 l^{-1} at -20^{o} C (some 6 orders of magnitude less plentiful than cloud condensation nuclei). For a $4-5^{o}$ C temperature warming, there is an approximate order of magnitude decline in activated ice nuclei. The average concentration of IN as a function of temperature can be estimated from the empirical function of Fletcher (1962):

$$IN\ (l^{-1}) = 10^{-5} \exp\ (0.6\ \Delta T) \qquad (2)$$

where ΔT is the degree of supercooling. While order-of-magnitude departures from this expression occur, it typifies measurements of natural IN concentrations made to date.

While the sources of naturally occurring ice nuclei are also tenuous, the activity spectra of several suspected materials have been analyzed. The earth's surface, a logical source, contains clays, silicates, and minerals that can serve as active IN (Schaefer, 1949; Mason and Maybank, 1958; Mason, 1971). Clays have activity thresholds (1 active nucleus in $\sim 10^{4}$) at temperatures as warm as -10^{o} C (common kaolinite at -9^{o} C) and reach high activity levels by -24^{o} C. Certain biological sources of IN are now suspected (Schnell and Vali, 1973), though the evidence is as yet inconclusive.

There is growing evidence for an anthropogenic source of ice nuclei. Steel mill exhaust is well known to be rich in ice nuclei, and may explain the high concentrations of IN sometimes observed downwind of industrial sites like Buffalo, New York (Weickmann, 1974). Of particular relevance to this NASA study, Al_2O_3 particles from coal fired plants are now suspected of being active IN and stimulating light snowfall in winter (Agee, 1971; Kramer et al., 1977).

C. Un-Neutralized Rocket Exhaust Particles - Al_2O_3

1. General Forms

Aluminas (Al_2O_3) take on many crystalline forms as indicated in Table IV-2. Some uncertainties exist as to the dominant crystalline phases and exact surface composition of the Al_2O_3 particles, particularly upon interaction with gaseous and aqueous HCl in the rocket exhaust. Electron diffraction studies by Dobbins and Strand (1970) of laboratory findings indicated that the larger exhaust particles (>0.2 to 1 μm) were presumably alpha-alumina while the smaller (more numerous) submicron particles were metastable gamma-alumina. Such was suspected by NASA-Langley investigators (Cofer and Pellett, undated). One might expect the alpha form, with its hexagonal symmetry and lattice constants (Tables IV-1 and 2) to be the more active ice nucleants of the aluminas; experimental confirmation is lacking.

The slower particle cooling rate in the actual exhaust plume of a large rocket may significantly increase the percentage of the alpha form. Varsi (1976) reported mostly alpha phase particles in the 0.1 μm size range, in contrast to earlier JPL sparse measurements at lower altitudes suggesting the gamma form.

Table IV-2

Crystal Structure and Density of Aluminas

Phase	Formula	Crystal System	Space Group	Molecules per Unit Cell	Unit Axis Lengths, Å				Measured Density g/ml	Reference
					a	b	c	Angle		
Molten									2.5	Wartenberg (1936)
Alpha Trihydrate	$Al_2O_3 \cdot 3H_2O$	Monoclinic	C_{2h}^5	4	8.62	5.06	9.70	85°26'	2.42①	Megaw (1934)
Beta Trihydrate	$Al_2O_3 \cdot 3H_2O$	Monoclinic	C_{2h}^5	2	4.72	8.68	5.06	90°11'	2.53①	Unmack
Alpha Monohydrate	$Al_2O_3 \cdot H_2O$	Orthorhombic	D_{2h}^{17}	2	2.868	12.227	3.700	.....	3.01①	Swanson and Fuyat
Beta Monohydrate	$Al_2O_3 \cdot H_2O$	Orthorhombic	D_{2h}^{16}	2	4.396	9.426	2.844	.....	3.44①	Swanson and Fuyat
Alpha	Al_2O_3	Hexagonal②	D_{3d}^6	2	4.758	.....	12.991	.....	3.98①	Swanson and Fuyat
Sodium Beta	$Na_2O \cdot 11Al_2O_3$	Hexagonal	D_{6h}^4	1	5.58	.....	22.45	.....	3.24	Beevers and Brohult
Potassium Beta	$K_2O \cdot 11Al_2O_3$	Hexagonal	D_{6h}^4	1	5.58	.....	22.67	.....	3.30	Beevers and Brohult
Magnesium Beta	$MgO \cdot 11Al_2O_3$	Hexagonal	D_{6h}^4	1	5.56	.....	22.55	.....	.....	Bragg
Calcium Beta	$CaO \cdot 6Al_2O_3$	Hexagonal	D_{6h}^4	2	5.54	.....	21.83	.....	.....	Lägerqvist
Strontium Beta	$SrO \cdot 6Al_2O_3$	Hexagonal	D_{6h}^4	2	5.56	.....	21.95	.....	.....	Lägerqvist
Barium Beta	$BaO \cdot 6Al_2O_3$	Hexagonal	D_{6h}^4	2	5.58	.....	22.67	.....	3.69①	Adelskôld
Lithium Zeta	$Li_2O \cdot 5Al_2O_3$	Cubic	O_h^7	2	7.90	.....	.....	.....	3.61	Kordes, Braun
Gamma	Nearly Anhydrous Al_2O_3	Cubic	....	..	....	.....	.....	.....	(3.2)①	Ginsberg
Delta		Orthorhombic	....	12	4.25	12.75	10.21	.....	(3.2)①	Stumpf
Delta (Rooksby)		Tetragonal	....	..	7.96	.....	23.4	.....	.....	Rooymans
Eta		Cubic (Spinel)	O_h^7	10	7.90	.....	.....	.....	2.5–3.6①	Stumpf
Theta②		Monoclinic	C_{2h}^3	4	5.63	2.95	11.86	103°42'	3.56①	Kohn
Iota		Orthorhombic	....	4	7.73	7.78	2.92	.....	3.71①	Stumpf
Kappa		Orthorhombic	....	32	8.49	12.73	13.39	.....	3.1–3.3①	Stumpf
Chi		Cubic (Not spinel)	....	10	7.95	.....	.....	.....	(3.0)①	Stumpf

①Anhydrous ②Rhombohedral ③Roth ④Fricke and Severin
⑤Dana ⑥Seemann ⑦Toropov ⑧Estimated ⑨Thibon

(Alcoa Research Laboratories Data)

Whatever the crystalline form, the aluminas' ice nucleating capability is also dependent on its solubility and HCl adsorption characteristics. Bailey and Wightman (1976) conducted such experiments for α and γ aluminas under a NASA-Langley grant, and some of their results are summarized in Tables IV-3 and 4. Some of the relevant conclusions from these tables and their work are as follows:

a. Neither alumina form is very soluble in water, but they are more soluble in HCl, particularly gamma Al_2O_3.

b. Water adsorption is of a reversible physical nature, while HCl adsorption is mainly a non-reversible chemisorption process.

c. The site for HCl adsorption on alumina is a surface aluminum ion, and for water adsorption two oxygen ions with hydrogen bonding.

d. Alpha alumina absorbs more HCl per unit area than gamma alumina; but on a mass basis gamma alumina has a greater adsorption capacity for HCl because of its greater surface area (Table IV-4).

e. Some 6 probable chemical reactions were given indicating the complexity of the $Al_2O_3 \cdot HCl \cdot H_2O$ system.

Cofer and Pellett (1978) indicated that several metastable (theta, delta, gamma) and stable alpha forms "chemisorb gaseous HCl, either dry or moist, to yield significant coverage of the surface by soluble chloride." Thus for reasons of solubility, lattice structure, and HCl adsorption cited above, one might expect alpha Al_2O_3 to be a more effective ice nucleant than the gamma form. Another suspected reactant - Gibbsite $[Al_2(OH)_6]$ - is also an effective IN at T = -11 C (Mason, 1971). The $HCl/H_2O/Al_2O_3$ system in the rocket exhaust is very complex (see Cofer and Pellett, 1978) and nucleation properties of resultant aerosols are not yet well known.

Table IV-3 Solubility of Alpha and Gamma Al_2O_3 in Water and in 0.1 N HCl*

Solution	Alumina Type	Average Aluminum Concentrations (ppm)
H_2O	Alpha α	0.3
H_2O	Gamma γ	0.9
HCl	Alpha	3.9
HCl	Gamma	62.0

Table IV-4 Cross-Sectional Areas of HCl and Water Adsorbed on α and γ Al_2O_3 *

Substance Adsorbed	Alumina Type	Outgas Temp.	Ave. Area Coverage on Al_2O_3 ($Å^2$/molecule)	HCl Surface Area (M^2/g)
H_2O	Alpha	80-400°C	12.4	
H_2O	Gamma	80-400	14.6	
HCl	Alpha	80-400	17.5	7.9
HCl	Gamma	80-200	33.4	48.2

*From Bailey and Wightman (1976)

2. Ice Nucleating Activity of Al_2O_3 Forms

The threshold temperature at which Al_2O_3 acts as an ice nucleus depends on the level of activity (% of total aerosol) tested for and somewhat the type of cold chamber employed. Table IV-5 presents virtually all the earlier tests reported in the literature that we are aware of (alpha form specified or presumed).

Table IV-5 Al_2O_3 Threshold Nucleation Temperatures

	Temp.
Mason and Van den Heuvel (1959)	
a. 1 in 10^4 activity (M)*	-12°C
b. 1 in 10^5 activity (D)*	- 8
c. On droplet surfaces	- 6
Fukuta (1958) 1 in 10^5 (M)	- 6.5
Serpolay (1968) (M)	-10
Sano et al. (1960) (D)	-12

*(M) - Mixing chamber; (D) - Diffusion chamber

Significant nucleation in clouds would probably require activation levels no less than 1 in 10^4 particles, such that a practical threshold in the neighborhood of T = -12° C appears reasonable. This is indirectly supported by recent field observations of induced snowfall downwind of coal-burning power plants in supercooled clouds $\leq$ -12° C (Kramer et al., 1977). Al_2O_3 was the suspected IN agent here and in a previously reported urban induced snowfall (Agee, 1971).

As reported previously (PS-V), the Naval Weapons Center at China Lake ran some laboratory Al_2O_3 nucleation tests for our task groups (data in Table IV-6) and additional tests for their research purposes.

Table IV-6 Ice Nuclei Output of Al_2O_3 (Naval Weapons Center)

Temp.	Output per gram
-14 to -15° C	$1\text{-}2 \times 10^{8}\ g^{-1}$
-20	$\sim 1 \times 10^{10}\ g^{-1}$

In one test involving the rocket propellant (18% Al plus an NH_4ClO_4 oxidizer), x-ray analysis indicated that the major alumina form was eta (Finnegan, private communication).

More recent tests conducted by the NWC and reported at the NASA-NOAA meeting at Estes Park, Colorado (Reinking, 1977) indicated that "plain" aluminum (Al-double base propellant devoid of an HCl byproduct) was an order of magnitude more effective as an IN agent than Al-NH_4ClO_4 at the warmer temperatures of -13 to -15 C; at colder temperatures approaching -20 C, respective results were similar. While such laboratory experiments obviously are subject to variation and may depart considerably from actual rocket burn conditions, they at least provide insights for preliminary assessments.

Because of Al_2O_3 solubility with time and the previously described evidance that metastable forms or chlorided stable forms may dominate (submicron size particles), the weather modification analysis was tentatively based on nucleation values 1-10% of those shown in Table IV-6. It was also stated (PS-V) that "the exact percentage (of effective IN) is highly important and must be determined accurately." In this context, the following cold cloud implications were previously reached (PS-V-17):

"In summary, on the assumption that 1-10% of the space shuttle rocket Al_2O_3 (and/or entrained earth material in the SGC) are effective ice nuclei with a threshold of -14° C:

a. The potential for inadvertent weather modification (IWM) exists.

b. The effect could be that of altering precipitation amounts, hail, and severe winds; in the uncontrolled situation involved, the net result could be either an increase or decrease.

c. Concerning rainfall it is more likely that such an effect would lead to an increase of modest amount and be of modest significance (based on non-orographic cloud seeding conducted to date); because of the crucial timing and sizable seeding required to modify hail development, significant alteration appears more improbable, though possible by chance.

d. Seeding effects are more likely in summer when strong convection can carry particulates upward to colder IN activation levels.

e. The levels most conducive to ice nuclei crystallization are approximately 5-10 km, the higher end of the range in summer and the lower levels in winter.

f. Any IWM is more probable at shorter times ($\leq$T + 3 hours), owing to higher IN concentrations, with the impact diminishing with time. Concentrations may still be somewhat above background after one day in continental type clouds but probably not enough so to perturb weather significantly. At 3 days and beyond, IWM is considered highly improbable.

g. Al_2O_3 (IN) released above the SGC in the 2-12 km altitude range are less concentrated by about an order of magnitude. Some near-term short-range IWM could result if susceptible clouds are present.

h. Because of washout and dilution effects of the SGC with time (particle residence time of a few days in the lower troposphere), no cumulative IWM effect from the projected 40 launches per year is likely. As an added precaution, spacing of rocket launches by several days is recommended."

Pending the recommended acquisition of more IN concentration measurements in Cape Canaveral rocket plumes, this assessment is still considered valid. In fact, aircraft penetrations of the plume from a static rocket burn at Edwards AFB by NWC (Reinking, 1977) could be construed to give added support to our assessment. With a Mee counter they measured IN concentrations of 850 l^{-1} maximum (150 l^{-1} average) at T = -25 C; such preliminary values are not too dissimilar from (actually less than) our lower 1% activity values, adjusting for time and temperature differences.* In another static Thiokol

* It was recently reported by NWC that the Mee Counter may underestimate IN concentrations in such burns by a factor of perhaps 10^3 (Hindman et al., 1978).

rocket burn, NCAR measured 120 IN l^{-1} at -20C on a membrane filter (G. Langer, private communication). IN concentrations on filters exposed in two actual Titan exhaust clouds at Cape Canaveral (SUNYA, NOAA) indicated substantially lower values (Lala, 1978[1]). Research is continuing in order to obtain reliable IN measurements in the laboratory and particularly in actual launch clouds and to resolve: a) apparent sizable aerosol property differences associated with the burn conditions of each environment, and b) differences in response of IN measuring apparatus.

D. Neutralized Rocket Cloud - Ice Nucleation Implications

The NASA goal of cloud neutralization is to reduce the deleterious effects of acidic particles and droplets. If successful, the HCl would be replaced by NH_4Cl. As stated in Chapter III, the probable end result, whether by diffusion or by coagulation process, will be Al_2O_3 particles combined with varying amounts of NH_4Cl. (In actuality, neutralization would not be 100% effective leading to some other particle types.)

No known information exists on the ice activation capability of those specific alumina-salt complexes. Clearly specific measurements and more research should be a high priority NASA item if the cloud neutralization concept is pursued. In the interim some logical deductions and qualified projects of related work can be presented.

1. Potential Ice Nucleus Types

From the discussion of types of ice nuclei in the atmosphere (Section A.2), we may conclude that the salt-complexed Al_2O_3 particles stand the best chance of acting as immersion ice nuclei. Considerable

[1]Lala, G., 1978: Measurements of Ice Nucleus Concentrations in Titan Rocket Exhaust Clouds. Final Report under NASA Contract NAS9-15538, 1978, 48 pp. (to be published as a NASA Contractor Report, 1979.) See also Hindman et al. reference.

salt should attach to each Al_2O_3 particle such that in any cloud forming situation, the mixed nuclei will act first as very effective condensation nuclei. The result likely will be sizable droplets with an imbedded insoluble Al_2O_3 particle that may subsequently initiate freezing if the drop supercools sufficiently.

The ample salt component (note soluble to insoluble volume ratios of Chapter III) would tend to lessen the likelihood of the particles acting as ice nuclei by

a) adsorption

b) condensation-freezing

c) contact and

d) sublimation.

In general, the mass of hygroscopic material would quickly attract too much water for the above processes to be operative. Only in the case of giant nuclei (> about 10 μm dia) where the salt volume percentage is $\leq$1%, might the film of water be sufficiently thin initially for condensation-freezing to take place; such events would be rare because of the low particle concentrations involved.

Table IV-7 presents for the determined aerosol distribution the following pertinent characteristics: percentage of soluble to insoluble material comprising the dry aerosol; equivalent diameter of the soluble (salt) component; approximate size of the condensation drop when and if it dilutes the soluble NH_4Cl to 1/1000 of its saturated concentration (molality $\tilde{\sim}6$); estimated time to reach this dilute drop concentration in a cloud at supersaturation S = 0.5%, T = -20C, and P = 500 mb. D_2 is simply given by:

$$D_2 = D_1 \text{ (Volume Ratio)}^{1/3}. \qquad (3)$$

Table IV-7 Mixed Aerosol Particles in Neutralized Cloud and Subsequent Droplet Growth Sizes and Times

Original Particle Dia. D_1	% Sol./Insol. Volume[1]	Equiv. Size D_2 of Soluble Component	Drop Size 1000 Dilution-D_3	∿Growth Time[2] to D_3
0.2 μm	99+%	∿0.2 μm	3.4 μm	14 sec
0.3	92	0.29	4.9	30
0.5	68	0.44	7.4	65
1.0	35	0.70	12	3.0 min
2.0	15	1.1	18	6.7
5.0	4.0	1.7	28	16
10	1.2	2.3	39	30
20	0.35	3.0	50	44

(1) Average volume ratios from Chapter III

(2) Approximate time for drop to grow from D_1 to D_3 at cloud S = 0.5%, T = -20, P = 500 mb

The approximate time for droplet growth to D_3 is:

$$t = \frac{D_3^2 - D_1^2}{8GS} \tag{4}$$

where G is a thermodynamic constant for given temperature and pressure conditions. This is a simplified form of the general drop growth equation

$$r\, dr/dt = G(S - a/r + b/r^3), \tag{5}$$

considered adequate here for purposes of illustration.

For example a 0.5 μm dia. mixed particle in the neutralized cloud would be 68% soluble (NH_4Cl) with an equivalent diameter of 0.44 μm. For a 1000 factor dilution by water of the hygroscopic material, the required drop size would be approximately 7 μm and take about 1 min. to grow to such a size under illustrative ambient cloud conditions. In short, drops can form readily on these nuclei with residual insoluble Al_2O_3 particles contained within them. These immersion IN can initiate drop freezing if sufficient supercooling ensues.

Particles less than about 0.3 μm possess so little insoluble material (Al_2O_3) that these minute aerosols may be considered prohibitively small for effective ice nucleation (note Fig. IV-1 on particle size dependence).

2. Immersion Nuclei Activation - IN

Hygroscopic particles go into solution and do not serve as ice nuclei (Hosler, 1951). In fact, in highly concentrated solutions they can depress the freezing point to temperatures colder than -50 C. As the solution dilutes, any immersed IN will initiate freezing at progressively "warmer" temperatures. Hoffer (1961) studied the freezing

temperatures of 100-200 μm dia. drops containing soluble salts (mixed $MgCl_2$ + Na_2SO_4) and insoluble ice nuclei. He measured the temperature at which 50% of the drops froze (median T) for different salt solution concentrations and IN. Table IV-8 typifies some of his results.

Table IV-8 Median Freezing Temperature for 100-120 μm Drops Formed on Mixed Nuclei (Hoffer, 1961)

($MgCl_2$+Na_2SO_4)	- Ice Nuclei -			
Solution Concentration	Illite	Montmorillonite	Kaolinite	AgI
Saturated	<-45°C	<-45°C	<-45°C	<-45°C
1/10 Sat.	-31.0	-30.0	-39.0	-19.0
1/100 Sat.	-28.0	-27.0	-35.0	-18.5
1/1000 Sat.	-27.0	-25.0	-34.5	-16.5
Pure Water	-24.0	-24.0	-32.5	-16.0

For dilute drops of 1/1000 saturated solutions, the immersed ice nuclei caused freezing within 0.5-3° C of the temperature for pure water. Hence the 1000 factor dilution was used in the calculations of the previous Table IV-7. The highest temperatures at which drops froze in the pure water case was some 6-12° C warmer than the median temperatures shown. Also of note, there was only a weak dependence of freezing on drop size over the range 50-200 μm dia.

Of considerable importance, this and other studies (Mason, 1971) suggest that immersion freezing is often less effective than say condensation-freezing in a cold chamber. Hoffer's (1961) data suggested 8-10° C differences in respective threshold nucleation values; Mason and Van den Heuvel (1959) reported little difference between nucleation modes for active IN such as AgI, but metallic oxides were much less

effective when immersed in a water drop than when tested as cloud chamber nuclei. Hence, a reasonable assumption is that the effective freezing temperature of immersed Al_2O_3 particles will be depressed, perhaps by a nominal 5-8° C.

3. Assumptions

It is quite appropriate to list the assumptions implicit or explicitly stated in the discussion thus far. Thereafter, the ice nuclei potential of aluminas and estimated concentrations in the neutralized rocket cloud can be better evaluated. The principal assumptions are:

a. The particle number concentration is governed by the distribution of Al_2O_3 particles (Chapter III).

b. All the particles are of mixed composition - Al_2O_3 plus NH_4Cl with the chemistry of each specie being preserved.

c. Ice nuclei are predominantly of the immersion-freezing type; effective Al_2O_3 particles act as IN when the attached salts dilute sufficiently in growing cloud drops.

d. Immersion nuclei (metallic oxides) are about 5-8° C less effective than drop forming ice nuclei (e.g. condensation-freezing nuclei).

e. Initial aerosol particles <0.3 μm dia. have too much hygroscopic material and too little Al_2O_3 to serve as effective IN.

f. The cloud is completely neutralized in the desired fashion (not realistic but a limiting condition).

4. Ice Nuclei Concentrations in the Neutralized Cloud

Estimates of IN concentrations can be approached in several ways. First using the mass budget approach described previously (PS-V), the concentration of IN can be calculated from:

$$IN = \frac{\text{Mass of } Al_2O_3 \times \text{Activity } (g^{-1}) \times \text{Efficiency Factor}}{\text{Cloud Volume}} \quad (6)$$

The efficiency factor (EF) is some uncertain value reflecting differences in actual rocket-cloud effective IN and that determined under laboratory conditions at very short times. An EF of 1-10% was hypothesized earlier for reasons stated in section C.2. Because of the elimination or reduction of HCl in the neutralized cloud, the dissolution of Al_2O_3 and formation of less-active aluminas presumably should diminish. Therefore, a tentative EF of 10% might be a more appropriate first approximation for this situation. Al_2O_3 activity values (cloud chamber - Naval Weapons Center) were listed in Table IV-6.

Thus, for example, at (T + 3) hours when the cloud volume is 3×10^2 km^3 and for T = -14° C (to circa -20 C) the IN concentration is estimated to be:

$$IN = \frac{(6.8 \times 10^7 \text{ g}) \ (10^8 \text{ g}^{-1}) \ (0.10)}{3 \times 10^{14} \text{ l}} \approx 2.3 \text{ l}^{-1}$$

The span of temperature is in recognition of the fact that immersion nuclei are reportedly less effective than cloud chamber nuclei (conditions of activity tests).

Proceeding as a function of time, expanding cloud volume, and temperature, Table IV-9 values were obtained. Depending on the precise corresponding temperature it is evident that for at least the first day after launch IN concentrations are well above natural background (e.g. 1.6 l^{-1} at -20° C; 30 l^{-1} at -25°C, based on Fletcher equation 2).

Table IV-9 Ice Nuclei Concentrations from Al_2O_3 - 10% Active
(Mass Budget Approach)

Time	Cloud Volume	IN Conc. (-14 to -20° C)	IN Conc. (-20 to -25° C)
(T+3 hrs)	$3x10^2$ km^3	2.3 l^{-1}	230 l^{-1}
(T+1 day)	$2.4x10^3$	0.3	30
(T+3 days)	$7.2x10^3$	0.1	10
(T+5 days)	$1.2x10^4$	0.06	6
(T+7 days)	$1.7x10^4$	0.04	4

As a second approach, we may consider the particle-size distribution of the total neutralized cloud (Chapter III, Figure III-4). All particles $\geq$0.3 μm dia. presumably are capable of serving as ice nuclei. From the discussion thus far of immersion ice nuclei in general and Al_2O_3 properties in particular, it is not too unreasonable to approximate the particle activation threshold level vs. temperature as follows: 1 IN/10^5 at T$\tilde{\sim}$-15° C, and 1/10^4 at T$\tilde{\sim}$-20° C. Using these values and the total aerosol concentration, the concentration of IN in the neutralized cloud can again be roughly estimated (Table IV-10). The results are reasonably consistent with the mass budget estimates of Table IV-9. It is evident that IN concentrations might remain well above background for periods of perhaps 3 days. Concentrations at temperatures colder than -20 to -25° C would probably not increase substantially, as metallic oxide IN activity is known to level off at such temperatures (Mason, 1971). In any event, the concentrations of potential IN generated are substantial and appear capable of influencing cloud behavior for more than a day.

Table IV-10 Al_2O_3 IN Concentrations (Particle-Size Distributions Approach)

Time	Total Aerosol Conc. $\geq$0.3 μm	IN Conc. ($1/10^5 \equiv -15^o$ C)	IN Conc. ($1/10^4 \equiv -20^o$ C)
(T+3 hrs)	$3x10^6$ l^{-1}	30 l^{-1}	300 l^{-1}
(T+1 day)	$3x10^5$	3	30
(T+3 days)	$1.3x10^5$	1	15
(T+5 days)	$7.7x10^4$	0.8	8
(T+7 days)	$5.5x10^4$	0.5	5

E. Cloud Seeding Implications

Clearly the potential for cold cloud seeding exists. The threat is greatest within several hours of launch but still persists for 1-3 days (Tables IV-9 and 10). Beyond that time, background IN concentrations should be approached via cloud expansion and particle washout and fallout.

Planned weather modification (Chapter II) often involves conparable or lesser IN concentrations, e.g. the addition of ~10 IN l^{-1} for precipitation enhancement and one to several 100 l^{-1} for thunderstorm modification.

By contrast with the regular rocket-exhaust cloud, the neutralized cloud would appear to have 4 main cold-cloud seeding effects:

1. The predominant IN are more apt to be immersion nuclei than condensation-freezing nuclei.
2. The nucleation activity of such particles is thereby shifted to colder temperatures.
3. The above beneficial effect is probably outweighed by the greater concentrations of IN produced.

4. A greater abundance of IN probably would result because fewer of the Al_2O_3 particles released should be de-activated by dissolution in HCl or conversion to less active IN alumina forms (assumption).

Significant Al_2O_3 activation at T<-15 to -20° C implies relatively deep clouds extending to altitudes above about 7 km in summer and 6 km in winter (standard sub-tropical lapse-rate conditions). During the summer rainy season in Florida, convective updrafts are strong and readily capable of carrying rocket-exhaust nuclei to effective levels (7-10 km); in winter less frequent tall cumuli and thunderstorms can occasionally transport material to an effective region of 6-9 km. Above these levels (∿-35° C), there are typically far higher concentrations of natural IN than can be produced artificially.

The significance of enhanced IN concentrations is difficult to assess. Exact cloud seeding effectiveness has been and continues to be a subject of debate. In broad terms, given suitable environmental conditions and substantial supercooled clouds, IN seeding of the order of 10 l^{-1} is believed by some to increase precipitation by perhaps 10-20%. More massive seeding (circa several 100 l^{-1}) in thunderstorm airmasses reportedly can diminish damaging hailfall (Sulakvelidze et al., 1967; Burtsev et al., 1973; Miller et al., 1974). These two weather modification effects--potential rainmaking and/or thunderstorm diminution--are most relevant to Florida. Neither are necessarily detrimental, especially the latter. Alternately, seeding at an inopportune time or with too many nuclei can have the effect of suppressing cloud development and rainfall (Braham, 1966).

In summary, we may list the most susceptible inadvertent weather modification conditions in Florida as follows:

a. short time periods after launch (with potential effects out to 1 to 3 days)

b. when thunderstorms or large cyclonic systems are in the vicinity of the rocket plume trajectory

c. the summer season

d. when winds are calm or easterly (on shore component)

e. unstable troposphere (thermal structure) with strong updrafts $\gtrsim 5$ m sec^{-1}

f. low natural ice concentrations as typified by continental air-mass trajectories.

Indications are that neutralization of the rocket cloud could aggravate the potential for inadvertent weather modification.

It should also be noted that an equivalent amount ($\sim 7 \times 10^7$ g) of Al_2O_3 is released in the troposphere (2-10 km altitude) above the neutralized zone. While much less concentrated because of the greater column depth and stronger dispersive winds, these potential IN particles may not be totally insignificant in cases of deep convection and at short time intervals from launch.

F. Recommendations - Neutralized Cloud Concept

It is advised that further NASA effort be conducted to provide more information for refining certain ice phase assunptions necessary in this evaluation. These recommendations concerning the neutralized rocket-cloud concept are as follows:

a. Measure the concentration of active Al_2O_3 generated in the exhaust plume with an automatic IN (ice particle) counter and with membrane filters.

b. Perform additional laboratory ice-nuclei activation spectra of Al_2O_3

   1. with the identical SRM propellant mix
   2. with interacting NH_4Cl
   3. with the particles immersed in liquid drops as well as dispersed in a cloud chamber
   4. as a function of aerosol aging.

c. Establish a ground network to evaluate possible downwind changes in precipitation (storm) patterns and to collect rain water for chemical analysis.

d. In view of the difficult logistics of cloud neutralization, the limited altitude zone involved, and the potentially adverse meteorological results, the neutralization concept might well be re-evaluated.

References

Agee, E., 1971: An artificially induced local snowstorm. Bull. Amer. Meteor. Soc., 52, 557.

Bailey, R. R., and Wightman, James P.: Interaction of Hydrogen Chloride With Alumina. NASA CR-2929, 1978.

Bradley, J., 1972: The climate of Florida, Climates of the States, Vol. 1, NOAA, U.S. Dept. of Commerce, 45-71.

Braham, R., 1966: Project Whitetop: a convective cloud randomization seeding project, Dept. Geophys. Sci., Univ. of Chicago.

Burtsev, I., Gaivoronsky, I., and A. Kartsivadze, 1973: Recent advances in studies of the physical processes producing hail, and results of anti-hail operations in the USSR, Proc. Intl. Conf. Wea. Mod., Tashkent, WMO, 189-197.

Cofer, W. and G. Pellett: Chemical characteristics and role of Al_2O_3 in SRM exhaust clouds, in Proceedings of the Space Shuttle Environmental Assessment Workshop on Tropospheric Effects, NASA TMX-58199, Feb. 1977, pp. E-5 to E-8.

Cofer, W. and G. Pellett, 1978: Adsorption and chemical reaction of gaseous mixtures of hydrogen chloride and water on aluminum oxide and application to solid-propellant rocket exhaust clouds, NASA Technical Paper 1105.

Dobbins, R. and L. Strand, 1970: A comparison of two methods of measuring particle size of Al_2O_3 produced by a small rocket motor, AIAA J., 8, 1544.

Fletcher, 1962: The Physics of Rainclouds, Cambridge Univ. Press, 390 pp.

Fukuta, N., 1958: Experimental investigations on the ice-forming ability of various chemical substances, J. Meteor., 15, 17.

Hindman, E., Odencrantz, F., and W. Finnegan, 1978: Airborne monitoring of long-lived, anthropogenic aerosol clouds. 71st Annual Meeting of APCA, Houston, Texas, Paper 78-45.8.

Hoffer, T., 1961: A laboratory investigation of droplet freezing. J. Meteor., 18, 766.

Houghton, H., 1950: A preliminary quantitative analysis of precipitation mechanisms. J. Meteor., 7, 363.

Kramer, M., Seymour, D., Smith, M., Reeves, R., and T. Frankenberg, 1977: Snowfall observations from natural-draft cooling tower plumes. Science, 197.

Hindman, E. E., II, et al.: Airborne Measurements of Cloud-Forming Nuclei and Aerosol Particles in Stabilized Ground Clouds Produced by Solid Rocket Booster Firings. Naval Weapons Center Report NWC TM-3589, Naval Weapons Center, China Lake, CA, Oct. 1978, 76 pp.

Mason, B., 1971: The Physics of Clouds, Clarendon Press, 671 pp.

Mason, B. and J. Maybank, 1958: Ice-nucleating properties of some natural mineral dusts. Quart. J. Roy. Met. Soc., 84, 235.

Mason, B. and A. Van Den Heuvel, 1959: The properties and behavior of some artificial ice nuclei, Proc. Phys. Soc., 74, 744.

Miller, J., Boyd, E., and R. Schleusener, 1974: Hail suppression data from western North Dakota, 1969-72, Proc. 4th Conf. Wea. Mod., Fort Lauderdale, AMS, 139.

Mohnen, V. et al., 1976: Position paper on the potential of inadvertent weather modification of the Florida peninsula resulting from the stabilized ground cloud. Final Report for period March-August, 1976, under NASA Grant NAS9-14940 000-001, NASA CR-151199, 1976, 201 pp.

Reinking, R., 1977: Meeting Summary-Joint conference on potentials for inadvertent weather modification caused by the ground cloud from space shuttle rocket launches. Estes Park, Colo., NOAA Weather Modification Program Office, Boulder.

Sano, I., Fujicani, Y., and Y. Maena, 1960: The ice-nucleating property of some substances and its dependence on particle size. Mem. Mar. Obs. Kobe., 14, 1.

Schaefer, V., 1949: The formation of ice crystals in the laboratory and the atmosphere. Chem. Rev., 44, 291.

Schnell, R. and G. Vali, 1973: World-wide source of leaf-derived freezing nuclei. Nature, 246, 212.

Serpolay, R., 1958: L'activité glacogens des aerosols d'oxydes métalliques. Bull. Obs. Puy de Dôme, 81.

Sulakvelidze, G., Bibilashvili, N., and V. Lapcheva, 1967: Formation of precipitation and modification of hail processes. Israel Sci. Translations (NSF), 208 pp.

Varsi, G., 1976: Particulate measurements. Presentation at Space Shuttle Environmental Workshop on Stratospheric Effects, March 24-25, 1976.

Weickmann, H., 1974: The mitigation of Great Lakes snow. In Weather and Climate Modification (ed. W. Hess), Wiley and Sons, 318.

Woodley, W. and R. Sax, 1976: The Florida area cumulus experiment: rationale, design, procedures, results, and future course. NOAA Tech. Rep. ERL-354-WMPO-6, Boulder, Colo., 204 pp.

Chapter V. Warm Clouds

A. Basic Assumptions

The discussion given in this chapter refers almost entirely to convective clouds, which are by far the most important precipitation-forming clouds in the Florida region. In "warm" clouds (i.e., those in which ice plays no significant role), precipitation can form as a result of the coalescence of droplets of varying sizes and fall speeds. The time taken to form raindrops naturally depends very strongly on the dispersion of droplet sizes. It is thought that two distinct mechanisms may contribute to this process:

(a) Especially in typical Florida "maritime" clouds (in which the droplet concentration (n) is not too large), coalescence can extend the droplet spectrum to larger and larger sizes, forming droplets which become the embryos of raindrops. The speed of this process depends very strongly on the size of the growing droplets, whose mass rate of growth increases very roughly as r^4. In suitable "maritime" cloud circumstances, the evolution of the spectrum can be quite rapid. In "continental" clouds where droplet concentrations are quite high, the droplets are relatively small and coalescence is usually too slow to be of importance.

(b) If very large hygroscopic particles (giant nuclei) are present, they may form (purely by condensation) droplets which are large enough to form raindrop embryos, growing rapidly by coalescence with much smaller droplets.

These processes are complex and variable, and it is possible only to make use of simple generalized criteria to distinguish those conditions in which the SGC aerosol might be expected to exert a significant influence on them, and hence affect the formation of rain in warm clouds in the Florida area ("warm rain").

The criteria which will be used here are:

(a) If the total concentration of droplets in a convective cloud (n) exceeds 10^3 cm^{-3}, it is assumed that the broadening of the droplet spectrum which can result from coalescence will proceed so slowly that the contribution of this process to the formation of warm rain will be significantly affected.

(b) If the concentration of giant nuclei is such that they give rise to droplets of radius $\geq$25 μm in concentrations exceeding 1 per liter, it is assumed that this will result in significantly accelerating the formation of warm rain.

The first of these criteria is discussed in Section B. Since, apart from the nature of the aerosol, the major factor determining n is the updraft speed at cloud base (V), it is necessary to investigate this question for a range of representative values of V. As will be seen below, this criterion is not met by natural clouds. The second criterion is discussed in Section C. In this case, the major factor determining whether a particular giant nucleus will form a droplet

of radius (r) exceeding 25 μm is the time it spends in the cloud growing by condensation. This time is likely to be rather variable. The average life of cumuli is of the order of 10^3 sec. The smaller short-lived clouds would not be expected to form rain. On the other hand, somewhat larger clouds capable of forming warm rain probably have lifetimes of the order 2 to $3x10^3$ sec.

The growth by coalescence of a droplet from r = 25 μm to raindrop size itself requires some time, and if a significant effect on rainfall is to result, some time must also be allowed for the resulting rain shower to continue. Thus, it would appear to be reasonable to define an "effective giant nucleus" as one which, if immersed in a cumulus for a time of order 10^3 sec, will form by condensation a droplet larger than r = 25 μm. Criterion (b) is then considered to be satisfied if the concentration of such particles exceeds one per liter.

B. Droplet Concentrations in Convective Clouds

The total mass of the exhaust products which form the SGC is of the order of 100 tons. By T+3 hours, this material has mixed with about $3x10^8$ tons of ambient air. Thus, although the aerosol content of the SGC is markedly different from that of the surrounding air, as described in Chapter III, at T+3 hours its original temperature excess has vanished, and in regard to properties such as mixing ratio and relative humidity, it has become indistinguishable from its surroundings.

The concentration of droplets formed in a convective cloud is determined chiefly by two factors: the spectrum of critical supersaturations (S_c) of the aerosol found in the updraft below cloud base, and the speed of this updraft as it passes through a region some tens of meters deep, just above the condensation level. In this region, the supersaturation of the air rises to a maximum (S_m) and begins to decline; thus those CCN for which $S_c < S_m$ form unstably growing cloud droplets, while those for which $S_c > S_m$ remain stable haze droplets (r of order 0.1 μm), and take no part in the formation of rain.

A number of numerical studies have been made of this complex process, for example by Howell (1949), Mordy (1959), Neiburger and Chien (1960), and Fitzgerald (1972). For the present purpose however such a complete treatment would not be appropriate, and a simpler and more general method is needed. One such approach is the very simplified treatment of this problem given by Squires (1958), which indicated that the maximum supersaturation achieved would be proportional to $V^{3/4}\ n^{-1/2}$, where V is the updraft speed and n the concentration of nuclei activated to form cloud drops. A significantly more complete treatment was given by Twomey (1959). This was based on a postulated cumulative distribution of critical supersaturations of the form $N = cS^k$, and led to the result that the concentration of droplets formed (n) is given by:

$$n = h\,\theta^{\frac{k}{(k+2)}}\,c^{\frac{2}{(k+2)}}\,v^{\frac{3k}{2(k+2)}}$$

where h is a numerical factor and θ is a thermodynamic parameter:

$$\theta = Q_1^{3/2}/\rho_L\, G^{3/2}\, Q_2 ,$$

where

$$Q_1 = \frac{M_o L\, g}{c_p\, RT^2} - \frac{M_a\, g}{RT}$$

$$Q_2 \quad \frac{M_o\, L^2}{M_a\, p\, c_p\, T} - \frac{1}{\rho_V}$$

$$G = D\,\rho_V/\rho_L\left(1+\frac{M_o\, L^2\, D\,\rho_V}{k\, RT}\right)$$

The treatment given by Squires may be used with any spectrum of CCN; if applied to one of the form $N = cS^k$ by writing $n = cS_m^k$, it yields an estimate for n which differs from that of Twomey only in that the numerical factor h is 10 to 20% lower, depending on the value of k.

Twomey's formula has been used by several authors to predict cloud droplet concentrations from the S_c spectrum and the updraft speed, V. However, the cumulative distribution of critical supersaturations of the SGC aerosol is not of the form $N = cS^k$, to which this formula applies (see Fig. V-1 below). Therefore the present discussion will be based on the simpler formulation of Squires, in which it is assumed that the droplets are monodisperse, and grow according to the law $r\frac{dr}{dt} = GS$. The conservation of water substance implies that

$dS = Q_1 dz - Q_2 dw$, whence

$$r\frac{dr}{dt} = GQ_1 Vt - \frac{4}{3}\pi GQ_2 \rho_L n r^3$$

where n is the concentration of droplets. (G, Q_1 and Q_2 are as defined above, or in Fletcher, 1962.) S is in absolute units, and Q_1 and Q_2 refer to a unit volume (1 cm^3). The critical phase of cloud formation is typically completed (and S begins to decrease) well before the air has risen 100 m, that is before the pressure of the air sample has decreased by as much as 10 mb. The temperature change is correspondingly small (<1°C). Consequently the functions Q_1, Q_2 and G may be treated as constants, and evaluated at the pressure and temperature occurring when the air reaches saturation (S = 0) (taken here as 900 mb, 10°C). The boundary conditions are conveniently taken as S = 0, r = 0 at t = 0.

Putting

$$r = \alpha^{\frac{1}{4}}\beta^{-\frac{1}{2}}\eta \ , \quad t = \alpha^{-\frac{1}{4}}\beta^{-\frac{1}{2}}\xi$$

where $\alpha = GQ_1 V$, $\beta = \frac{4}{3}\pi GQ_2 \rho_L n$, the equation reduces to:

$$\eta\frac{d\eta}{d\xi} = \xi - \eta^3 \ .$$

S is proportional to $\xi - \eta^3$, and is therefore stationary at the point (ξ_1, η_1), the intersection of the solution curve through the origin with $\xi = (\eta^3 + \frac{1}{3\eta})$. It is found numerically that $\xi_1 = 0.8370$, $\eta_1 = 0.7209$.

Consequently, expressing S_m in absolute units,

$$S_m = (\xi_1 - \eta_1^3)\ \alpha^{\frac{3}{4}}\ \beta^{-\frac{1}{2}}\ G^{-1}$$

i.e. $$S_m^2 = \frac{3}{4\pi}(\xi_1 - \eta_1^3)^2\ \Theta\ V^{\frac{3}{2}}\ n^{-1}$$

or $$nS_m^2 = 2.679 \times 10^{-6}\ V^{\frac{3}{2}} \quad .$$

Thus, for a given value of V, the updraft at cloud base, n and S_m are functionally related. If the corresponding curve is superimposed on a cumulative distribution curve relating the concentration (N(S)) of aerosol particles with critical supersaturations less than S to S, the intersection of the two curves will give an estimate of n, the concentration of cloud droplets formed.

As a result of the mixing of the SGC with ambient air, the aerosol within the diluted SGC consists of two components -- the natural ambient aerosol, and that derived from the exhaust products. Figure III-6 shows that this latter component consists of particles all of which have S_c values less than about 0.043%, or 4.3×10^{-4} absolute. Hence, for values of S exceeding this, the cumulative distribution over land is given by:

$$N(S) = 5913\ S^{0.53} + \frac{2.97 \times 10^4}{H}$$

where H is the time elapsed since launch in hours (see Table III-4 and Fitzgerald's results quoted in Chapter III; note however that here, S is expressed in absolute units).

Over the sea, the corresponding distribution is:

$$N(S) = 2420\ S^{0.46} + \frac{2.97 \times 10^4}{H} \quad ,$$

Figure V-1 includes the S_c distributions over the land at T+3h, T+1d, T+2d, T+3d and T+∞ (the natural distribution), together with four lines representing the relationship between n and S_m for four values of V which correspond to clouds ranging from moderate cumuli to thunderstorms. It is seen that n exceeds 10^3 cm^{-3} for over a day, but falls below this level after two days, except with very strong updrafts. The intersections with the curve marked T+∞ ,which represents the natural distribution, show that in the natural situation, the predicted value of n lies below 10^3 cm^{-3}.

The conclusion may be drawn that for a period of about two days, the concentration of particles in the SGC is high enough to cause some degree of "overseeding" with CCN and so tend to inhibit warm rain forming processes.

C. Giant Nuclei

1. Introduction

As described in Chapter III, following neutralization with NH_3, the particles in the original Al_2O_3 aerosol acquire a coating of NH_4Cl. In the case of the larger Al_2O_3 particles, the mass of NH_4Cl is small compared with that of the Al_2O_3 core, but nevertheless may be sufficient to enable the mixed particle to act as a giant nucleus and form by condensation a droplet with a radius exceeding 25 μm, which could become the

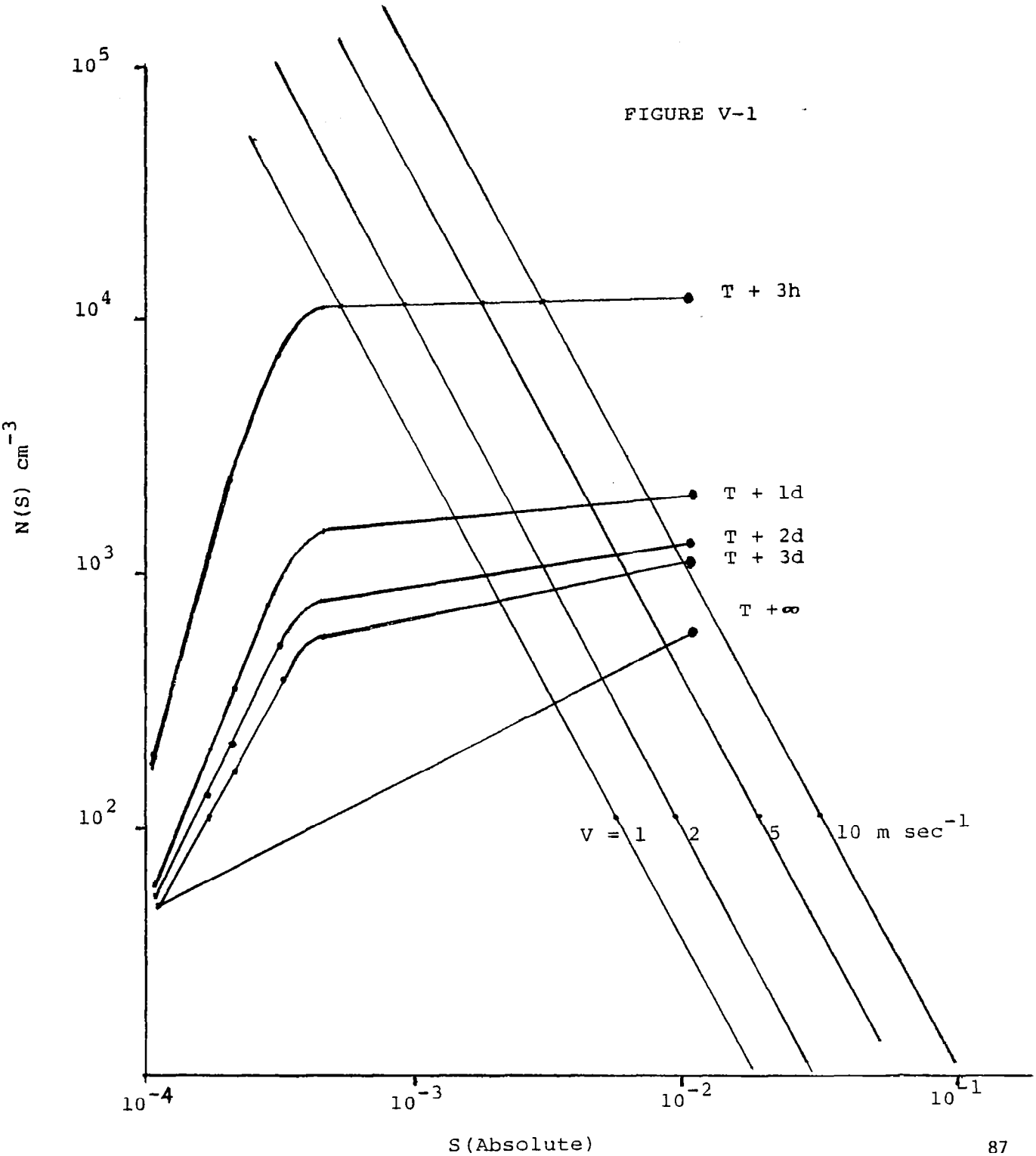
FIGURE V-1
10^5
10^4
10^3
10^2
N(S) cm^{-3}
T + 3h
T + 1d
T + 2d
T + 3d
T + ∞
V = 1
2
5
10 m sec^{-1}
10^{-4}
10^{-3}
10^{-2}
10^{-1}
S(Absolute)

embryo of a raindrop (i.e., act as an "effective giant nucleus" as defined in Section A).

The question of whether such additional giant nuclei would influence warm rain formation must be considered in the context of the fact that in all probability, most of the time, the natural atmosphere in the Florida region already contains more than one particle per liter which qualifies as an "effective giant nucleus." The Florida region is essentially a maritime one, so that it must be expected that in many weather situations, the data of Woodcock (1952) concerning the concentration of giant sea-salt particles over the sea will be representative of the region. Woodcock found that the concentrations in the sub-cloud layer depended on the strength of the surface wind. It is shown (in the Appendix to this section) that a sea salt particle of mass 1.2×10^{-10} g or greater can act as an "effective giant nucleus," and according to Woodcock's data, even with a surface wind as light as force 3, these particles are present in a concentration of about 5 per liter. As will be shown later, the concentration of exhaust-product derived "effective giant nuclei" within the SGC is likely to fall to about 1 per liter at T+3 hours. Therefore, it seems likely that at and beyond T+3 hours these particles are likely to influence rainfall significantly only in rather special weather situations -- for example, if there were a period of very light winds following a general rainfall which

could have scavenged out much of the normal giant nucleus population of the lower atmosphere.

At the beginning of Section B, it was pointed out that by T+3 hours, the original SGC has been greatly diluted by mixing with relatively huge volumes of ambient air. As a result, it soon becomes indistinguishable from its surroundings as regards temperature and humidity although, in terms of the aerosol which it contains, it remains quite distinct for some days. In the case of CCN, as illustrated by the distribution curves in Figure V-1, it is essential to take account of the ambient aerosol which is mixed into the SGC. However, in the case of giant nuclei, it is impracticable to consider the total aerosol within the SGC as being made up of two components (the natural one and that derived from exhaust products) as was done in relation to CCN in Section B. The discussion of this section will therefore be carried out as if the ambient air which mixes into the SGC were devoid of a significant concentration of "effective giant nuclei," on the understanding that such situations are probably rare.

2. Droplet Growth

In the Florida region, the relative humidity near the surface is usually fairly close to the triple point value for the salt under consideration (NH_4Cl). It is therefore to be expected that in the sub-cloud layer the SGC particles will quickly form droplets which consist of a concentrated

solution of NH_4Cl, enclosing an insoluble particle of Al_2O_3. When at some point the SGC becomes involved in an updraft which forms a convective cloud, the relative humidity will begin to increase, and the droplets will grow as discussed in the case of sea salt particles by Keith and Arons (1954). When the air reaches the condensation level, unstably growing droplets will form (in concentrations of order 10^3 cm^{-3}) on natural or SGC cloud condensation nuclei as discussed in Section B, so forming a visible cloud, in which the concentration of droplets is high enough to prevent the relative humidity from rising much beyond 100%.

Within cloud therefore the growth of a droplet formed on a giant nucleus may be evaluated by assuming that the air is close to saturation. Below cloud, however, the situation is more complex, the relative humidity in an updraft increasing with height. However, cloud bases in the Florida region are typically below 1 km, so that with a moderate updraft speed of (say) 2 m sec^{-1}, a particle will spend on the average only 200 to 300 seconds rising to cloud base in the updraft below a convective cloud. Within cloud, as discussed in Section A, the time available for condensational growth would appear to be of order 10^3 sec. Most of the growth therefore occurs in cloud (where the relative humidity is higher and more time is available). Since the estimated growth times are necessarily crude averages, the additional

complexity of evaluating sub-cloud growth does not seem justified, and droplet growth will be evaluated assuming that at cloud base the giant particle consists of an insoluble Al_2O_3 particle surrounded by a layer of saturated solution. As shown in the Appendix to this section, in the case of the larger particles which might act as giant nuclei, the volume of this solution is quite small compared with that of the Al_2O_3 core. Consequently, in discussing droplet growth, it is assumed that the thickness of the layer of NH_4Cl on the surface of the Al_2O_3 particle, and also that of the saturated solution which forms at the triple point, are negligible compared with the radius of the Al_2O_3 core particle (less than 1% in the case discussed in the Appendix).

The vast majority of cloud droplets form on particles with diameters of only a few hundredths of a micron, so that by the time they reach sizes of several microns, the solution of which they consist is extremely dilute. Consequently, the effect of the Raoult vapor pressure lowering on their further growth is negligible. In the case of a giant nucleus, however, the Raoult effect remains appreciable even at $r = 25$ μm. Compared with this effect and with the ambient supersaturation present in the cloud, the Kelvin curvature effect may however be neglected, as will be shown in the Appendix to this section.

On this basis, the droplet growth equation (after Fletcher, 1962) takes on a simplified form:

$$r\frac{dr}{dt} = Gf\left(\frac{b}{r^3 - r_o^3} + S_o\right)$$

where r is the radius of the droplet, r_o that of the insoluble Al_2O_3 particle within it; G is a thermodynamic parameter which for the in-cloud conditions assumed typical here (800 mb, 10°C) has a value of about 9.8×10^{-7} cm^2 sec^{-1}; S_o is the ambient supersaturation within the cloud, taken to be a constant; $b = 4.30 \frac{mi}{M}$ where m is the mass of NH_4Cl present, M its molecular weight (53), and i the van't Hoff factor (2); f is an average value (taken as 1.1) of $f(R_e, P_r')$, the ventilation factor ($f(R_e, P_r')$ increases with droplet size, reaching a value of about 1.14 when r = 30 μm at 800 mb, 10°C).

Preliminary investigations having indicated that the effect of giant nuclei derived from the SGC is of short duration, it is appropriate to investigate first whether or not there exists at T+3 hours a concentration of one particle per liter which is capable of forming a droplet of radius 25 μm after being immersed in a cloud for of order 10^3 sec. Inspection of Fig. III-5 shows that the volume fraction of NH_4Cl in the mixed particles is smaller for larger particles, but that the rate of decrease of this fraction is such that the volume of NH_4Cl present in a particle is an increasing function of its size (as would be expected from their mode of formation). Thus, if it is supposed that two different sized particles have formed droplets of the same radius, the

concentration of the solution formed on the larger one will be the greater, both because the mass of NH_4Cl present is greater, and because the Al_2O_3 core occupies more of the total droplet volume. Therefore, the droplet formed on the larger particle will grow faster, and it may be assumed that in a cloud, larger particles will form larger droplets.

According to Table III-6, at T+3 hours, the total particle concentration in the SGC (ignoring those originating in the ambient air and neglecting the depletion of the giant nucleus population of the SGC by fall-out) is 9.9×10^6 per liter, so that those particles which are present in a normalized concentration of $\frac{1}{9.9 \times 10^6} = 1.01 \times 10^{-7}$ have at that time a concentration of one per liter. Figure III-2 shows that this corresponds to a diameter of about 17.8 μm. If then there is to be a concentration of one per liter of effective giant nuclei present, particles with radii (r_o) down to 8.9 μm must qualify for this role. Figure III-5 shows that if r_o = 8.9 μm, the volume fraction of NH_4Cl is about 4.35×10^{-3}. Taking the density of NH_4Cl as 1.5 g cm^{-3}, as in Chapter III, this implies that $m = 1.93 \times 10^{-11}$ g, so that (with i = 2, M = 53), $b = 3.13 \times 10^{-12}$.

A representative value for S_o may be derived from the quasi-static approximation given by Squires (1952), according to which, above the quite shallow activation region discussed in Section B, the supersaturation (in absolute units) in the bulk of the cloud is about

$$S_o = \frac{1.6\times10^{-6}V + 1.15\times10^{-7}n}{n\bar{r}}$$

where V is the updraft velocity, $\bar{r}$ the mean radius of all the cloud droplets and n their concentration. As shown in Section B(Fig. V-1), at T+3 hours, n is about 10^4 cm^{-3}. Taking as average values an updraft speed of V = 300 cm sec^{-1} and a liquid water content of 10^{-6} g cm^{-3}, it results that $\bar{r}$ = 2.88 μm, $n\bar{r}$ = 2.88 cm cm^{-3}, so that $S_o \approx 5.7\times10^{-4}$ (absolute). It would appear reasonable therefore to compute the growth of droplets formed on giant nuclei for values of S_o of this order.

As mentioned above, the layer of saturated NH_4Cl solution formed initially on the surface of the Al_2O_3 particle is of negligible thickness compared with the radius of the latter (r_o). Therefore it will be assumed that at cloud base (t = o), the droplet has a radius r = r_o. Treating the ventilation factor f as a constant (1.1), the droplet growth equation may be rearranged to read:

$$GfS_o \frac{dt}{dr} = r - \frac{br}{S_o(r^3+\frac{b}{S_o}-r_o^3)} \quad ,$$

so that by quadrature it is found that the time taken for the droplet radius to increase from r_o to r is:

$$t(r,r_o) = \frac{1}{GfS_o}\left[\frac{r^2}{2} - \frac{b}{\ell S_o}\left\{\frac{1}{6}\ln\frac{\ell^3+r^3}{(\ell+r)^3} + \frac{1}{\sqrt{3}}\tan^{-1}\frac{(2r-\ell)}{\ell\sqrt{3}}\right\}\right]_{r=r_o}^{r=r}$$

where $\ell^3 = \frac{b}{S_o} - r_o^3$.

Based on the values quoted above ($r = 25$ μm, $r_o = 8.9$ μm, $f = 1.1$, $b = 3.13\times10^{-12}$, the values derived for $t(r,r_o)$ are given in Table V-1 below for $S = 5\times10^{-4}$ (the likeliest value), 10^{-3} and 2×10^{-3}.

TABLE V-1

Growth times to r = 25 μm for those particles which at T+3 hours are present in a concentration of one per liter ($r_o = 8.9$ μm)

S_o (absolute)	$t(r,r_o)$ (sec)
5×10^{-4}	2220
10^{-3}	1460
2×10^{-3}	890

Thus, unless the ambient supersaturation S_o is much larger than would seem to be likely, at T+3 hours the concentration of "effective giant nuclei" derived from exhaust products will have fallen below one per liter. Possible exceptions to this conclusion may occur in situations where deep and long-lived stratiform clouds are present.

At T+1 day, the total SGC particle concentration has fallen to 1.2×10^{6} per liter, so that a concentration of one per liter corresponds to a normalized concentration of 8.33×10^{-7}. According to Figure III-2 (ignoring the depletion of the larger particles by fall-out) this corresponds to a particle diameter ($2r_o$) of about 11 μm. From Figure III-5, it can be seen that in such a particle, the volume fraction of NH_4Cl is about 1.1×10^{-2}, so that the mass of NH_4Cl present is about 1.1×10^{-11} g. Thus in this case, $b = 1.8 \times 10^{-12}$. At T+1 day, the total droplet concentration (Fig. V-1) has fallen to about 1500 cm^{-3}, and assuming a mean liquid water content of 10^{-6} g cm^{-3} as before, $\bar{r} = 5.4$ μm, so that $n\bar{r} = 0.81$. With $V = 300$ cm sec^{-1}, the quasi-static formula indicates that $S_o \approx 8 \times 10^{-5}$.

Based on the values quoted above ($r = 25$ μm, $r_o = 5.5$ μm, $f = 1.1$, $b = 1.8 \times 10^{-12}$) the values derived for $t(r, r_o)$ are given in Table V-2 below for $S_o = 5 \times 10^{-4}$, 10^{-3} and 2×10^{-3}.

TABLE V-2

Growth times to r = 25 μm for those particles which at T+1 day are present in a concentration of one per liter ($r_o = 5.5$ μm)

S_o (absolute)	$t(r,r_o)$ (sec)
5×10^{-4}	2990
10^{-3}	1840
2×10^{-3}	1060

The concentrations given in Table III-2 on which these calculations were based ignore the depletion of the giant nucleus population of the SGC by fall-out, and are therefore somewhat above the true values. Thus the particle radius corresponding to a concentration of one per liter at T+1 day will in fact be somewhat smaller than 5.5 μm, and the times required to grow to r = 25 μm correspondingly longer than those quoted.

It therefore appears that after one day, the concentration of "effective giant nuclei" will have fallen distinctly below one per liter.

D. Conclusion

The neutralized SGC could influence warm rain formation in two opposing ways: the addition of CCN may delay it, while the addition of giant nuclei may accelerate it. On the basis of the discussion of the formation of the original aerosol and of the rate of growth of the SGC volume given in Chapter III, it is expected that convective clouds formed from the SGC will contain significantly higher concentrations of droplets (over 10^3 cm^{-3}) than natural clouds for a period approaching two days. On the other hand, it is expected that the additional giant nuclei will be of significance beyond T+3 hours only in rather special conditions; normally, the natural concentration of such nuclei will be dominant. When the preceding weather situation has been such that the natural concentrations are much lower than usual, the giant nuclei derived from the SGC may be of

marginal significance at T+3 hours, especially in stratiform cloud. They are unlikely however to influence warm rain formation beyond T+1 day.

The overall influence of the SGC will probably be to delay warm rain formation processes for one to two days; in view of the limited lifetimes of the convective clouds (the dominant rain forming cloud in the area), this is expected to lead to some reduction in precipitation. These conclusions may well require modification, however, unless the launch pad is paved over a sufficient area to prevent the blast from lifting large numbers of soil particles into the trench cloud; such particles could add very appreciably to the population of giant nuclei in the SGC.

The profound modification of the microphysical properties of clouds caused by the addition of CCN may of course have other effects not discussed here. For example, the reduction in the sizes of the main population of cloud droplets may affect certain ice multiplication processes, or again, the slowing-down of rain formation may result in significantly increased water loading of updrafts, leading to some reduction in the vigor of convective cells.

It is clear that a high priority item for investigation would be to obtain field measurements of the CCN supersaturation spectrum in a neutralized SGC.

REFERENCES

Fitzgerald, J.W., 1972: A study of the initial phase of cloud growth by condensation. U. of Chicago, Cloud Physics Lab Tech Note No. 44.

Fletcher, N.H., 1962: The Physics of Rainclouds. Cambridge U. Press.

Howell, W.E., 1949: J. Met., 6, 134.

Keith, C.H. and A.B. Arons, 1954: J. Met., 11, 173-184.

Mordy, W.A., 1959: Tellus, 11, 16.

Neiburger, M. and C.W. Chien, 1960: Computations of the growth of cloud drops. Physics of Precipitation, Geophysical Monographs No. 5, 191.

Squires, P., 1952: Aust. J. of Sci. Res., A5, 59.

Squires, P., 1958: Tellus, 10, 262.

Woodcock, A.H., 1953: J. Met., 10, 362.

APPENDIX TO SECTION C, CHAPTER V

1. The growth of droplets on sea-salt particles.

In order to show that on the basis of the data of Woodcock (1952) the natural concentration of "effective giant nuclei" consisting of sea-salt particles significantly exceeds one per liter over the sea with a force 3 wind, it is sufficient to estimate their growth in cloud conservatively. Thus, if the ambient in-cloud supersaturation (S_o) is taken to be zero, the growth law (from r = o at t = o) for the droplets formed in cloud becomes simply

$$r^5 = 5Gbft \ .$$

With i = 2, M = 58 (the molecular weight of NaCl), and $t = 10^3$ sec, the right hand side equals 8.0×10^{-4} m. Putting r = 25 μm, it results that particles for which $m > 1.2 \times 10^{-10}$ g will be "effective giant nuclei."

2. The Kelvin Curvature Effect and Giant Nuclei

The terms in the full droplet growth equation which express the effective supersaturation available to drive droplet growth are the ambient supersaturation (S_o) which is positive, the Kelvin curvature effect (negative) and the Raoult effect (positive). In the cases of interest here, the Kelvin term is small compared with the other two.

The ratio of the Kelvin to the Raoult term in the growth equation of a droplet formed on an SGC particle of radius r_o

is proportional to $\frac{r^3-r_o^3}{r} = r^2 - \frac{r_o^3}{r}$, which is clearly an increasing function of r. It is sufficient therefore to evaluate this ratio for r = 25 μm.

As described in Section C, the SGC particles of interest have a radius (r_o) of about 9 μm, and the mass of NH_4Cl on their surface is about $2x10^{-11}$ g. When a droplet of radius r has formed on such a particle, the effective supersaturation which is due to the Raoult effect is $\frac{3\ m\ M_o\ i}{4\pi M \rho_L (r^3-r_o^3)}$, where M_o is the molecular weight of water. When r = 25 μm, this has the value $2.2x10^{-4}$. The estimate of the value of S_o derived in Section C at T+3 hours was $5.7x10^{-4}$. Thus the two positive terms add up to a total of $8x10^{-4}$ when r = 25 μm.

The negative Kelvin term, on the other hand, is about $\frac{1.15x10^{-7}}{r}$ which, for r = 25 μm, equals $5x10^{-5}$, i.e. about 1/16th of the positive terms. At earlier times, when the droplet is smaller, the relative magnitude of the Kelvin term is even smaller; thus its neglect in the treatment of droplet growth in Section C is justified.

3. The Thickness of the NH_4Cl Solution Layer at the Triple Point

The particles of interest have a radius of about 9 μm or larger, and contain about $2x10^{-11}$ g of NH_4Cl. The solubility of NH_4Cl at 10°C is 333 g in 1000 g of water, so that the volume of the saturated solution is about $6x10^{-11}$ cm^3. If therefore

the Al_2O_3 particle has a radius of 9.00 μm (and a volume of $3x10^{-9}$ cm^3), the saturated solution layer is only 0.06 μm thick.

Thus it is reasonable to calculate droplet growth assuming that the layer of NH_4Cl solution is of negligible thickness.

CHAPTER VI. FLORIDA SYNOPTIC CLIMATOLOGY

TABLE OF CONTENTS

I OVERVIEW

The following description of the climate of Florida has been synthesized from many different published data sources. Special tabulations of unpublished data have also been constructed to supplement the published sets. In particular, extensive use has been made of the tabulated climatic summaries from Bradley (1972), Newell et al. (1972), Baldwin (1974), Court (1974), various NOAA publications, Air Weather Service Climatic Briefs, US Navy Station Climatic Summaries and selected NASA Technical Memorandums and Notes. The staff of the Kennedy Space Center Weather Service Office, headed by Mr. Jesse Gullick, provided many useful local and unpublished climatological studies.

Appendix I contains selected climatological information put together in our previous document entitled "Position Paper on the Potential of Inadvertent Weather Modification of the Florida Peninsula Resulting from the Stabilized Ground Cloud". This chapter provides additional details and provides newer information. Appendix II is a climatography of the Cape Canaveral-Merritt Island, Florida area prepared by Richard Siler of the Kennedy Space Center Weather Office. It gives a nice overview of the local climate.

The reader should refer to the map of the Cape Canaveral area (Figure 44 of Appendix I) for general orientation. Note in particular the location of the weather stations for Cape Canaveral, Kennedy Space Center and Titusville.

II SELECTED SURFACE CLIMATOLOGY

(a) Relative humidity

The variation of relative humidity for selected hours is shown in Table 1 as a function of month. Note the diurnal and seasonal variations with the driest period occurring in late winter and early spring during the early afternoon.

(b) Cloud cover distribution

Cloud cover variations for the Cape Canaveral weather station are listed in Table 2. The period of record is relatively short but the numbers suggest that there is relatively little relation between cloud cover and rainfall with a strong rainfall peak in mid summer. Mean cloud cover for the Florida peninsula in general is shown in Figure 15 and Figure 16 of Appendix I.

(c) Winds

Table 3 shows the most frequent wind direction and the average wind speed from that direction for Cape Canaveral. During the warm season the prevailing wind direction is easterly (July exception) with the highest frequencies in September and October. Northerly or northwesterly flow prevails during the cool season with slightly higher wind speeds.

Table 4 portrays selected percentile values, maximum, and standard deviation of peak surface winds (knots) for a 15 year period. This data is included for completeness.

(d) Present weather

Table 5 shows the mean number of hours of rain or drizzle, fog and smoke or haze by month at the Cape Canaveral weather station for

a 10 to 11 year period. Fog is confined mainly to the cool season and is nearly non-existent during summer. The same appears to be true for haze and smoke incidence. A May exception is noted but this may reflect a temporary local smoke source and would probably not be reflected in long term climatology. Summer mixing heights considerably exceed winter values in Florida which is consistent with the observed summer fog and smoke/haze minimum. Precipitation frequencies will be discussed later.

(e) Fog

A Cape Canaveral-Patrick AFB fog frequency comparison is given in Table 6. Despite slightly different record periods the fog frequencies are identical at the two locations with a strong winter maximum. Fog duration, however, would appear to be 20 percent greater at Patrick AFB. It is difficult to assess the reality of this discrepancy in view of possible differences in observational procedures between the two locations. Patrick AFB is, however, very close to water on two sides. Fog information is not available from Titusville for comparison. The large coastal fog frequency gradient is worthy of note with fog reported only on 25 to 30 days 20 or more kilometers inland from the coast in central Florida.

(f) Flying weather

Another perspective on visibility and ceilings is provided in Table 7 for various flying weather categories at Patrick AFB and Cape Canaveral. For example, at Cape Canaveral over a 15 year record period the ceiling is less than 150 meters and/or the visibility is less than 1.6 kilometers under one percent (0.9%) of the time. Individual hours by month for various categories are tabulated for Patrick AFB. These

should be compared with the detailed summary for Cape Canaveral given by Figure 43 of Appendix I.

(g) Hurricanes

Table 8 lists the number of hurricanes found within 185 kilometers of Cape Canaveral by month over an 80 year record period. The highest frequencies are found in August and September with an average of one hurricane every 11 years. The statistics may be somewhat misleading, however, because hurricane landfall patterns appear to exhibit geographical cycles. Additionally, extensive hurricane related rainfall may extend considerably more than 200 kilometers from the storm center.

III PRECIPITATION

(a) Rainfall frequencies

Mean rainfall maps for the state of Florida are given in Figures 17 to 20 of Appendix I for the months of December, March, June and September. The prominent feature is the coastal minimum during the warm season due to partial suppression of convective activity during the afternoon sea breeze regimes. This section will concentrate on more local variations.

Table 9 gives a Titusville-Kennedy Space Center monthly rainfall comparison for the last 11 year period. Titusville is located about 18 kilometers west of Kennedy Space Center. The monthly rainfall differences are rather dramatic with Titusville receiving approximately 25 percent more rainfall than the Kennedy Space Center on an annual average (comparable to the Miami-Miami Beach observed difference). This difference is rather pronounced in all months with the exception

of June and January and is particularly strong from mid summer through early autumn. The usual explanation for this discrepancy is that rainfall is enhanced inland from the coast in the vicinity of the sea breeze convergence (see, e.g., Byers and Rodebush [1948], Frank et al. [1967] and Pielke [1973]). During the cool season, however, this explanation would not appear to be as sufficient. Synoptic scale controls are stronger and sea-breeze regimes are correspondingly weaker. During the cool season the bulk of the central Florida precipitation is frontal related. It may be that a weak inland sea breeze convergence is set up under warm and humid conditions just prior to the arrival of a cold front. More research is needed on this point.

In an effort to assess the risk of precipitation on a diurnal basis 25 years of hourly rainfall were tabulated for Daytona Beach airport. Daytona Beach is the closest station to Cape Canaveral (hourly rainfall not tabulated) which tabulates hourly rainfall in readily accessible published form. The climate regimes of Daytona Beach and Cape Canaveral are very similar. The results for Daytona Beach are tabulated in Table 10 for the four key months of March, June, September and December.

The March data suggest that trace amounts are most prevalent around 8 AM and 8 PM LST. Heavier rainfall amounts (greater than 15 mm) show no particular time preference while intermediate rainfall amounts peak near sunrise and from mid-afternoon through early evening. Overall from seven to 10 percent of all hours record rainfall in March at Daytona Beach.

By June a different picture emerges as a strong diurnal variation is noted. Heavy hourly rainfalls (greater than 25 mm) are strongly concentrated from early to mid afternoon with a secondary maximum just before sunrise. Trace amounts are most likely from mid afternoon through early evening. Intermediate rainfall totals show a broad peak from late morning through early evening. The percentage of June hours that record at least a trace of rain at Daytona Beach ranges from five to six percent just after midnight to near 20 percent by 4 PM.

The September rainfall frequencies while similar to June values, are somewhat reduced for rainfall amounts in excess of 15 mm and increased for trace and .25 to 1 mm rainfalls. The daybreak secondary trace maximum is evident again while the overall diurnal rainfall variation is reduced somewhat from June. Hourly rainfall frequencies in September range from seven to eight percent to 17 to 18 percent.

December shows the absence of the warm season convective regime with no hourly rainfalls in excess of 25 mm recorded in 25 years. If anything, the heavier rainfalls tend to be concentrated near 8 AM and 8 PM LST. Hourly rainfall frequencies range from seven to 10 percent with maxima near sunrise and sunset.

A few cautionary notes on the use of the Daytona Beach data. While the record length is longer than for any previously published study the actual rainfall frequencies will be less than indicated because when hourly rainfall is tabulated it does not mean that rain fell for all 60 minutes. Table 5 shows the actual number of hours of rain or drizzle at Cape Canaveral for a much shorter record period. Rainfall frequencies range from three percent in May and November to eight percent in September.

The representativeness of the Daytona Beach data is also open to question. Considerable total rainfall variation has already been noted along an east-west line normal to the coastline from Table 9. However, it is not obvious that there would be any significant variation in the rainfall frequencies along this same line. Titusville may just rain significantly more than Cape Canaveral when it does rain. The data is not in hand to support or refute this statement. There is some indirect evidence, however. Miami International Airport averages 30 percent more rain on an annual basis than does Miami Beach yet the number of days of rainfall $\geq$ 0.25 mm runs between 125 and 130 at both locations. The corresponding rainfall frequency ($\geq$ .25 mm) at Cape Canaveral is 111 days. Additional details on Florida peninsula rainfall variations can be found in Appendix I (Table 1), with the monthly distribution as shown in Table 2.

(b) Thunderstorms

The reader is invited to review the general Florida thunderstorm climatology given in Appendix I (Table 2 and Figures 25 and 26). Additional climatology for the Kennedy Space Center area is given in Table 12. Two separate data sets are given for Cape Canaveral (different record lengths) in addition to a tabulation for Patrick AFB. More thunderstorm days are indicated for the Cape Canaveral region but the difference may not be significant although there is a 22 percent difference in the average number of hours of thunderstorms. Undoubtedly these numbers would increase westward towards Titusville (recall Table 9 rainfall comparison) as the sea breeze convergence zone is reached.

Additional information from Neumann (1970) will now be presented. This should be compared with Figures 46 to 49 from Neumann (1970) in Appendix I. Figure 1c shows the probability of a thunderstorm event starting on a particular day and continuing for n-consecutive days (the event may be interrupted) while Figure 1d shows conditional and unconditional thunderstorm probabilities during the warm season. The higher conditional as opposed to unconditional probabilities suggest a measure of synoptic control over thunderstorm events.

Figure 46 of Appendix I established that the maximum daytime thunderstorm frequency occurs near 1 July and 1 August with a secondary maximum in late March. Nightime frequencies are considerably reduced and peak in September. Figure 2 shows the Cape Canaveral afternoon thunderstorm probability as a function of the 1200 GMT 900 meter wind speed and direction. The probability is most sensitive to changes in wind direction with winds between 180 and 300 degrees leading to very high probabilities, a fact well known to Florida forecasters. This is further seen in Figure 3 where the afternoon thunderstorm probability as a function of 900 m wind direction is plotted against the time of the year. Morning westerly winds at 900 m (900 mb) are highly favorable for afternoon thunderstorms at Cape Canaveral in summer. A westerly flow regime near the surface layer inhibits the inland penetration of the sea-breeze convergence zone and leads to relatively high thunderstorm incidence along the immediate Florida east coast.

Finally, Figure 4 shows the average thunderstorm starting time during the warm season as a function of 900 meter wind speed and direction. Morning thunderstorms are very unlikely under a westerly flow regime with

a slight exception for relatively strong ($\sim$ 10 ms^{-1}) due westerly flow. Thunderstorms are apt to be particularly late with a northwesterly flow regime. Late morning thunderstorms, on the other hand, are considerably more likely with a southeasterly flow regime. As a general rule lower tropospheric easterlies favor morning convective activity with little active afternoon convection. The reverse is true under a lower tropospheric westerly regime although morning thunderstorms can not be ruled out in this latter case.

(c) Radar echo coverage

A factor of considerable importance to this position paper is the percentage of radar echo coverage as a function of the time of the day. Unfortunately very little in the way of hard quantitative evidence is available. An early investigation by Byers and Rodebush (1948) established the strong diurnal variation of the Florida convective and postulated the possible significance of the summer time double sea breeze regime. Frank et al. (1967) then sought to establish the seasonal diurnal cycle of echo frequencies over the Florida peninsula for the months May through August 1963 using the Daytona Beach, Tampa and Miami WSR-57 radar data. Some of the key results are shown in Figure 5. Surface convergence is strongly peaked around 1 PM LST for the four months. Echo coverage has a very strong diurnal variation with a peak at 1 PM and 4 PM LST. Note the inland maximum along both coasts. The data suggest an average 15 percent radar echo coverage in the Cape Canaveral vicinity at 4 PM LST with 20 percent just inland. Unfortunately it is difficult to assess the overall significance of these results because only one season of data was included. The warm season of 1963

was somewhat below normal in average precipitation over the Florida peninsula. Fhe Florida Area Cumulus Experiment (Woodley 1977) recorded an average 7.1 percent echo coverage (2PM LST) on the Miami radarscope for all echoes within 185 km of the radar site. Highly disturbed days were excluded from the sample.

Dr. William Woodley (personal communication) of the National Hurricane Research Laboratories has emphasized that the percentage area of deep convection is very strongly time dependent during the warm season. Over land on a disturbed day cumulonimbus coverage may reach 50 percent during the afternoon of which anywhere from one to 10 percent is active updraft. Thus as an upper bound we can probably take five percent as the percentage area of active updraft accompanying deep convection over Florida on an afternoon of a disturbed day. In a general easterly flow regime very little active updrafts are noted, especially over the water with less than one percent of the area covered. These figures, of course, are much higher for westerly flow. During the late nightime and early morning hours echo coverage is a relative maximum along the coast and just offshore along the edge of the Gulf Stream.

IV LOWER TROPOSPHERIC WINDS

Cape Canaveral 850 mb (≈ 1500 meters) relative wind directional frequencies are given in Table 13. A 10 year period of record (1960-1969) is used with all available 0000, 0600, 1200 and 1800 GMT observations used in an effort to assess diurnal variations. Nearly 300 observations were available at 0000 and 1200 GMT, 200 observations at 0600 GMT and

160 observations at 1800 GMT. Thus the 0600 and 1800 GMT should be viewed more cautiously. The data are tabulated by 30 degree increments beginning with 340 to 009 degrees. This choice is dictated by the 340 to 160 degree orientation of the coast line in the vicinity of Cape Canaveral. Onshore winds then refer to any wind from 340 clockwise through 160 degrees with offshore components otherwise. A down peninsula wind component then refers to winds from 250 clockwise through 070 degrees with up peninsula components otherwise. Mean wind speeds (ms^{-1}) for the 30 degree segments are tabulated in parentheses for the 0000 and 1200 GMT time periods where observations are abundant.

The March data reflect the predominant southwesterly flow at 850. Onshore components occur less than 30 percent of the time with a maximum at 1200 GMT. Overall diurnal variations are rather small as cool season synoptic patterns dominate the flow. A significant difference is seen by June. Southwesterly flow is still most prevalent but easterly components are now significant. These easterly components are most pronounced at 0000 GMT. Onshore components exhibit considerable variability, peaking at 0000 and 0600 GMT. The up-peninsula southerly components are most pronounced at 0600 and 1200 GMT and to a lesser extent at 1800 GMT.

By September the easterly flow components become dominant as the subtropical high pressure system reaches its northernmost position. Again onshore components are most pronounced at 0600 GMT and up-peninsula components at 1200 GMT. Cool season circulation patterns take over again by December with strong prevailing westerly flow. Onshore components

average 30 percent with a maximum at 1200 GMT. The strong offshore flow at 1800 GMT may be a reflection of the more limited data sample.

Table 14 shows the percentage of Cape Canaveral 850 mb wind observations with wind speeds ≤ 2 ms^{-1}. With the assumption of relatively light surface winds the numbers can be viewed as an upper bound on the probability that the ground cloud will still be within 10 km of the launch site more than an hour after launch. Pronounced seasonal and diurnal variations are evident with an overall peak in summer and at the 0600 GMT observation (except for March) in particular. The diurnal variation is particularly strong in June at the time of maximum solar heating.

V SYNOPTIC REGIMES

In this section some soundings are presented for the lowest two kilometers of the Cape Canaveral atmosphere for some characteristic synoptic regimes. The data are taken from Susko and Stephens (1976). Autumn and spring soundings are presented in Tables 15 and 16 with a sea-breeze regime given in Table 17. The autumn sounding will lead to an inland transport of the ground cloud. The 1000 m mixing height may or may not be typical. The mixing height often reaches 2000 m during a typical spring regime. The sea breeze regime has an average 300 m mixing height. Exhaust material would be carried northwest of the launch site under a typical sea breeze regime and then return offshore with the return circulation in the vicinity of 1500 m.

A major cool season weather factor in the Cape Canaveral area is the cold front. Some typical cold front vicinity soundings are given in Tables 18 through 20. The pre-frontal southwesterly flow regime at all

levels is given in Table 18. Table 19 gives the corresponding profiles immediately after cold frontal passage. Deep easterlies are present with wind speeds reaching 15 ms^{-1}. This is a typical post frontal sounding near the beginning and end of the cool season. Post frontal precipitation is not unknown with such soundings so the deep easterly flow poses a problem for possible interaction of the exhaust cloud with a convective cell. Continued post frontal easterly flow is still in evidence two days later in Table 20.

Finally, a typical cool season anticyclone regime is given in Table 21 with light, westerly flow at low levels and a relatively shallow surface mixing layer.

VI CONCLUSIONS AND RECOMMENDATIONS

The key findings are reviewed here and some risk factors are assigned which represent upper bound probabilities for the respective events.

(a) Thunderstorms

The risk of any day with thunder peaks at 50 percent in August. The average warm season thunderstorm duration is 1.7 hours. The conditional probability of a thunderstorm given the previous day recorded a thunderstorm is high, reaching 70 percent in August.

The Cape Canaveral data suggest the following percentage of actual thunderstorm hours = July-August 6.0 percent; June 4.4 percent; September 2.8 percent; October, March and April 1 percent. The Patrick AFB figures are comparable except for June (3.8%), July (4.4%) and August (3.8%). The figures for Titusville (data not available) are

probably somewhat higher in summer. A very strong diurnal variation exists in thunderstorm frequency with a maximum near 4 PM LST.

The skill in predicting such thunderstorms measured against improvement over a conditional persistence climatology is probably non-existent beyond 24 hours and only marginal in the 0-12 hour forecast projection. The onset of thunderstorm activity at the Kennedy Space Center (warm season) is likely to be late morning with a lower tropospheric onshore flow (southeasterly) regime. This activity usually ceases by mid to late afternoon. Convective activity may be especially pronounced with a lower tropospheric southwesterly flow. It peaks during the afternoon and early evening and may be non-existent during the morning under such a regime.

(b) Hurricanes

On the basis of an 80 year period of record a hurricane is likely to reach within 185 kilometers (100 nautical miles) of Cape Canaveral one year out of 11 in August through October, one year out of 40 in July and one year out of 80 in June. The episode is likely to last less than 24 hours under this criteria.

Disturbed conditions over land and water accompanying hurricanes or tropical storms may encompass the Cape Canaveral region one year out of three or four years (storm center may be as far as 500-1000 km away). These relatively disturbed conditions (cumulonimbus coverage 20-50%) may persist from 24 to 72 hours.

Current skill levels suggest a 500 km radius error envelope for a tropical storm center in a 72 hour forecast.

(c) Winds

Onshore 850 mb flow ranges from 20-27 percent in March (maximum at 1200 GMT), 40-50 percent in June (maximum at 0000 and 0600 GMT), 55-64 percent in September (maximum at 0600 GMT) to 27-33 percent in December (maximum at 1200 GMT).

June exhibits the largest diurnal variation. Southerly 850 mb wind components are most pronounced in June with a large diurnal variation peaking at 0600 and 1200 GMT.

(d) Precipitation

In the Cape Canaveral region a 30 percent annual rainfall variation exists with the amounts increasing steadily inland to Titusville. The inland maximum occurs in all months except January and June and is most prominent from mid summer to early autumn.

A strong seasonal and diurnal variation for hours with precipitation (trace or more) exists, ranging from seven to 10 percent in March and December to 7.5 to 17.5 percent in September and 5.5 to 20 percent in June. These numbers refer to the percentage of hours recording a trace or more of precipitation when the data is sampled every hour. Undoubtedly the actual number of hours with rain is less, especially during convective regimes. Convective activity is strongly peaked from early afternoon through early evening in summer with a 4 PM LST maximum in June. The highest frequencies of hourly rainfall in excess of 25 mm occur from 2-4 PM LST in June with an average frequency of one percent (Daytona Beach long term data). The cool season shows a daybreak and sunset relative maximum in trace and light precipitation with a very weak afternoon maximum in the heavier rainfalls.

Radar echo coverage is highly variable and may average 20 percent in summer along the sea breeze convergence zone along the central Florida east coast, 15 percent right along the coast and less than 10 percent offshore. On a disturbed summer day over land cumulonimbus echo coverage may reach 50 percent of which one to 10 percent represents active updraft regions (5% of total area maximum).

Synoptic weather regimes which favor near surface onshore flow in the absence of strong westerlies above the planetary boundary layer and in the presence of active convective elements should especially be avoided in terms of the space shuttle launch. Characteristic synoptic regimes that would fall into this category include

(1) hurricanes

(2) easterly waves of summer

(3) stagnating frontal zones

(4) cool season squall lines

(5) cool season low latitude mid tropospheric troughs

(6) warm season weak mid tropospheric troughs

(7) coastal sea breeze convergence regimes

The hurricane risk has been assessed above. Easterly waves with disturbed conditions (50% Cb average) may reach Florida every four or five days from mid July through September with the disturbed conditions persisting 12-24 hours.

Stagnating fronts across central Florida (Morgan 1975) carry risk factors of five to six days in March and December (less in January and February) and two to three days in early June and late September. Extensive precipitation may occur, particularly in September, in the low

level easterly flow just to the north of the frontal zone. Disturbed conditions and accompanying rainfall may persist for 12 to 24 hours. Such events can be predicted with some skill relative to climatology 12 to 36 hours in advance. Occasional squall lines in advance of strong cold fronts may sweep across central Florida in winter (especially in December and March). The strong westerly flow accompanying such fronts results in precipitation duration of an hour or less--predictability is usually restricted to a general statement of likelihood 12 to 24 hours in advance of the event.

Cool season extensive precipitation (24-48 hours) may occur in the presence of very rare low latitude extratropical cyclogenesis accompanying deep, cold troughs aloft one year out of three. A recent example is the storm of 10-13 February 1973. Predictability can be poor because of the rarity of the event although antecedent conditions may provide useful clues to the experienced forecaster.

Finally, warm season weak mid tropospheric troughs can interact with the sea breeze convergence regime to produce highly disturbed conditions several days each month. This leads to a general rule. With southwesterly flow at 850 mb at 1200 GMT a morning launch as opposed to afternoon launch is preferred. The reverse is usually true with morning southeasterly flow.

VII REFERENCES

Baldwin, J.L., 1974: "Climates of the United States", U.S. Dept. of Commerce, 113 pp.

Bradley, J.T., 1972: "The Climate of Florida", Climates of the States, Vol. I, NOAA, U.S. Dept. of Commerce, 45-71.

Byers, H.R. and H.R. Rodebush, 1948: "Causes of Thunderstorms of the Florida Peninsula", J. Meteor, Vol. 5, 6, 275-280.

Court, A., 1974: "The Climate of the Coterminus United States", in World Survey of Climatology, Vol. II, Climates of North America, edited by R. Bryson and F.K. Hare.

Frank, N.L., P.L. Moore and G.E. Fisher, 1967: "Summer Shower Distribution over Florida Peninsula as Deduced from Digitized Radar Data", J. Appl. Meteor., Vol. 6, #3, 309-316.

Morgan, G.M., D.G. Brunkow and R.C. Beebe, 1975: "Climatology of Surface Fronts", Illinois State Water Survey, ISWS-75-CIR-122, 46 pp.

Neumann, C.J., 1970: "Frequency and Duration of Thunderstorms at Cape Kennedy, Part II", ESSA Tech. Memo., WBTM-SOS-6.

Pielke, R., 1973: "An Observational Study of Cumulus Convection Patterns in Relation to the Sea Breeze over South Florida", NOAA Tech. Memo. ERL-OD-16, 81 pp.

Susko, M. and J. Stephens, 1976: "Baseline Meteorological Soundings for Parametric Environmental Investigations at Kennedy Space Center and Vandenberg Air Force Base", NASA TM X-64986, 35 pp.

Wallace, J.M., 1975: "Diurnal Variations in Precipitation and Thunderstorm Frequency over the Caterminus United States", Mon. Wea. Rev., 103, #5, 406-419.

Woodley, W.L., J. Simpson, R. Bondini and J. Berkeley, 1977: "Rainfall Results, 1970-1975: Florida Area Cumulus Experiment", Science, Vol. 195, No. 4280, 735-742.

LIST OF TABLES

TABLE 1

Kennedy Space Center Surface Relative Humidity
by Selected Hour by Month

	0100	0700	1300	1900
January	83	84	61	78
February	78	83	54	70
March	78	80	55	70
April	73	78	54	66
May	79	81	57	71
June	85	85	65	82
July	87	87	65	82
August	88	90	68	82
September	85	87	68	79
October	81	84	65	74
November	81	83	80	78
December	80	83	59	78

TIME (LST)
PERIOD OF RECORD: April 1965-December 1976

TABLE 2

Percentage Frequency Distribution of Total Cloud Cover (in Tenths)
for Cape Canaveral, Florida
Period of Record: August 1950-February 1954,
April 1954, April 1956-July 1962

	0-3	4-7	8-10
January	44.1	18.7	37.2
February	45.2	20.1	34.7
March	39.6	18.4	42.0
April	43.5	20.8	35.7
May	45.0	21.5	33.5
June	36.4	24.8	38.8
July	36.3	29.8	33.9
August	36.2	28.7	35.1
September	35.7	25.8	38.5
October	37.2	25.1	37.7
November	44.7	23.1	32.2
December	44.6	20.4	35.0
Year	40.6	23.2	36.2

TABLE 3

Most Frequent Wind Direction and the Average Wind Speed (ms^{-1}) from that Direction, Cape Canaveral, Florida
Period of Record: 1951-52; 1957-70

	Prevailing Wind		Percent
January	NW	4.5	12.0
February	N	5.0	11.6
March	N	5.0	9.9
April	ESE	4.0	12.8
May	E	4.5	14.6
June	E	4.0	12.3
July	S	3.0	14.1
August	E	3.5	11.9
September	E	4.0	17.4
October	E	4.5	14.7
November	NW	4.0	12.2
December	NW	4.0	14.3
Year	E	4.0	10.6

TABLE 4

Selected Percentile Values, Maximum, and Standard Deviation
of Peak Surface Winds, in Knots, at Cape Canaveral, Florida

Reference height: 10 meters

	Percentile											
Month	1	5	10	25	50	75	90	95	99	99.9	Max	Std Dev
Jan	6.0	8.0	8.9	12.0	15.9	22.0	27.0	31.1	35.9	42.9	46.0	7.2
Feb	7.0	8.9	9.9	13.0	15.9	22.0	29.0	33.0	41.0	42.9	44.1	7.6
Mar	8.0	9.9	12.0	13.0	17.1	22.0	30.0	33.0	41.0	54.0	58.1	7.4
Apr	7.0	9.9	12.0	13.0	15.9	21.0	28.0	32.1	42.9	47.0	49.0	7.0
May	8.9	9.9	11.1	13.0	15.9	20.0	24.1	30.0	36.9	49.0	58.1	5.8
Jun	17.9	9.9	11.1	12.0	15.0	20.0	26.0	32.1	42.9	63.9	72.1	7.4
Jul	7.0	8.9	9.9	12.0	14.0	19.0	25.1	31.1	42.0	48.0	49.0	7.0
Aug	7.0	8.9	9.9	12.0	14.0	19.0	25.1	28.9	40.0	49.9	51.1	6.8
Sep	7.0	8.9	9.9	12.0	15.0	22.0	28.0	35.0	41.0	42.9	44.1	7.6
Oct	7.0	8.9	9.9	13.0	15.9	22.9	27.0	31.1	36.9	54.0	59.1	7.2
Nov	7.0	8.0	8.9	12.0	15.0	20.0	25.1	28.0	40.0	55.9	64.0	6.8
Dec	7.0	8.0	8.9	12.0	15.0	22.0	28.0	31.1	40.0	56.9	60.0	7.8
Year	7.0	8.9	9.9	12.0	15.0	21.0	27.0	32.1	41.0	55.9	72.1	7.2

PERIOD OF RECORD: Jan 1951-Dec 1952
Jan 1957-Dec 1970

TABLE 5

Mean Number of Hours of Specified Weather Occurrences
for Cape Canaveral, Florida
Period of Record: August 1950-February 1954,
April 1954, April 1956-July 1962

	Rain or Drizzle	Fog	Smoke or Haze
January	38.0	50.1	4.6
February	39.8	33.5	3.2
March	53.0	21.9	5.6
April	29.8	7.2	1.0
May	22.2	6.6	10.5
June	38.1	4.0	1.1
July	27.0	.9	.1
August	34.6	4.2	1.4
September	57.0	3.9	2.0
October	54.0	7.8	1.4
November	23.4	14.8	6.8
December	33.1	27.3	3.2
Year	446.8	183.9	43.8

NOTE: Fog Defined for Surface Visibility ≤ 10 km.

TABLE 6

Cape Canaveral--Patrick AFB
Fog Frequency Comparison

	Jan	Feb	Mar	Apr	May	Jun	Jul	Aug	Sep	Oct	Nov	Dec	ANN
Cape Canaveral													
Days with Fog	10	8	6	4	3	2	2	2	2	2	6	8	55
Avg. No. Hrs.	43	33	21	10	7	4	2	4	4	8	19	35	180
Patrick AFB													
Days with Fog	10	8	7	5	2	2	1	1	2	3	6	8	55
Avg. No. Hrs.	50	39	26	15	4	6	2	2	5	9	16	43	217

PERIOD OF RECORD
Cape Canaveral: Aug 1950-Nov 1952, Dec 1956-Dec 1972
Patrick AFB: Jan 1950-Dec 1973

TABLE 7

Flying Weather (Hours) Patrick AFB
Period of Record: Jan 1970-Dec 1973

	Jan	Feb	Mar	Apr	May	Jun	Jul	Aug	Sep	Oct	Nov	Dec	ANN
Ceiling ≥ 450 meters and Visibility ≥ 5 km	694	623	718	703	731	705	739	737	702	721	696	706	8475
Ceiling 60-450 m and Visibility ≥ 5 km or Visibility ≥ 0.4 km but < 5 km and Ceiling ≥ 60 m	46	46	24	16	11	15	5	7	18	22	23	33	266
Ceiling < 60 m and Visibility ≤ 0.4 km	4	3	2	1	1	1	0	0	0	1	1	5	17

Flying Weather (Annual Percentages): Cape Canaveral
Period of Record: Aug 1950-Nov 1952
Jan 1957-Dec 1970

A - Ceiling ≥ 300 m and Visibility ≥ 5 km	97.6%
B - Ceiling 150-275 m and Visibility ≥ 1.6 km or Visibility ≥ 1.6 km but < 5 km and Ceiling ≥ 150 m	1.5%
C - Ceiling < 150 m and/or Visibility < 1.6 km	0.9%

DATA SOURCE: Uniform Summary of Surface Observations

TABLE 8

Number of Hurricanes Within 185 Kilometers
of Cape Canaveral, Florida
Period of Record: 1886-November 1966

	Number of Hurricanes Centered Within 185 Kilometers
January	0
February	0
March	0
April	0
May	0
June	1
July	2
August	7
September	7
October	6
November	0
December	1
Total	21

TABLE 9

Kennedy Space Center--Titusville
Simultaneous Rainfall Comparison
Period of Record: April 1966-December 1976
Units (mm)

	Jan	Feb	Mar	Apr	May	Jun	Jul	Aug	Sep	Oct	Nov	Dec	ANN
Titusville	40.6	67.6	72.4	36.3	124.7	233.7	229.4	181.4	153.4	144.5	50.0	59.2	1393.2
Cape Canaveral	39.1	52.1	59.7	21.1	91.2	238.3	136.9	138.9	122.4	108.5	45.5	54.6	1108.2

TABLE 10

Daytona Beach, Florida
Relative Frequency of Precipitation by Amount and by Hour

	1	2	3	4	5	6	7	8	9	10	11	12	1	2	3	4	5	6	7	8	9	10	11	12
March																								
Trace	3.8	3.3	4.1	4.6	4.5	4.1	4.5	5.3	6.6	5.2	4.0	4.5	4.5	4.6	4.3	4.1	4.2	4.3	4.6	5.2	3.2	3.8	3.2	3.5
.25-1	2.2	2.3	1.1	2.2	1.6	1.6	1.7	3.3	2.1	2.2	2.5	2.1	3.1	2.9	2.6	3.0	2.5	2.0	2.1	2.2	3.0	1.9	2.6	2.5
> 1-5	1.0	1.1	1.5	1.4	2.1	2.3	1.6	1.1	1.0	1.0	1.6	2.0	1.7	1.3	2.0	2.2	2.5	2.4	1.9	1.5	2.0	1.4	1.0	0.9
> 5-15	0.4	0.1	0.5	0.1	0.6	0.4	0.4	0.5	0.1	0.4	0.6	0.5	0.8	0.8	0.5	0.4	0.9	0.6	0.5	0.8	0.1	0.4	0.1	0.6
> 15-25			0.1	0.1					0.1					0.1	0.3				0.1			0.1		
> 25		0.1		0.1					0.1	0.1														
June																								
Trace	2.7	2.7	2.9	3.3	2.5	3.0	3.3	2.5	3.0	3.5	3.3	6.1	6.9	7.5	9.7	10.5	8.7	9.1	10.7	8.5	8.3	4.8	4.5	3.6
.25-1	1.5	1.9	2.1	1.3	2.0	1.6	1.5	1.6	1.9	2.4	2.9	3.7	4.5	4.4	4.1	5.3	6.1	4.1	3.7	5.2	3.5	2.7	2.0	1.7
> 1-5	0.9	0.9	0.5	0.9	1.0	0.9	0.9	1.0	1.3	1.6	1.5	2.5	2.7	3.3	3.6	2.7	3.3	2.9	4.1	2.9	2.7	1.9	2.0	1.7
> 5-15	0.3	0.1	0.7	0.4	0.4	0.5	0.3	0.8	0.4	0.7	0.5	1.3	1.0	1.6	1.3	2.0	1.6	1.3	0.8	1.0	0.8	0.9		
> 15-25	0.1	0.1		0.4							0.3	0.1	0.5		0.7	0.4	1.0	0.7	0.4	0.4	0.3	0.1		
> 25				0.3	0.1	0.1		0.1			0.1	0.1	0.3	0.9	0.4	1.2	0.1		0.1					
September																								
Trace	4.9	4.3	3.7	3.9	4.1	6.1	4.7	5.9	4.4	4.3	7.5	6.4	9.3	9.1	8.4	9.9	8.1	8.0	8.3	10.7	7.7	6.5	6.1	5.9
.25-1	2.7	2.0	2.4	2.4	2.0	2.1	2.8	3.0	2.7	2.3	2.9	4.5	4.3	3.7	2.8	3.3	4.7	4.5	4.4	3.6	3.0	3.9	2.8	2.3
> 1-5	1.6	1.6	1.5	2.0	1.7	0.9	1.3	1.9	1.7	2.0	2.1	2.0	2.8	2.8	2.7	2.4	3.0	3.5	2.9	3.6	4.3	2.0	1.9	1.5
> 5-15	0.3	0.3	0.7	0.1	0.7	0.4	0.8	0.5	0.7	1.9	0.8	0.5	1.3	1.1	2.0	1.9	2.5	1.6	1.3	0.5	0.7	0.4	0.5	0.5
> 15-25		0.1		0.1	0.3		0.3		0.1			0.3	0.1	0.7	0.4	0.8	0.1'		0.3	0.3			0.4	
> 25			0.1	0.1				0.1				0.1	0.3	0.3	0.4	0.3	0.1	0.1	0.1		0.1			0.1
December																								
Trace	5.2	4.1	4.3	3.7	3.7	5.3	5.4	5.9	5.7	4.9	5.3	4.4	5.9	6.5	4.9	4.5	5.0	4.8	4.6	4.5	5.5	5.3	5.3	5.9
.25-1	1.2	2.6	2.1	2.6	1.8	2.6	2.1	2.6	1.8	2.5	2.2	2.3	1.8	1.5	1.8	2.2	2.1	1.8	2.7	2.3	2.2	1.8	2.2	2.3
> 1-5	1.5	1.0	1.0	0.6	1.3	0.9	1.7	1.4	1.4	1.2	1.8	1.4	1.4	1.2	1.3	0.8	0.6	1.7	1.5	1.3	1.7	1.2	1.3	0.9
> 5-15			0.1	0.3	0.3	0.4	0.1	0.1	0.3	0.5	0.3	0.6	0.3	0.1	0.1	0.3	0.6	0.1	0.4	0.3	0.4	0.6	0.3	0.1
> 15-25									0.1											0.1			0.1	0.1
> 25																								

Rainfall Units (mm)
Period of Record: 1952-1976
Data Source: Local Climatological Data (NOAA)
Time (LST)

TABLE 11

Cape Canaveral
Percentage Frequency of Days with Rainfall 0.25 mm
Period of Record: Nov 1950, Feb 1951-Nov 1952
Dec 1956-Dec 1965

January	22.9
February	28.6
March	29.0
April	20.3
May	23.8
June	35.5
July	34.3
August	34.1
September	46.4
October	37.8
November	26.4
December	21.7
ANNUAL	30.3 (111 days)

TABLE 12

Thunderstorm Days at Cape Canaveral, Florida
Period of Record: January 1951-December 1952,
January 1957-December 1965

	Mean Thunderstorm Days	Percent of Thunderstorm Days	Mean Duration (Hours) of Thunderstorms
January	0.5	1.5	0.5
February	1.2	4.2	1.3
March	3.1	10.0	1.6
April	3.5	11.8	1.4
May	6.9	22.3	1.6
June	12.3	40.1	1.7
July	13.9	44.9	2.0
August	15.1	50.3	1.7
September	9.2	30.6	1.4
October	3.1	10.0	1.3
November	1.0	3.3	2.2
December	0.7	2.4	1.0
Year	70.5	19.3	1.7

Thunderstorm Climatology

	Cape Canaveral AFS Period of Record: Aug 1950-Nov 1952, Dec 1956-Dec 1972		Patrick AFB Period of Record: Jan 1950-Dec 1973	
	Days with Thunderstorms	Avg. # of Hours	Days with Thunderstorms	Avg. # of Hours
Jan	1	1	1	1
Feb	1	2	1	2
Mar	3	7	3	7
Apr	3	6	4	6
May	7	16	7	13
Jun	13	32	11	27
Jul	13	44	13	33
Aug	15	45	14	28
Sep	9	20	9	18
Oct	4	7	3	6
Nov	1	3	1	2
Dec	1	1	1	1
Year	72	184	68	144

Cape Canaveral 850 mb Relative Wind Directional Frequencies; Onshore, Offshore and Down and Up Peninsula Frequencies

	340-009	010-039	040-069	070-099	100-129	130-159	160-189	190-219	220-249	250-279	280-309	310-339	Onshore	Offshore	Down Peninsula	Up Peninsula
March																
0000	6.1	1.8	3.6	5.0	2.2	5.0	4.3	10.8	20.5	20.1	14.7	5.8	23.7	76.3	52.9	47.1
	(5.5)	(6.8)	(4.6)	(5.8)	(7.3)	(6.6)	(6.5)	(9.1)	(9.9)	(10.2)	(11.7)	(7.0)				
0600	2.4	4.0	4.0	0.0	4.8	4.8	7.2	14.4	20.0	14.4	18.4	5.6	20.0	80.0	48.8	51.2
1200	3.4	3.0	5.7	3.7	4.4	6.4	6.4	8.7	17.8	16.4	15.4	8.7	26.6	73.4	52.6	47.4
	(7.7)	(4.0)	(8.2)	(5.5)	(4.7)	(6.2)	(7.3)	(9.2)	(11.7)	(9.0)	(11.2)	(8.8)				
1800	1.4	2.1	2.7	2.1	1.4	4.1	6.8	11.6	23.3	20.5	16.4	7.5	13.8	86.2	50.6	49.4
June																
0000	6.6	5.6	8.0	9.4	13.3	5.2	4.2	9.8	10.8	11.5	8.0	7.3	48.1	51.9	47.0	53.0
	(3.8)	(4.3)	(6.8)	(5.4)	(6.0)	(5.3)	(4.5)	(7.1)	(6.7)	(5.6)	(5.4)	(4.4)				
0600	4.2	5.2	6.1	7.5	13.7	14.6	13.2	7.5	11.3	6.1	5.2	5.2	51.3	48.7	32.0	68.0
1200	3.1	5.1	7.2	7.5	7.2	9.9	12.3	13.4	16.4	11.6	3.1	3.1	40.0	60.0	32.2	66.8
	(3.2)	(4.5)	(5.5)	(4.7)	(5.7)	(5.4)	(4.9)	(5.8)	(6.5)	(6.4)	(5.4)	(3.2)				
1800	4.9	3.5	7.0	6.3	9.8	7.0	9.1	11.9	18.2	10.5	10.5	1.4	38.5	61.5	37.8	62.2
September																
0000	4.2	10.5	15.7	12.6	10.5	6.3	3.8	3.8	8.0	11.2	6.3	7.0	59.8	40.2	36.2	63.8
	(5.7)	(6.0)	(7.7)	(7.4)	(6.0)	(5.1)	(6.3)	(10.5)	(7.9)	(6.7)	(5.9)	(4.2)				
0600	4.7	5.1	12.1	15.0	17.3	9.8	7.0	8.4	8.9	5.1	3.3	3.3	64.0	36.0	33.6	66.4
1200	3.5	4.9	11.5	17.8	13.3	7.3	4.9	10.1	13.6	6.6	3.1	1.7	58.3	41.7	31.3	68.7
	(5.6)	(6.9)	(6.2)	(6.3)	(5.9)	(6.0)	(5.9)	(8.7)	(6.7)	(5.3)	(4.3)	(10.4)				
1800	5.5	7.6	12.4	16.6	13.1	6.9	5.5	11.0	7.6	10.3	3.4	0.0	62.1	37.9	39.2	60.8
December																
0000	4.4	3.0	6.7	5.1	3.7	4.7	8.4	7.7	13.8	15.8	17.5	9.1	27.6	72.4	56.5	43.5
	(7.8)	(8.6)	(7.2)	(7.1)	(5.4)	(5.5)	(6.2)	(9.1)	(9.0)	(9.1)	(10.0)	(9.5)				
0600	3.4	5.4	4.0	6.0	4.7	7.4	9.4	11.4	14.1	12.1	18.1	4.0	30.9	69.1	47.0	53.0
1200	2.7	4.4	4.1	3.4	6.5	4.5	7.5	11.6	14.4	16.8	16.4	7.5	33.1	66.9	51.9	48.1
	(5.8)	(6.1)	(5.9)	(5.9)	(5.9)	(5.6)	(7.3)	(8.3)	(9.6)	(10.1)	(9.8)	(7.6)				
1800	3.7	1.8	2.4	3.7	0.6	5.5	8.0	14.7	14.7	19.0	15.3	10.4	17.7	82.3	52.6	47.4

Period of Record: 1960-1969
Data Source: WBAN 33 (NOAA)
Speeds (ms^{-1}) given in parantheses where available
Times are GMT
Onshore (340-160)

TABLE 14

Percentage of Cape Canaveral 850 mb Wind Observations with Wind Speeds Less Than or Equal to 2 ms^{-1}

Time (GMT)	March	June	September	December
0000	6.5	15.7	15.4	7.7
0600	6.5	22.0	17.7	11.5
1200	6.7	14.8	13.0	5.8
1800	5.4	12.5	14.5	6.7

PERIOD OF RECORD: 1960-1969

TABLE 15

KSC Fall, Normal Launch

Standard deviation of the azimuth surface wind angle is 12.000 deg.
Surface air density is 1183.550 g/m^3.
Height of surface mixing layer is 10000.000.*

Layer Boundary Height (m)	Wind Direction (deg)	Wind Speed (m/s)	Temperature (°C)	Pressure (mb)
18.000	90.0000	4.7000	26.000	1013.000
60.000	91.9000	5.1200	25.440	1007.000
200.000	95.8000	5.9700	24.300	995.000
400.000	101.6000	6.3900	22.600	972.500
600.000	107.4000	6.6500	20.900	950.000
800.000	113.2000	6.8500	19.200	926.000
1000.000	119.0000	7.0000	17.500	905.000
1200.000	121.5000	6.7000	16.800	885.000
1400.000	124.0000	6.4500	16.100	865.000
1600.000	126.0000	6.1800	15.400	845.000
1800.000	129.0000	5.9000	14.700	825.000
2000.000	131.0000	5.6000	14.000	805.000

*The height of mixing layer in all tables is a suggested altitude.

SOURCE: Susko and Stephens (1976)

TABLE 16

KSC Spring, Normal Launch

Standard deviation of the azimuth surface wind angle is 7.000 deg.
Surface air density is 1183.550 g/m^3.
Height of surface mixing layer is 2000.000.

Layer Boundary Height (m)	Wind Direction (deg)	Wind Speed (m/s)	Temperature (°C)	Pressure (mb)
18.000	100.0000	6.0000	27.000	1013.000
66.000	104.0000	6.2400	26.500	1007.000
200.000	108.0000	6.7200	25.500	995.000
400.000	116.0000	6.9500	23.900	972.500
600.000	124.0000	7.0800	22.300	950.000
800.000	132.0000	7.1800	20.700	926.000
1000.000	140.0000	7.2600	19.000	905.000
1200.000	148.0000	7.3200	17.450	885.000
1400.000	156.0000	7.3700	15.800	865.000
1600.000	164.0000	7.4200	14.200	845.000
1800.000	172.0000	7.4600	12.600	825.000
2000.000	180.0000	7.5000	11.000	805.000
2500.000	200.0000	7.5000	11.000	757.500

SOURCE: Susko and Stephens (1976)

TABLE 17

KSC Sea Breeze, Normal Launch

Standard deviation of the azimuth surface wind angle is 12.000 deg.
Surface air density is 1183.550 g/m^3.
Height of surface mixing layer is 300.000.

Layer Boundary Height (m)	Wind Direction (deg)	Wind Speed (m/s)	Temperature (°C)	Pressure (mb)
18.000	140.0000	4.5000	21.000	1013.000
44.000	141.6000	5.8000	20.020	1008.700
150.000	145.0000	7.9000	20.050	1000.000
300.000	150.0000	9.5000	19.000	985.000
500.000	161.5000	5.6000	19.000	961.000
700.000	172.5000	4.0000	19.000	937.500
1000.000	190.0000	2.7000	19.000	905.000
1500.000	240.0000	2.9000	16.750	855.000
2000.000	250.0000	3.1000	14.400	805.000

SOURCE: Susko and Stephens (1976)

TABLE 18

19 October 1972, 1115 Z (0715 EDT)
Cold Front North of KSC, Normal Launch

Standard deviation of the azimuth surface wind angle is 7.000 deg.
Surface air density is 1204.880 g/m^3.
Height of surface mixing layer is 218.000.

Layer Boundary Height (m)	Wind Direction (deg)	Wind Speed (m/s)	Temperature (°C)	Pressure (mb)
18.000	253.0000	2.6000	18.900	1018.000
33.000	248.0000	2.9000	20.400	1016.000
65.000	238.0000	3.5000	23.300	1011.000
218.000	194.0000	3.0000	24.000	993.500
400.000	198.0000	3.0000	22.700	973.000
600.000	199.0000	3.0000	21.400	951.000
800.000	211.0000	2.5000	20.400	929.000
1076.000	235.0000	2.0000	18.700	200.000
1200.000	229.0000	2.0000	16.800	887.000
1400.000	215.0000	3.0000	15.550	867.000

SOURCE: Susko and Stephens (1976)

TABLE 19

20 October 1972, 1115 Z (0715 EDT)
Cold Front Near KSC, Normal Launch

Standard deviation of the azimuth surface wind angle is 1.130 deg.
Surface air density is 1185.220 g/m^3.
Height of surface mixing layer is 250.000.

Layer Boundary Height (m)	Wind Direction (deg)	Wind Speed (m/s)	Temperature (°C)	Pressure (mb)
18.000	41.0000	8.8000	23.700	1018.600
53.000	42.2000	10.2000	23.580	1014.000
125.000	44.5000	13.0000	23.350	1006.000
250.000	48.0000	15.0000	22.900	990.500
400.000	49.0000	15.0000	21.500	974.000
613.000	51.0000	15.0000	19.600	950.000
800.000	54.0000	13.7000	18.300	929.000
100.000	59.0000	12.0000	17.200	908.400
1200.000	66.0000	11.3000	16.100	887.000
1400.000	73.5000	10.4000	14.800	867.000
1600.000	80.0000	8.8000	13.550	847.000
1800.000	86.5000	8.0000	12.200	827.000
2000.000	91.0000	7.0000	11.300	807.500

SOURCE: Susko and Stephens (1976)

TABLE 20

21 October 1972, 1115 Z (0715 EDT)
Cold Front South of KSC, Normal Launch

Standard deviation of the azimuth surface wind angle is 9.000 deg.
Surface air density is 1197.070 g/m^3.
Height of surface mixing layer is 1400.000.

Layer Boundary Height (m)	Wind Direction (deg)	Wind Speed (m/s)	Temperature (°C)	Pressure (mb)
18.000	80.0000	6.0000	22.600	1022.000
53.000	80.2000	6.7000	22.520	1017.700
125.000	80.5000	8.2000	22.350	1009.000
250.000	82.0000	9.0000	22.100	993.700
400.000	80.0000	9.6000	20.550	977.000
600.000	78.0000	10.0000	18.150	954.000
800.000	75.0000	11.0000	16.400	932.000
1000.000	71.0000	11.0000	14.600	910.600
1200.000	65.0000	11.0000	12.750	890.000
1400.000	57.0000	10.4000	11.000	868.000
1700.000	40.5000	8.6000	9.950	838.000

SOURCE: Susko and Stephens (1976)

TABLE 21

27 November 1972, 1115 Z (0715 EDT)
Fair Weather, High Pressure, Normal Launch

Standard deviation of the azimuth surface wind angle is 15.000 deg.
Surface air density is 1262.230 g/m^3.
Height of surface mixing layer is 250.000.

Layer Boundary Height (m)	Wind Direction (deg)	Wind Speed (m/s)	Temperature (°C)	Pressure (mb)
2.000	280.0000	2.0000	7.100	1020.000
18.000	284.0000	2.1300	7.380	1018.000
50.000	292.0000	2.4000	8.050	1015.000
100.000	304.0000	2.8000	9.000	1010.000
150.000	317.0000	3.2000	10.000	1004.000
200.000	329.0000	3.6000	11.050	999.000
250.000	343.0000	4.0000	11.900	990.000
500.000	332.0000	4.0000	10.200	960.000
750.000	309.0000	3.0000	9.000	930.000
1200.000	292.0000	5.4000	10.050	885.000

SOURCE: Susko and Stephens (1976)

LIST OF FIGURES

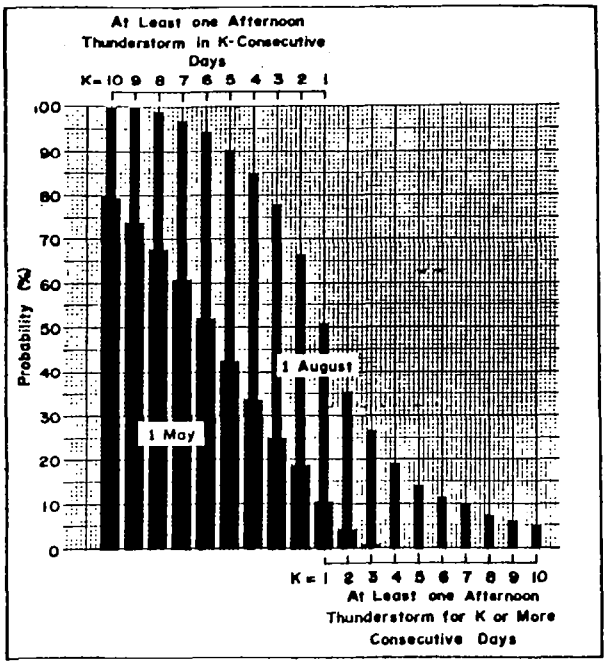

Probability (%) of specified thunderstorm event starting on August 1 and on May 1 and continuing for k-consecutive days (data derived from Part I).

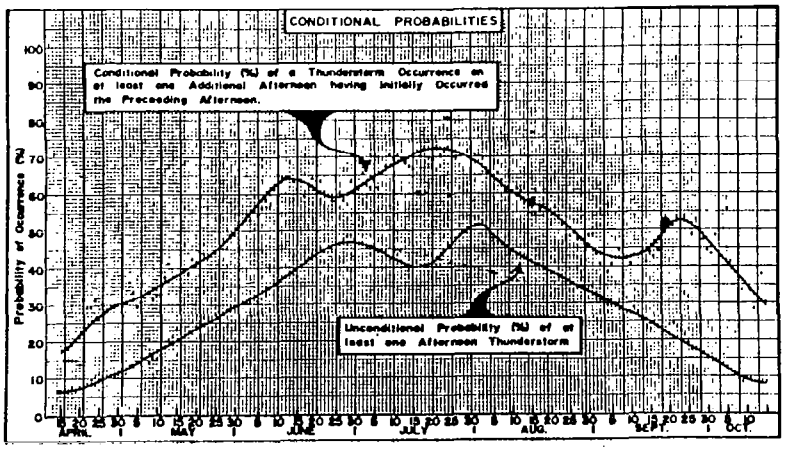

Conditional thunderstorm probabilities (data derived from Part I).

Fig. 1. Cape Canaveral thunderstorm probabilities

Source: Neumann (1970

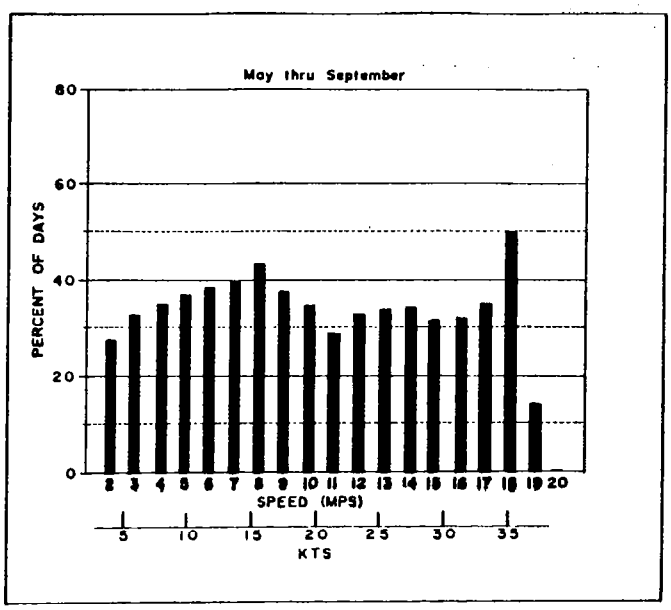

Probability of afternoon thunderstorms with 1200 GMT 3000-foot wind speeds between 2 and 20 meters per second.

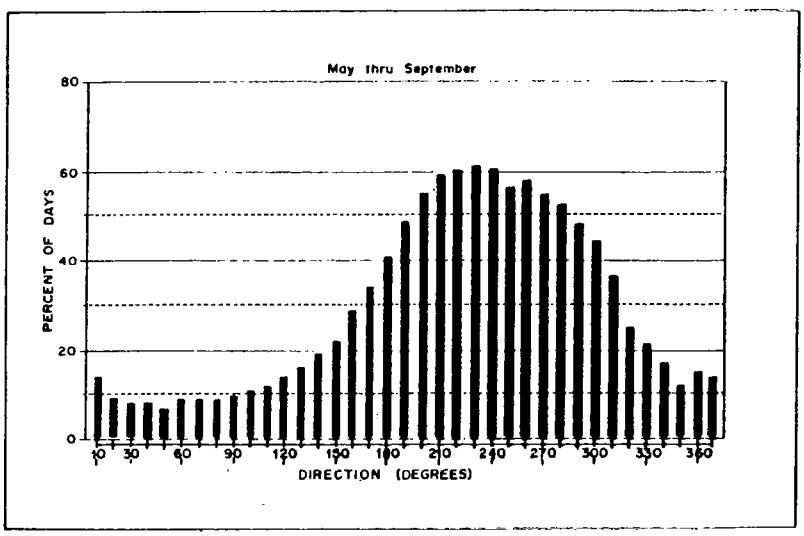

Probability of afternoon thunderstorms with each 1200 GMT 3000-foot wind direction in 10 degree increments.

Fig. 2. Cape Canaveral thunderstorm probabilities

Source: Neumann (1970

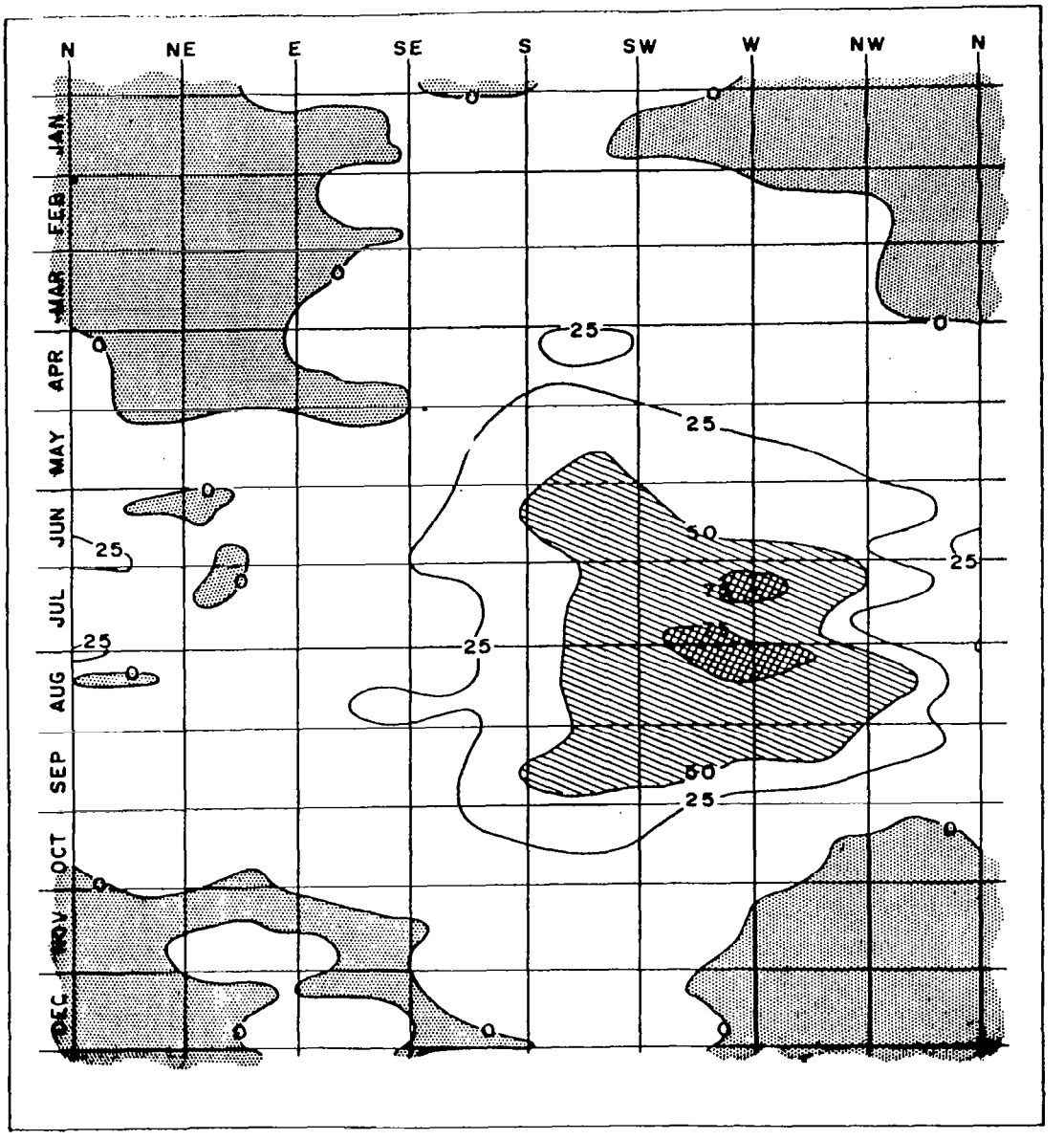

Probability (%) of afternoon thunderstorms on any given date as a function of the 1200 GMT 3000-foot wind direction only. The dot pattern shows areas where, after smoothing, thunderstorms did not occur during the period of record. Cross-hatching shows areas where, after smoothing, afternoon thunderstorms occurred over 75 percent of the time. The maximum value of 81 percent occurs about August 6 with a direction of 260 degrees. For operational use, a wind speed correction factor should be applied to the probabilities obtained from this figure.

Fig. 3. Cape Canaveral thunderstorm frequency as a function of the 900 meter wind direction

Source: Neumann (1970)

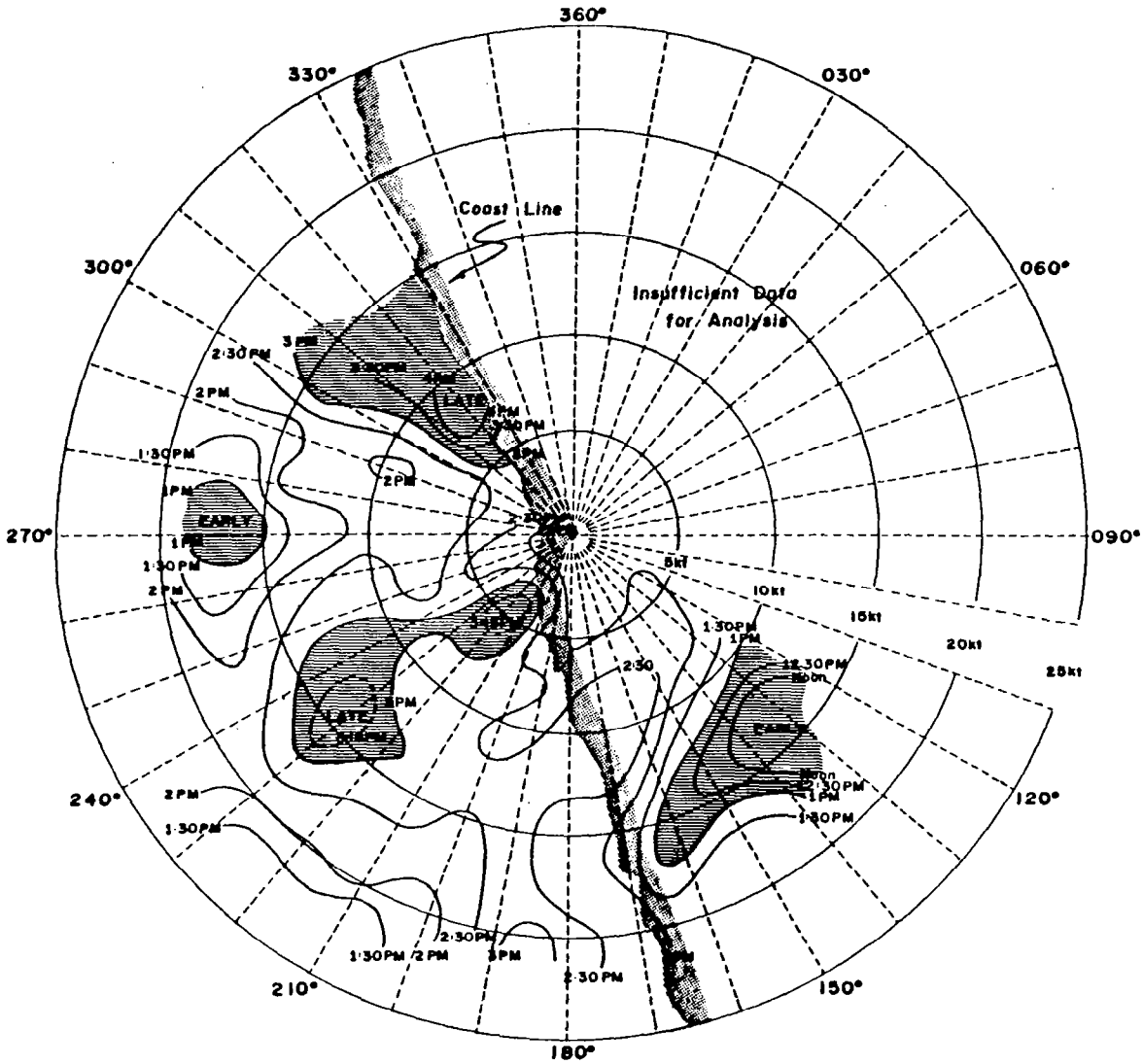

Average thunderstorm starting time between May and September as a function of the 1200 GMT 3000-foot wind speed and direction. Times are EST.

Fig. 4. Cape Canaveral average thunderstorm starting time as a function of the 1200 GMT 900-meter wind direction and speed.

Source: Neumann (1970)

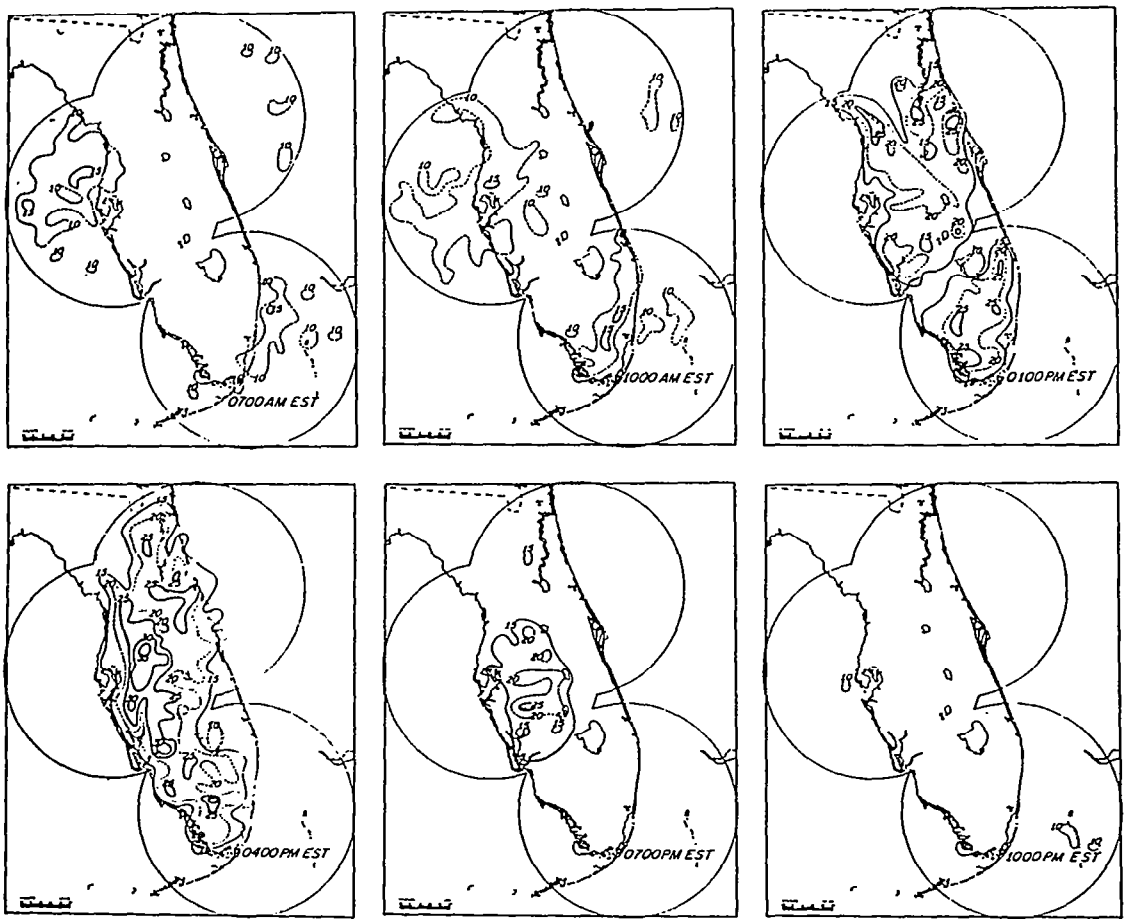

. The seasonal diurnal cycle of echo frequencies over the Florida peninsula for the months May through August 1963 excluding the 0100 and 0400 charts. Frequency isolines have been drawn in 5 per cent intervals beginning with the 10 per cent line.

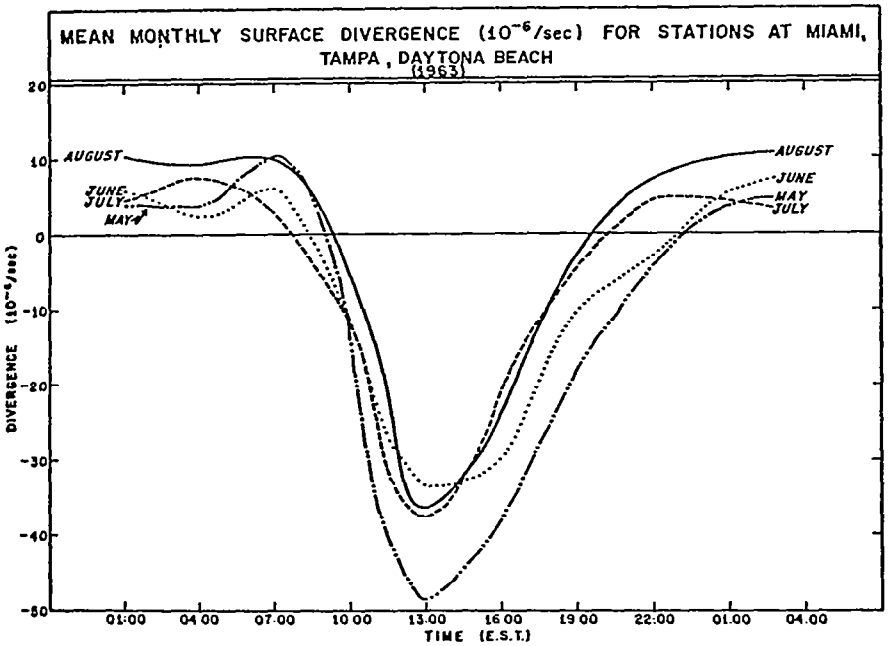

The mean monthly diurnal surface divergence curves for the months May through August 1963 over the Florida peninsula. The divergence was computed by the Bellamy (1949) method using the triangle of stations, Miami, Tampa, and Daytona Beach.

Fig. 5. Echo frequency and monthly surface divergence

Source: Frank, et al. (1967

APPENDIX I

Selected tables and figures follow from previous document entitled "Position Paper on the Potential of Inadvertent Weather Modification of the Florida Peninsula Resulting from the Stabilized Ground Cloud".

Table numbers and figure numbers correspond to the original document for ease of reference.

TABLE VI -I (Wallace - 1975)

Diurnal Frequency of Precipitation by Amount and Category by Season

Station	Percentage of hours with Precipitation (Trace or More)		Phase of Diurnal Cycle (Time of Maximum--GMT)		Normalized Amplitude	
	Jun-Aug	Nov-Mar	Jun-Aug	Nov-Mar	Jun-Aug	Nov-Mar
Jacksonville	10	10	2100	1300	.90	.10
Orlando	12	9	2100	2000	1.10	.15
West Palm Beach	11	9	1800	2000	.65	.20
Miami	10	7	1900	1800	.40	.10
	Percentage of Hours with Precip > 2.5 mmh^{-1}		"		"	
	Jun-Aug	Nov-Mar	Jun-Aug	Nov-Mar	Jun-Aug	Nov-Mar
Jacksonville	1.8	1.1	2100	1400	1.05	.20
Orlando	2.2	1.1	2100	2300	1.15	.40
West Palm Beach	2.1	1.1	1900	2100	.70	.35
Miami	2.0	0.9	2100	2000	.60	.25
	Percentage of Hours with a Trace		"		"	
	Jun-Aug	Nov-Mar	Jun-Aug	Nov-Mar	Jun-Aug	Nov-Mar
Jacksonville	5	5	2100	1300	.60	.05
Orlando	6	4	2100	2100	.55	.20
West Palm Beach	5	5	1800	2000	.50	.15
Miami	5	4	1900	1800	.35	.20

TABLE VI -II (Wallace - 1975)

Diurnal Cycle in the Thunderstorm Frequency by Season

Station	Percentage of Hours of Audible Thunder		Phase of Diurnal Cycle (Time of Max-GMT)		Normalized Amplitude	
	Jun-Aug	Nov-Mar	Jun-Aug	Nov-Mar	Jun-Aug	Nov-Mar
Eglin AFB	4.5	5.5	2000	0300	.65	.20
Panama City	3.2	4.8	2000	1000	.70	.45
Tallahassee	4.8	7.6	2100	1600	1.30	.30
Jacksonville	2.8	1.7	2100	2300	1.40	.40
Daytona Beach	4.9	3.2	2100	2300	1.50	.65
Orlando	3.8		2200		1.60	
Tampa	4.4	2.2	2200	0000	1.55	.35
Vero Beach	5.6		2100		1.40	
Fort Myers	4.4		2200		1.60	
West Palm Beach	3.2	2.0	2100	0000	1.10	.30
Miami	3.7		2100		1.10	

TABLE VI -III

Mandatory Level Temperatures Across Florida

After Newell, et al. (1972)

Station	850 mb		700 mb		500 mb	
	Dec-Feb	Jun-Aug	Dec-Feb	Jun-Aug	Dec-Feb	Jun-Aug
Eglin AFB	7.6	17.5	1.5	8.1	-14.2	-7.1
Jacksonville	8.0	17.5	1.8	8.4	-13.9	-7.2
Cape Canaveral	10.0	17.7	3.8	8.1	-12.3	-7.4
Tampa	9.6	17.8	3.6	7.9	-12.0	-7.3
Miami	11.3	17.4	5.1	8.2	-10.4	-7.4
Key West	12.2	17.8	5.7	8.4	- 8.7	-7.1

Units (°C)

TABLE VI -IV

Mandatory Level Winds Across Florida After Newell et al. (1972)

December-February

Station	Surface		850 mb				700 mb		500 mb			
	u	v	u	σ(u)	v	σ(v)	u	v	u	σ(u)	v	σ(v)
Eglin AFB	0.2	-0.0	5.2	6.9	0.4	7.8	13.0	1.5	23.3	10.8	3.5	10.9
Jacksonville	0.1	-0.7	6.3	6.6	1.4	6.9	12.8	1.5	22.9	10.9	2.1	9.7
Cape Canaveral	0.5	-0.8	8.1	6.1	2.2	8.7	10.1	1.7	29.4	6.1	5.1	14.5
Tampa	1.0	-1.2	3.7	6.7	1.1	5.8	15.7	2.8	18.1	8.2	3.6	7.8
Miami	-0.8	-0.2	2.2	6.9	0.6	4.9	7.2	1.6	15.5	8.6	5.0	7.0
Key West	-1.1	-1.7	1.5	6.5	0.3	5.1	6.1	1.0	17.0	8.3	1.7	6.2

June-August

	u	v		σ(u)	v	σ(v)	u	v	u	σ(u)	v	σ(v)
Eglin AFB	0.9	1.8	0.4	4.6	0.2	4.1	1.3	0.0	2.7	5.9	0.1	5.0
Jacksonville	-1.9	1.4	1.2	4.6	0.5	4.1	1.6	0.3	2.5	5.6	0.2	4.7
Cape Canaveral	-1.8	0.4	-1.0	6.6	1.7	5.0	1.3	1.4	2.0	8.4	0.6	6.0
Tampa	0.5	-0.3	-0.7	4.4	1.1	3.5	1.0	0.8	1.0	5.4	0.6	4.3
Miami	-1.9	0.9	-1.6	4.3	0.6	3.2	- 0.7	0.9	- 0.4	5.2	1.1	4.0
Key West	-2.0	0.6	-2.3	4.1	0.7	3.1	- 1.0	0.9	- 0.9	4.8	0.5	3.5

UNITS: ms^{-1}

TABLE VI -V

Cape Canaveral: Selected Upper Air Data by Pressure

		Jan	Apr	Jul	Oct
1000 mb	T(°C)	15.7	20.5	25.6	23.2
	(T)	4.8	2.9	1.7	2.7
	%RH	73	70	80	75
850 mb	T(°C)	9.3	12.5	17.3	14.3
	(T)	3.7	3.1	1.2	2.5
	%RH	56	56	71	69
700 mb	T(°C)	3.1	5.0	7.9	6.7
	(T)	3.1	2.4	1.2	2.1
	%RH	33	34	59	46

Data Source: Patrick AFB 1950-1956
Cape Canaveral 1956-1970 0000 GMT Only

TABLE VI -VI

Cape Canaveral: Selected Upper Air Data by Height

	March		June		September		December	
	T(°C)	%RH	T(°C)	%RH	T(°C)	%RH	T(°C)	%RH
Surface	20.7	81	27.5	79	27.9	80	18.5	85
500 m	17.5	74	23.2	80	23.7	83	16.1	78
1000 m	14.7	75	20.0	72	19.7	79	13.2	78
1500 m	12.4	75	17.2	73	17.2	78	10.8	75
2000 m	10.1	63	13.9	69	14.7	74	9.4	57
3000 m	5.0	41	8.5	65	9.4	70	5.1	25
4000 m	- 0.6	33	2.9	42	3.9	64	- 0.3	--
5000 m	- 6.9	33	- 2.8	42	- 1.8	57	- 6.3	--

Data Source: NASA - Cape Canaveral (1950-1960)
0000 GMT Data Only

TABLE VI -VII

Cape Canaveral: 50% Cumulative Frequency Winds by Height

	March					June				
	u	v	θ	V_r	$\|\bar{V}\|$	u	v	θ	V_r	$\|\bar{V}\|$
Surface	- 0.4	-0.4	045	0.6	3.7	- 0.9	-0.0	090	0.9	2.8
1000 m	2.6	0.8	253	2.7	7.4	- 0.3	0.7	156	0.8	4.6
2000 m	6.0	0.6	264	6.0	8.4	0.5	0.0	270	0.5	4.6
3000 m	9.4	0.4	268	9.4	11.7	1.0	-0.2	281	1.0	4.5
4000 m	13.5	-0.3	271	13.5	15.5	1.2	-0.4	288	1.3	4.6
5000 m	17.2	-0.3	271	17.2	19.2	1.3	-0.4	287	1.4	4.8

	September					December				
	u	v	θ	V_r	$\|\bar{V}\|$	u	v	θ	V_r	$\|\bar{V}\|$
Surface	- 2.8	-0.6	078	2.9	3.0	- 0.0	-1.4	360	1.4	3.1
1000 m	- 3.7	-0.4	084	3.7	5.5	- 0.6	-0.7	041	0.9	7.1
2000 m	- 2.6	-0.4	081	2.6	5.2	1.7	-0.2	083	1.7	6.3
3000 m	- 1.3	-0.3	077	1.3	4.8	5.0	-0.0	270	5.0	8.1
4000 m	- 1.8	-0.2	084	1.8	4.8	9.1	0.2	269	9.1	11.4
5000 m	- 0.7	-0.4	060	0.8	4.9	11.8	0.4	268	11.8	14.3

UNITS: ms^{-1}
θ = resultant wind direction
V_r = resultant wind speed
$|\bar{V}|$ = scalar mean wind speed

Data Source: 1950-1960 - NASA
0000 GMT Only

TABLE VI -VIII

Cape Canaveral: Diurnal Variation of Height
Temperature and Relative Humidity

Time GMT	Surface			950 mb			900 mb			850 mb		
	PRES(mb)	T(°C)	%RH	HT(m)	T(°C)	%RH	HT(m)	T(°C)	%RH	HT(m)	T(°C)	%RH
March												
0000	1017.0	18.4	73	587	16.1	65	1045	13.1	66	1524	10.3	63
1200	1017.7	14.8	85	588	14.6	71	1045	12.1	67	1522	10.0	60
June												
0000	1014.6	25.9	78	583	22.3	74	1052	19.6	71	1542	16.6	70
1200	1015.2	23.3	89	585	21.4	79	1058	18.9	72	1542	16.2	70
September												
0000	1013.7	26.1	80	577	22.5	79	1046	19.7	77	1536	16.8	76
1200	1014.0	23.7	89	577	22.0	83	1046	19.2	79	1536	16.5	76
December												
0000	1018.6	15.9	79	596	14.5	67	1052	12.0	64	1529	9.7	59
1200	1019.1	12.9	85	595	13.6	72	1049	11.6	66	1528	9.7	58

DATA SOURCE: WBAN 33 Forms 1960-1969
National Climatic Center

TABLE VI -IX

Cape Canaveral: 850 mb Diurnal Wind Frequencies (%)

Time (GMT)		Direction Frequency (%)				Onshore	Offshore	Northerly	Southerly
		001-090	091-180	181-270	271-360	← (%) →			
June	0000	23	24	29	24	47	53	53	47
	1200	19	26	44	11	45	55	30	70
Dec.	0000	14	15	35	36	29	71	50	50
	1200	12	17	40	31	29	71	43	57

DATE SOURCE: WBAN 33 Forms 1960-1969
National Climatic Center

TABLE VI -X

Florida Mean Seasonal and Annual Morning and Afternoon

Mixing Heights (H) and Wind Speeds (u) for NOP[1] and ALL[2] Cases After Holzworth (1972)

Station	Time[3]	Winter					Spring					Summer					Autumn					Annual				
		H, m			U, m sec^{-1}		H, m			U, m sec^{-1}		H, m			U, m sec^{-1}		H, m			U, m sec^{-1}		H, m			U, m sec^{-1}	
		NOP	All	% NOP	NOP	All	NOP	All	% NOP	NOP	All	NOP	All	% NOP	NOP	All	NOP	All	% NOP	NOP	All	NOP	All	% NOP	NOP	All
Jacksonville, Florida	M	345	403	79.4	5.2	5.9	447	477	90.4	5.3	5.6	567	583	91.1	4.3	4.4	418	458	85.9	4.7	5.0	444	480	86.7	4.9	5.2
	A	1058	1104	80.1	6.7	7.0	1639	1667	86.1	7.1	7.2	1681	1712	68.0	5.6	5.8	1321	1342	80.4	6.5	6.5	1424	1456	78.6	6.5	6.7
Tampa, Florida	M	394	436	85.8	5.8	6.1	503	526	91.7	5.6	5.8	656	674	91.1	4.2	4.3	419	439	89.2	5.4	5.6	493	519	89.4	5.3	5.4
	A	1052	1079	81.4	6.4	6.6	1523	1544	87.8	6.7	6.8	1460	1526	68.9	5.0	5.3	1401	1429	84.4	6.4	6.8	1359	1394	80.6	6.2	6.4
Miami, Florida	M	654	707	87.2	5.4	5.7	947	980	91.1	5.7	5.9	1041	1071	88.3	4.3	4.5	872	933	82.4	5.0	5.3	878	923	87.2	5.1	5.3
	A	1208	1221	89.2	6.4	6.5	1440	1459	87.4	6.8	6.9	1360	1383	73.7	5.3	5.5	1315	1341	78.7	6.6	6.9	1330	1351	82.2	6.3	6.5

DATA SOURCE: 1960-1964

[1]NOP: Omitting Cold Advection and Precipitation Cases

[2]ALL: Includes all Available Data

TABLE VI -XI

Episode-Days of High Meteorological Air Pollution Potential

(After Holzworth [1972])

Station	Wind Speed (ms^{-1})	Mixing Heights (M) 500	10000	1500	2000
Jacksonville	2	0(0)	0 (0)	0 (0)	0 (0)
	4	0(0)	2 (5) Win.	12 (28) Win.	23 (50) Win.
	6	1(3) Win.	12(29) Win.	43(116) Win.	105(314) Aut.
Tampa	2	0(0)	0 (0)	0 (0)	0 (0)
	4	0(0)	1 (2) Spr.	9 (23) Win.	15 (38) Sum.
	6	1(2) Win.	14(29) Win.	79(234) Win.	127(406) Sum.
Miami	2	0(0)	0 (0)	0 (0)	0 (0)
	4	0(0)	0 (0)	17 (38) Sum-Aut.	25 (60) Sum.
	6	0(0)	3(11) Win.	79(207) Sum.	128(406) Sum.

DATE SOURCE: 1960-1964

First figure is the number of episodes; the number of episode-days is given in parentheses. Seasonal Peaks as Indicated.

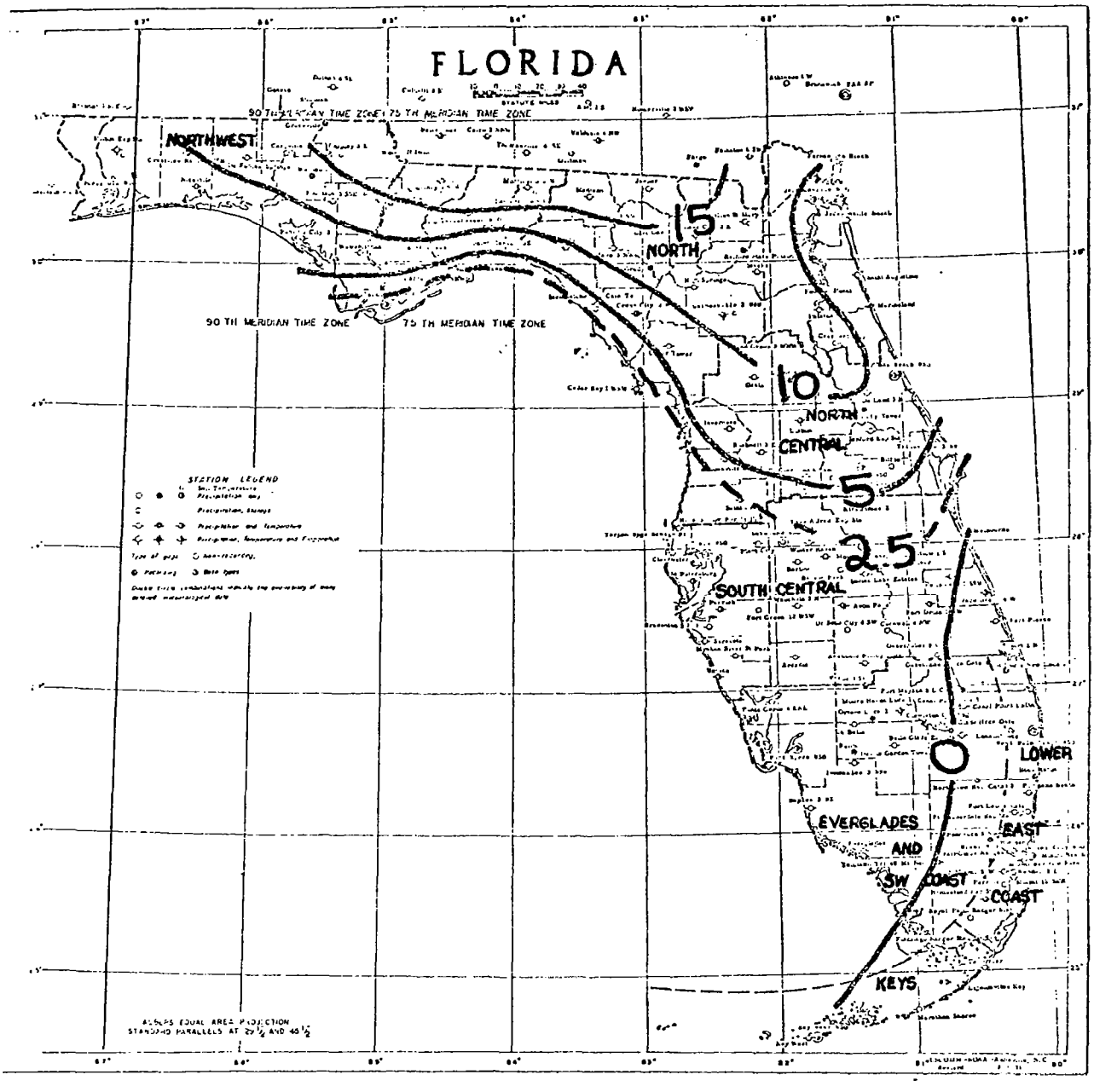

Figure VI -11: Days of Heavy Fog: Visibility $\leq$ 0.4 km
May-October

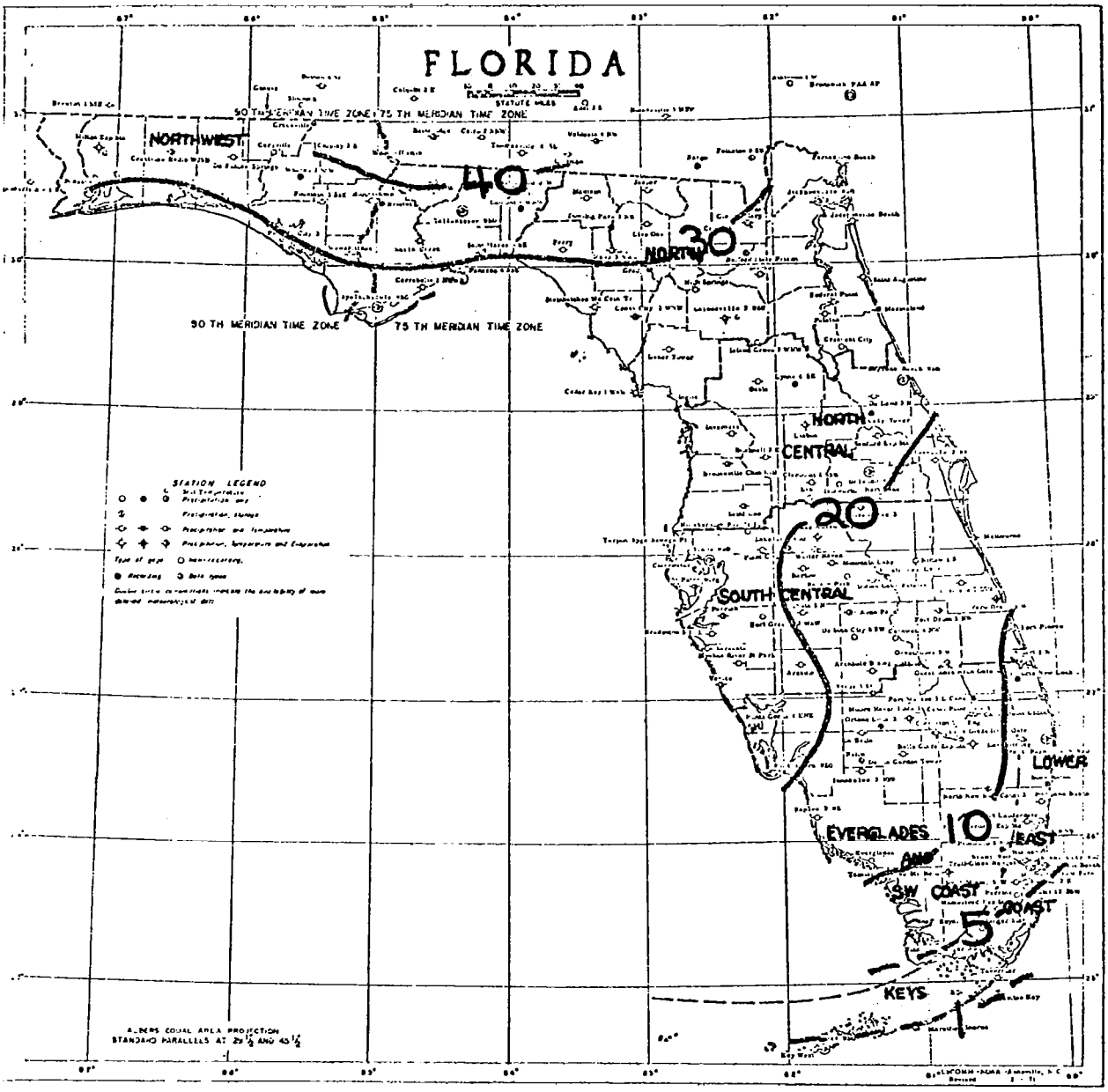

Figure VI -12: Days of Heavy Fog: Visibility ≤ 0.4 km
November-April

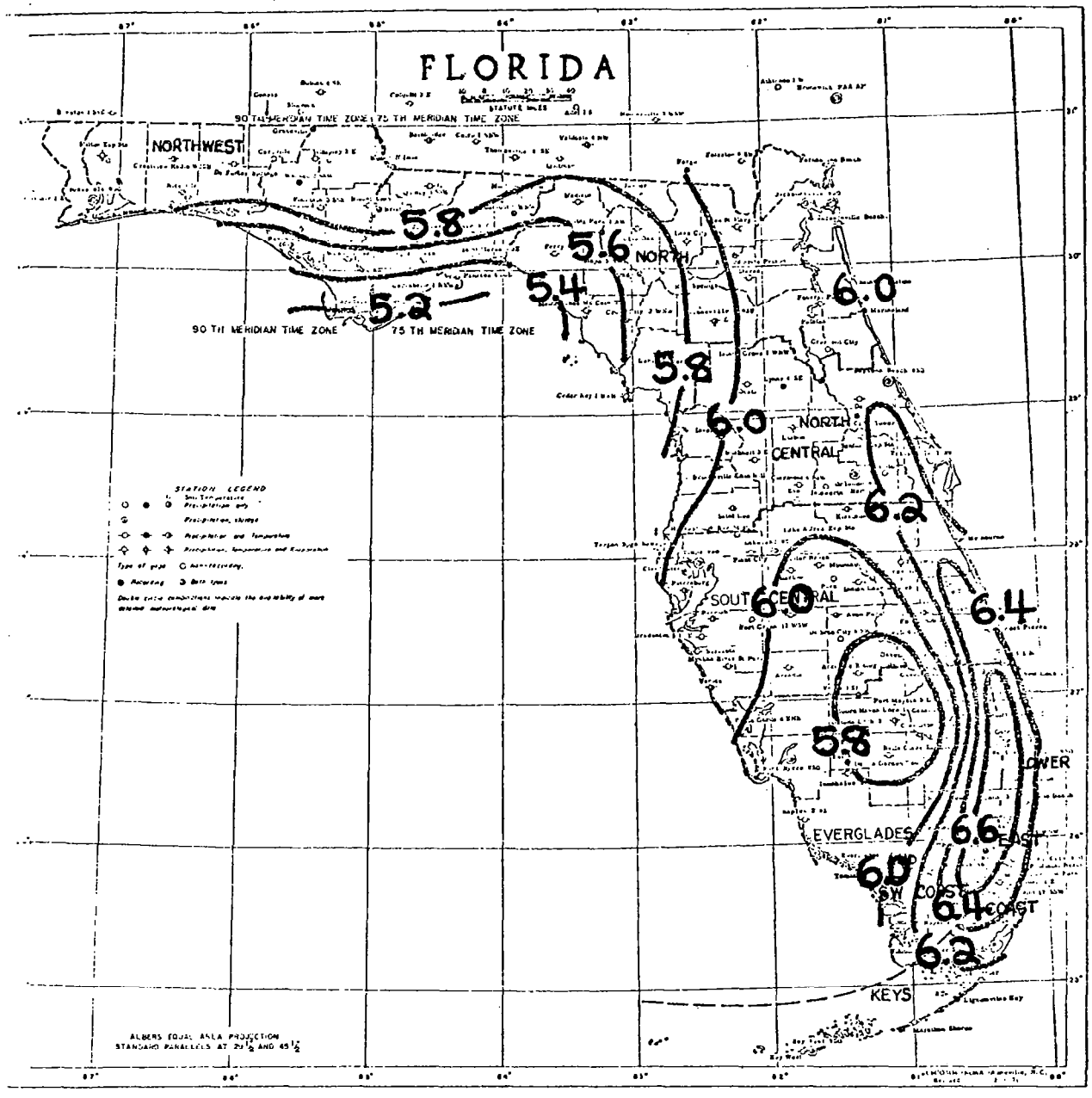

Figure VI -15: Mean Cloud Cover (Tenths) Sunrise-Sunset
May-October

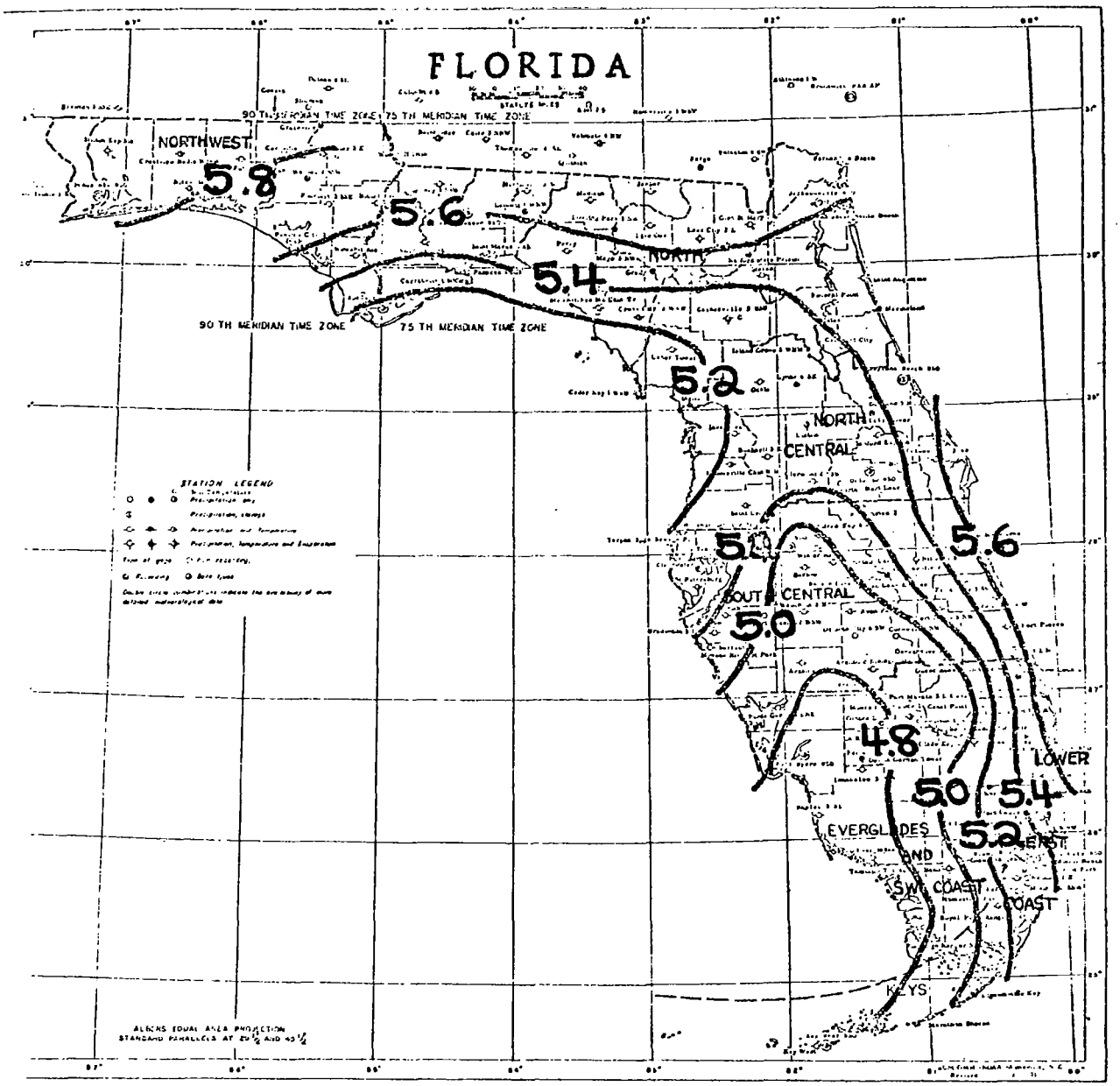

Figure VI -16: Mean Cloud Cover (Tenths) Sunrise-Sunset November-April

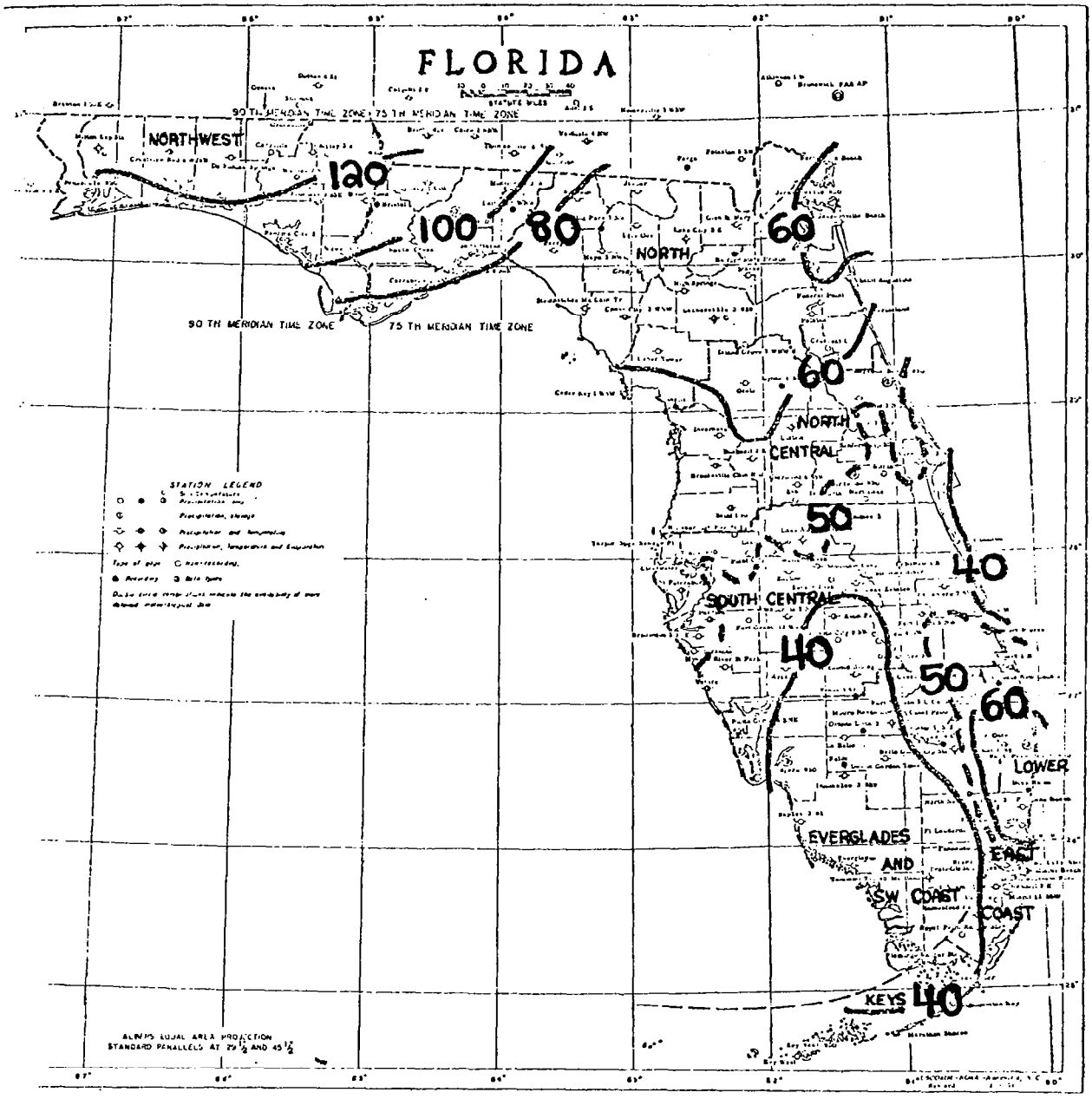

Figure VI -17: Mean Monthly Precipitation (mm)
December

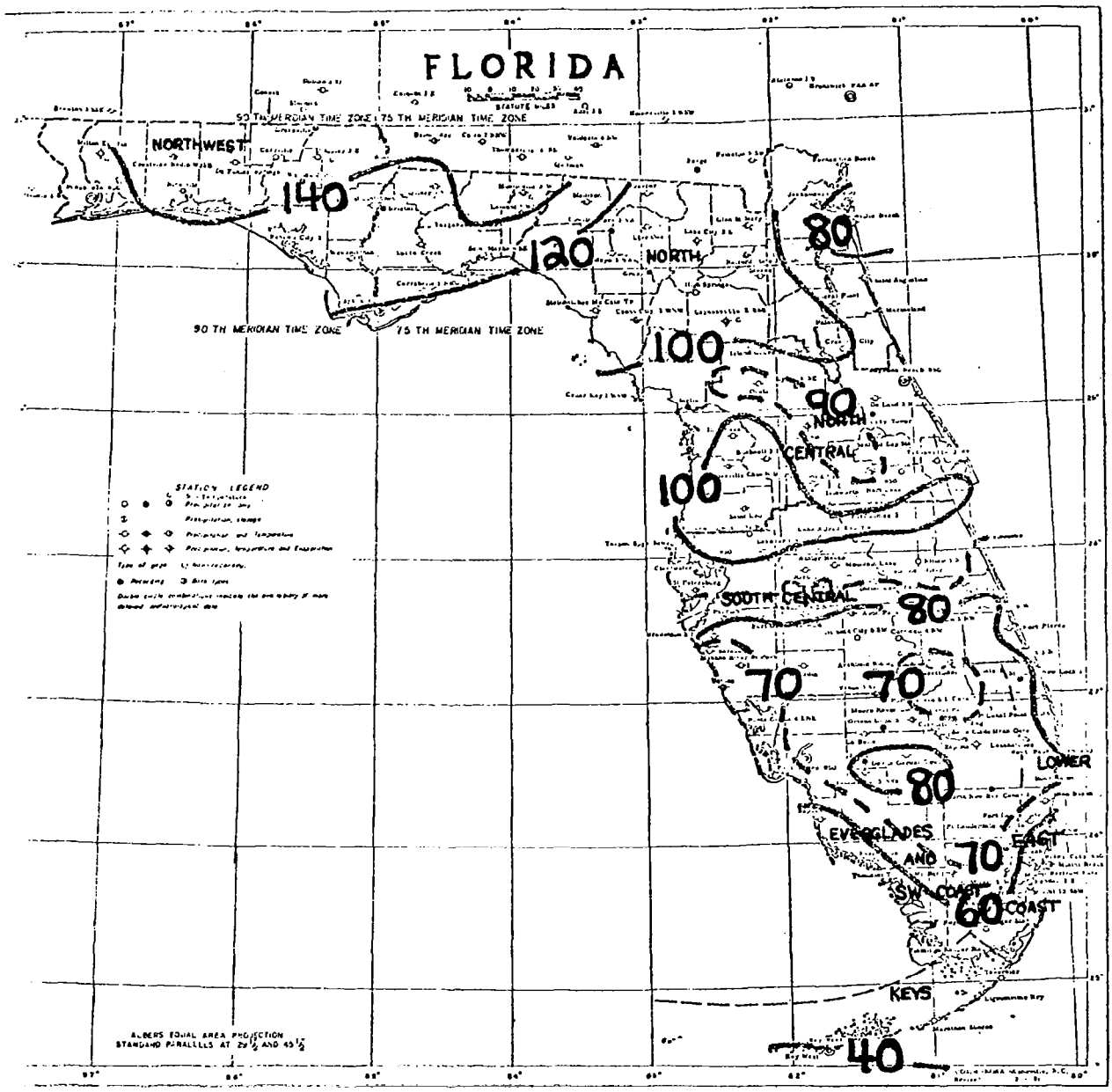

Figure VI -18: Mean Monthly Precipitation (mm)
March

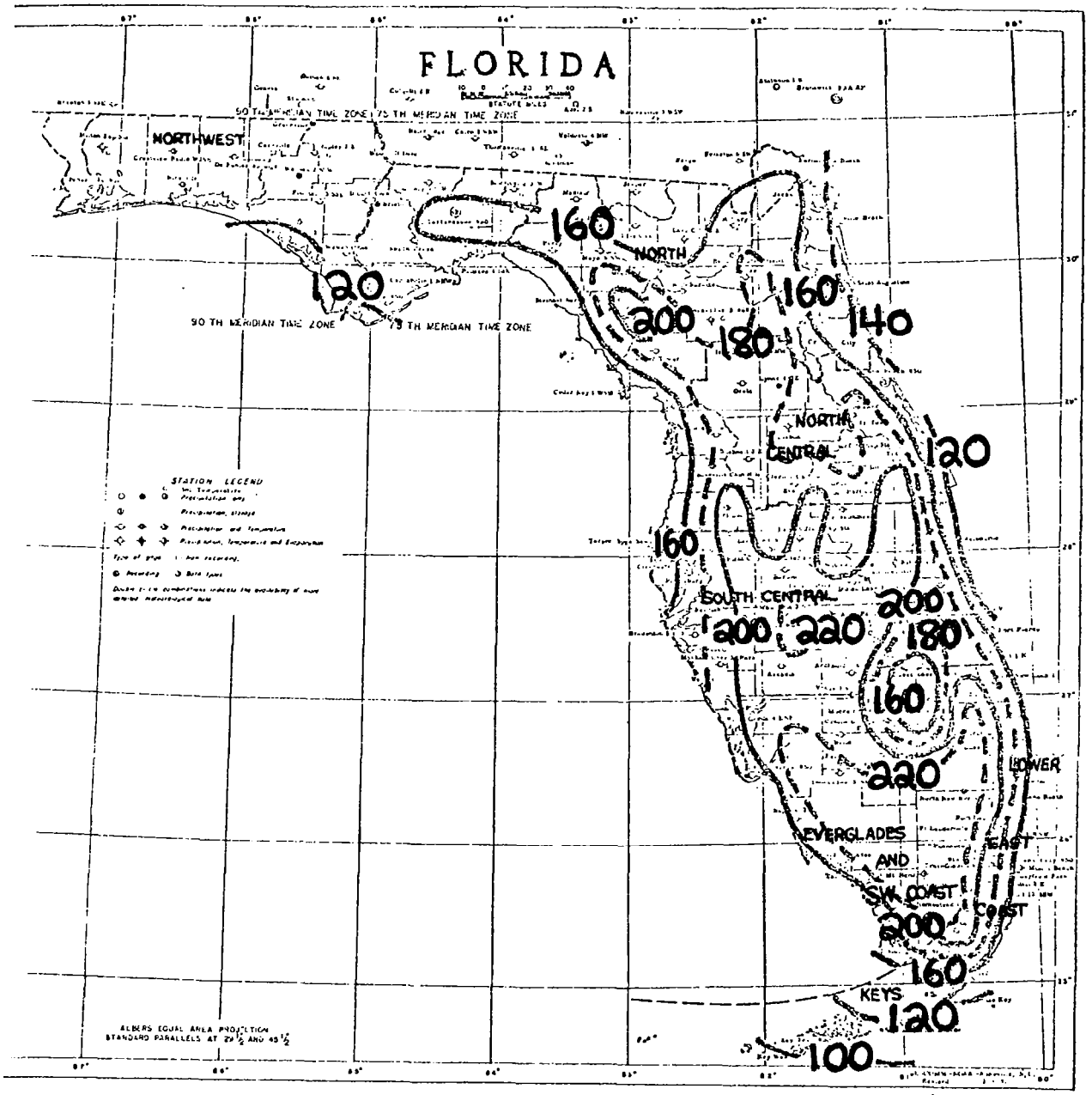

Figure VI -19: Mean Monthly Precipitation (mm)
June

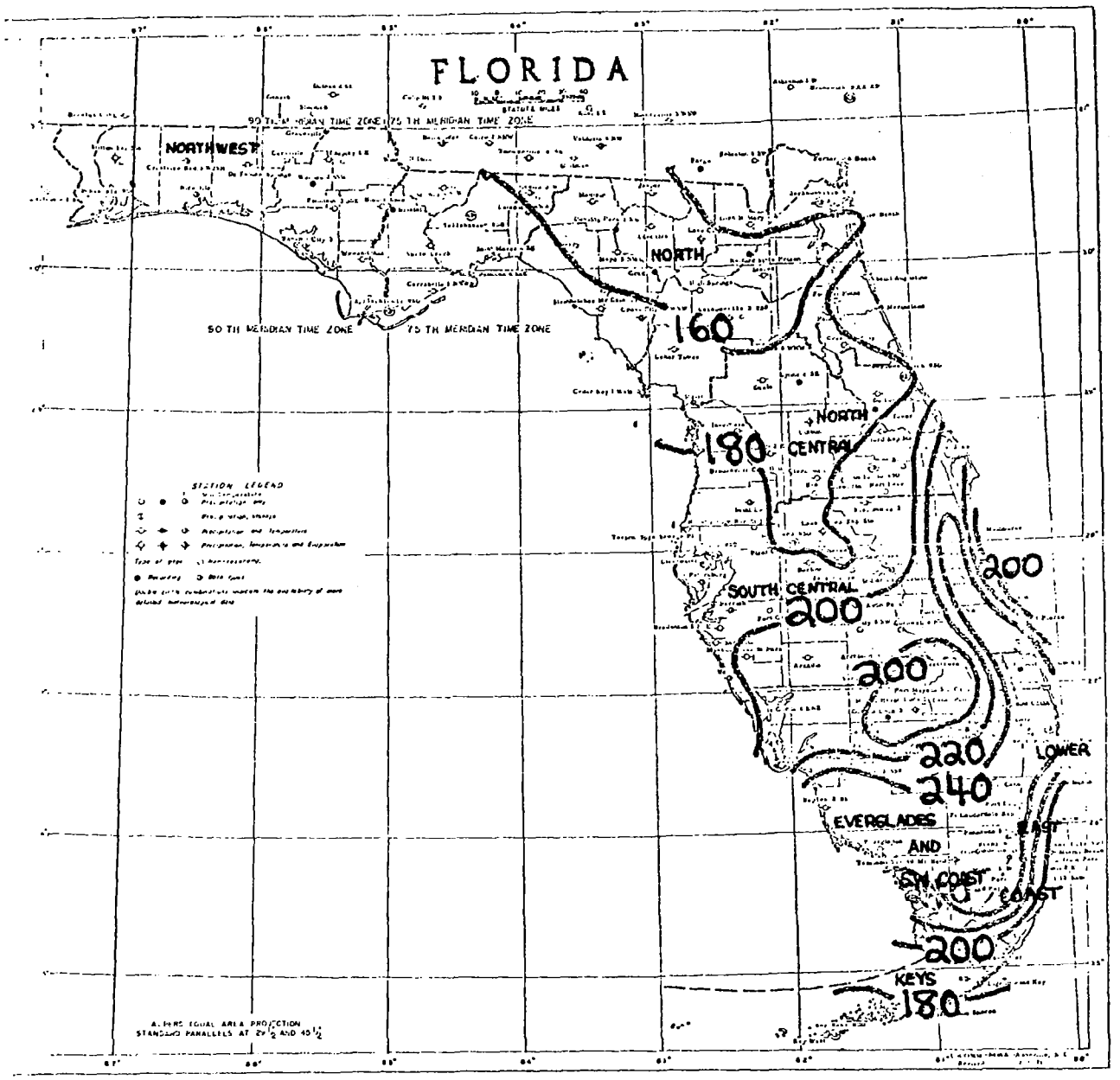

Figure VI -20: Mean Monthly Precipitation (mm)
September

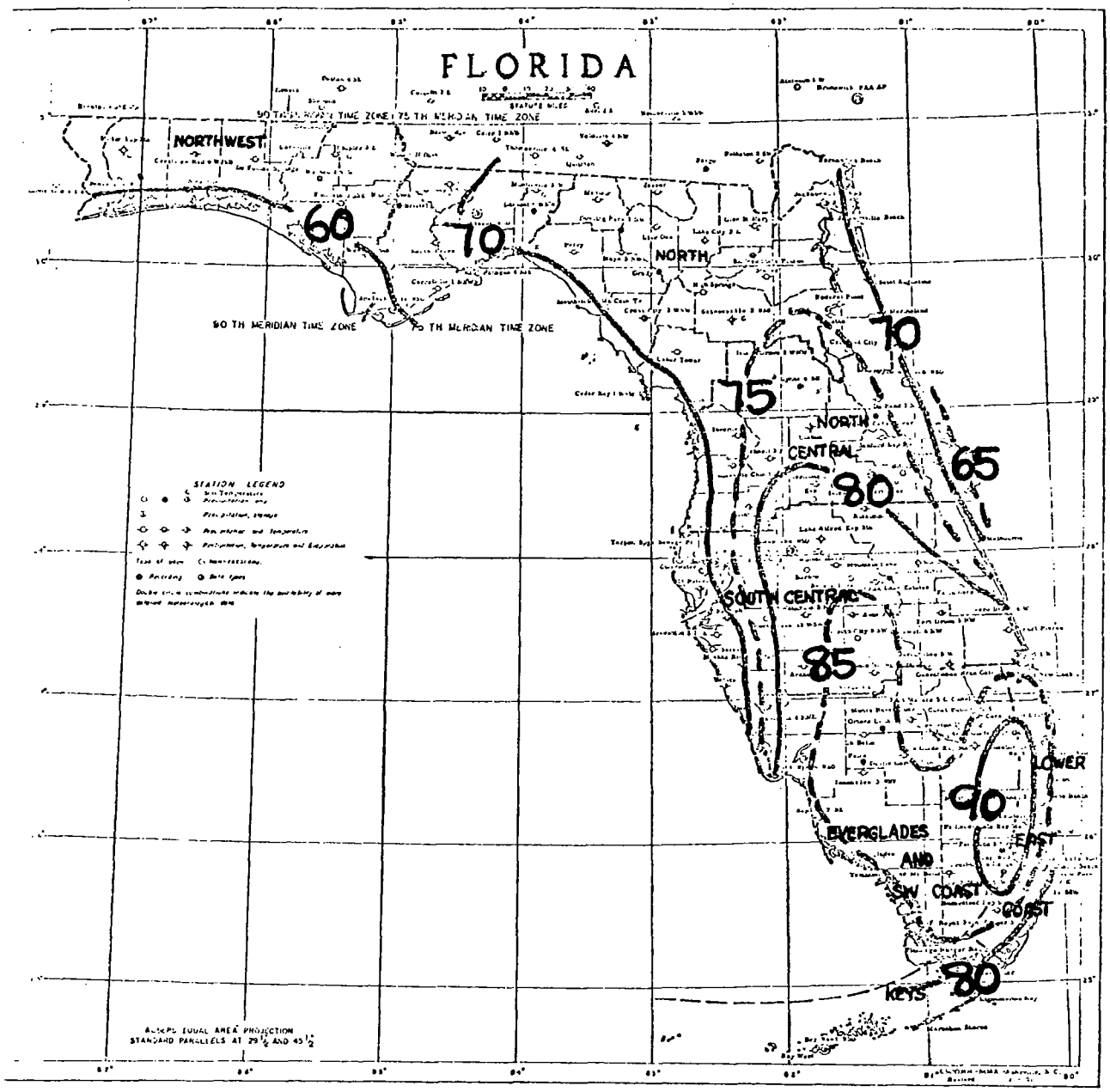

Figure VI -21: Mean Number of Days Precipitation ≥ 0.25 mm
May-October

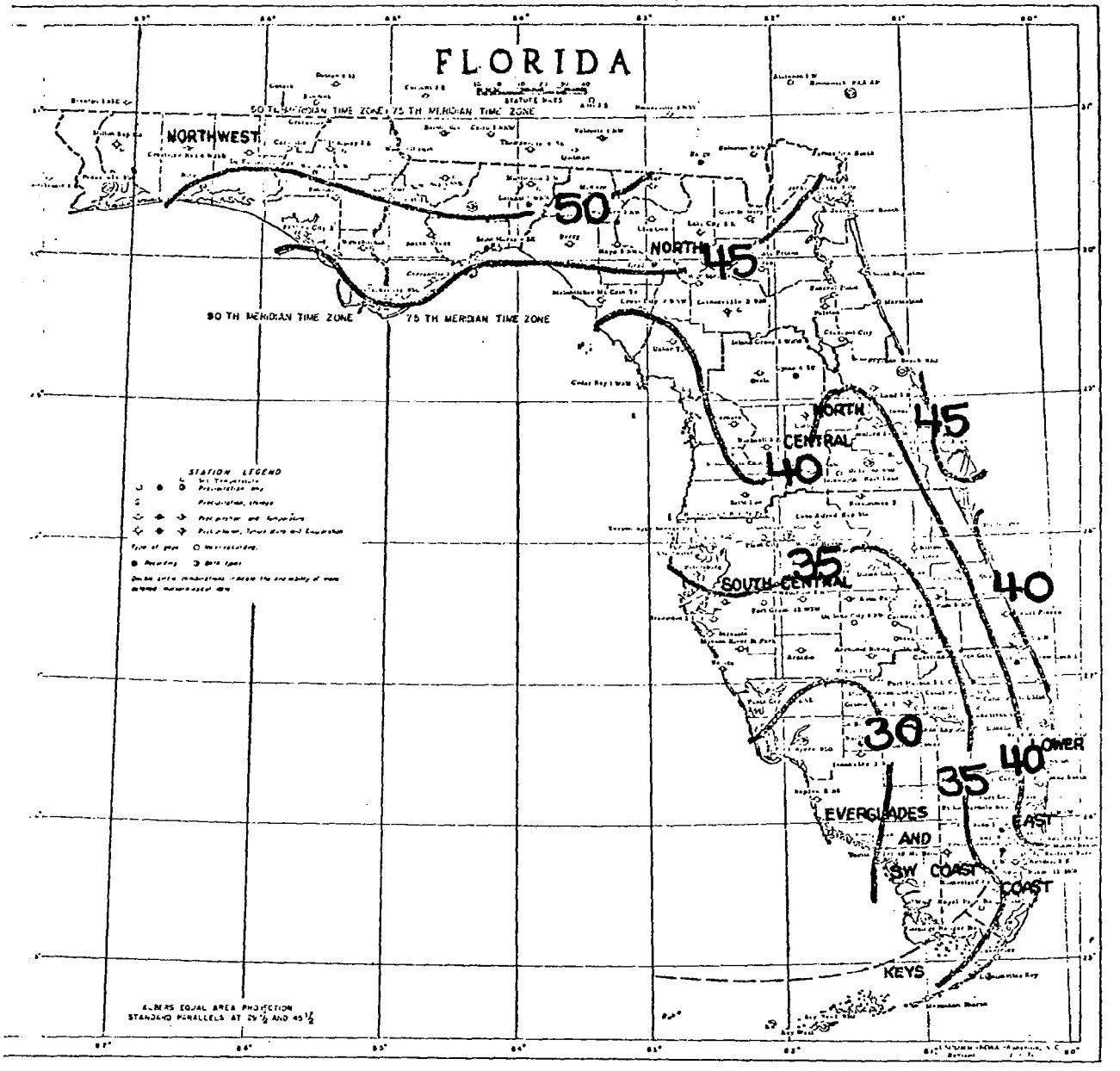

Figure VI -22: Mean Number of Days Precipitation ≥ 0.25 mm
November-April

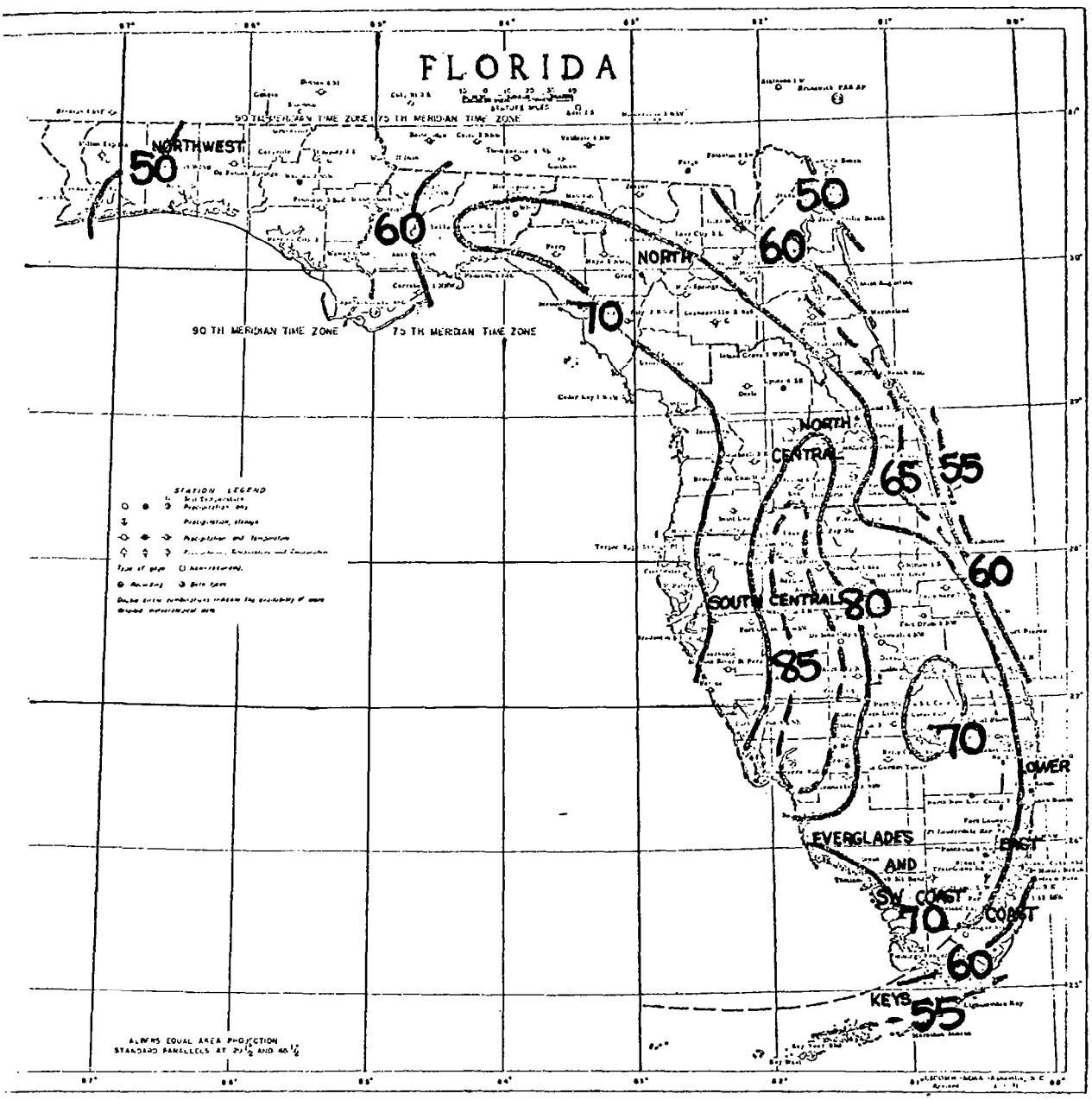

Figure VI -25: Number of Thunderstorm Days
May-October

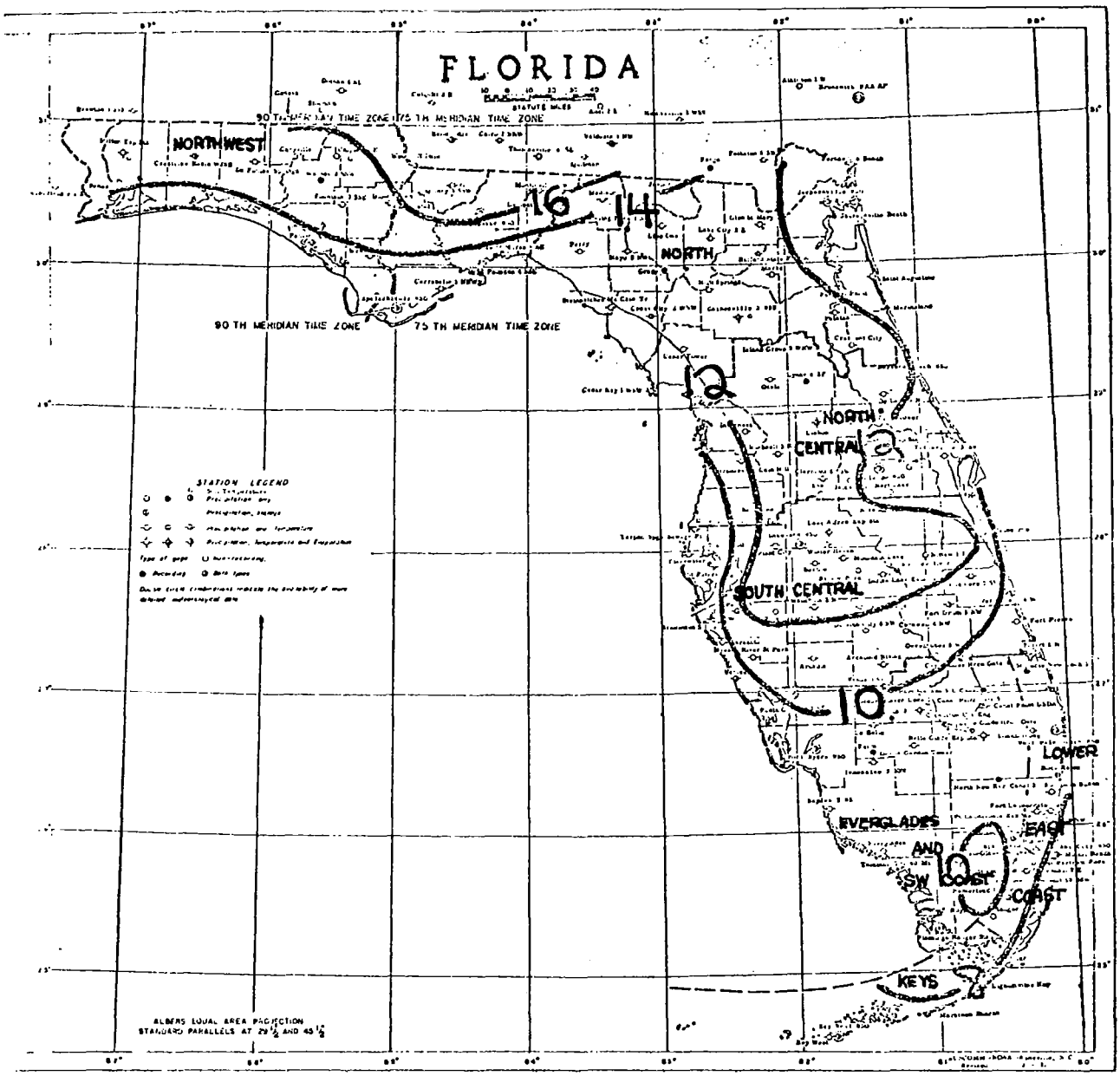

Figure VI -26: Number of Thunderstorm Days
November-April

AWS CLIMATIC BRIEF — CAPE KENNEDY AFS, FLORIDA — PERIOD 1950-65 — WBAN # 12836 — WMO # 74794

Prepared by ETAC (FEB 1970) — N 28 29 W 80.33 — ELEVATION: 29 ft — STN LTRS: XMR

MONTH	TEMPERATURE (°F) EXTREME MAXIMUM	MEAN DAILY MAXIMUM	MEAN DAILY MINIMUM	EXTREME MINIMUM	PRECIPITATION (in) MEAN TOTAL	MAXIMUM IN 24 HOURS	MEAN SNOWFALL	MAX SNOWFALL IN 24 HOURS	WIND (KT) PREVAILING DIRECTION	MEAN SPEED	EXTREME (FAST-MILE) (GUSTS) SPEED	MEAN 0400 RELATIVE HUMIDITY (%)	MEAN 1300 RELATIVE HUMIDITY (%)	MEAN DEW POINT (°F)	MEAN VAPOR PRESSURE (in Hg)	PRESSURE ALTITUDE (Feet) 99.95%	MEAN NUMBER OF DAYS PRECIP ≥ 0.01 in	PRECIP ≥ 0.5 in	SNOWFALL ≥ 0.1 in	SNOWFALL ≥ 1.5 in	THUNDERSTORMS	FOG (< 7 miles)	TEMPERATURE (°F) MAXIMUM IV 90	MAXIMUM IV 80	MINIMUM IA 32	MINIMUM IA 0	MEAN CLDS (TENTHS)
JAN	82	69	52	29	3.0	3.0	0	0	NW	8	46	89	65	53	.40	350	7	2	0	0	1	11	0	1	1	0	5
FEB	86	70	53	28	3.4	2.1	0	0	N	9	43	89	67	55	.43	350	8	2	0	0	1	8	0	3	#	0	5
MAR	88	73	57	34	4.1	5.6	0	0	N	9	46	88	64	57	.47	350	9	3	0	0	3	7	0	5	0	0	5
APR	89	77	62	44	2.0	2.6	0	0	ESE	9	53	86	62	61	.54	350	6	1	0	0	4	3	0	10	0	0	5
MAY	94	82	67	47	1.8	1.4	0	0	E	8	37	90	64	67	.66	250	7	1	0	0	7	3	1	25	0	0	5
JUN	98	86	72	61	4.2	2.7	0	0	S	7	43	93	69	72	.78	200	10	3	0	0	13	2	4	30	0	0	5
JUL	95	88	74	67	5.7	3.6	0	0	S	6	41	94	70	74	.84	150	11	4	0	0	13	1	6	31	0	0	5
AUG	94	88	74	67	6.0	5.8	0	0	E	6	60	95	71	74	.84	200	11	4	0	0	16	2	6	31	0	0	6
SEP	94	86	74	62	8.9	6.9	0	0	E	8	68	90	72	73	.81	250	14	5	0	0	9	1	1	29	0	0	6
OCT	91	81	70	50	5.1	6.4	0	0	N	8	38	87	68	67	.66	350	12	3	0	0	4	3	#	21	0	0	5
NOV	86	75	60	31	3.5	5.9	0	0	NW	8	37	87	66	61	.54	300	8	2	0	0	1	7	0	7	#	0	5
DEC	85	70	53	25	1.6	1.4	0	0	NW	8	37	87	65	54	.42	250	7	1	0	0	1	8	0	1	1	0	5
ANN	98	79	64	25	49.2	6.9	0	0	E	8	68	90	65	64	.60	300	110	31	0	0	73	56	18	194	2	0	5
EYR	11	11	11	11	11	11	11	11	14	14	7	14	14	14	14	10	11	11	11	11	13	13	11	11	11	11	14

REMARKS

RUSSWO:
POR: Hourly Obsns: Jun 50-Dec 53, Apr 56-Apr 66.
Daily Obsns : Jun 50-Dec 53, Apr 56-May 65.

NOTE: *DATA NOT AVAILABLE. #LESS THAN 0.5 DAY, 0.5 OR 0.05 INCH, OR 0.5 PERCENT (%) AS APPLICABLE.

FLYING WEATHER (%FREQ)	HOURS (LST)	JAN	FEB	MAR	APR	MAY	JUN	JUL	AUG	SEP	OCT	NOV	DEC	ANN	EYR
CIG less than 3000 feet and/or VSBY less than 3 miles	00-02	14	15	7	4	4	4	1	2	8	9	11	12	7	
	03-05	19	18	9	7	5	5	1	4	8	11	12	12	9	
	06-08	21	21	13	8	5	6	2	5	8	9	13	15	10	
	09-11	12	14	13	7	4	7	4	7	9	10	11	11	9	
	12-14	10	11	11	5	3	8	7	9	12	12	11	9	9	
	15-17	7	10	8	4	4	8	8	8	12	12	8	7	8	
	18-20	8	9	7	4	5	4	4	5	11	10	7	8	7	
	21-23	10	11	7	3	4	4	1	3	9	9	7	10	7	
	ALL HOURS	12	14	9	5	4	6	4	5	9	10	10	11	8	14
CIG less than 1500 feet and/or VSBY less than 3 miles	00-02	8	9	4	1	1	1	#	#	1	2	5	6	3	
	03-05	13	12	6	4	2	2	#	2	1	3	7	7	5	
	06-08	15	14	10	4	2	3	1	2	2	4	7	10	6	
	09-11	8	8	7	2	1	1	1	1	2	3	4	6	4	
	12-14	4	5	4	1	#	1	1	1	2	2	3	4	2	
	15-17	2	5	3	2	1	1	1	1	3	2	3	3	2	
	18-20	4	4	3	1	1	#	1	1	3	2	3	2	2	
	21-23	5	5	4	1	#	1	#	1	1	1	3	3	2	
	ALL HOURS	7	8	5	2	1	1	1	1	2	2	4	5	3	14
CIG less than 1000 feet and/or VSBY less than 2 miles	00-02	5	6	2	1	1	1	#	#	#	1	3	4	2	
	03-05	10	9	5	3	1	1	#	1	1	2	5	5	4	
	06-08	12	11	6	3	2	2	1	2	2	3	5	8	5	
	09-11	6	6	4	1	1	1	#	#	1	1	3	4	2	
	12-14	2	3	1	1	#	1	1	#	1	1	1	2	1	
	15-17	1	3	2	1	#	1	1	#	1	1	2	2	1	
	18-20	2	3	2	#	#	0	#	#	1	1	2	2	1	
	21-23	3	3	2	#	#	0	#	#	#	#	2	3	1	
	ALL HOURS	5	5	3	1	1	1	#	1	1	1	3	4	2	14
CIG less than 200 feet and/or VSBY less than ½ mile	00-02	2	1	0	#	0	#	0	0	0	1	#	2	#	
	03-05	4	2	1	1	#	#	0	#	#	#	#	2	1	
	06-08	5	4	1	#	0	0	0	#	1	#	1	3	1	
	09-11	1	1	#	0	0	0	0	0	#	#	#	1	#	
	12-14	0	#	0	0	0	0	#	0	#	#	0	0	#	
	15-17	0	#	#	0	#	#	0	#	0	#	0	#	#	
	18-20	#	#	0	0	0	0	#	0	0	0	0	0	#	
	21-23	1	#	0	0	0	0	0	#	0	0	#	1	#	
	ALL HOURS	2	1	#	#	#	#	#	#	#	#	#	1	#	14

Figure VI -43: Cape Canaveral Climatic Summary

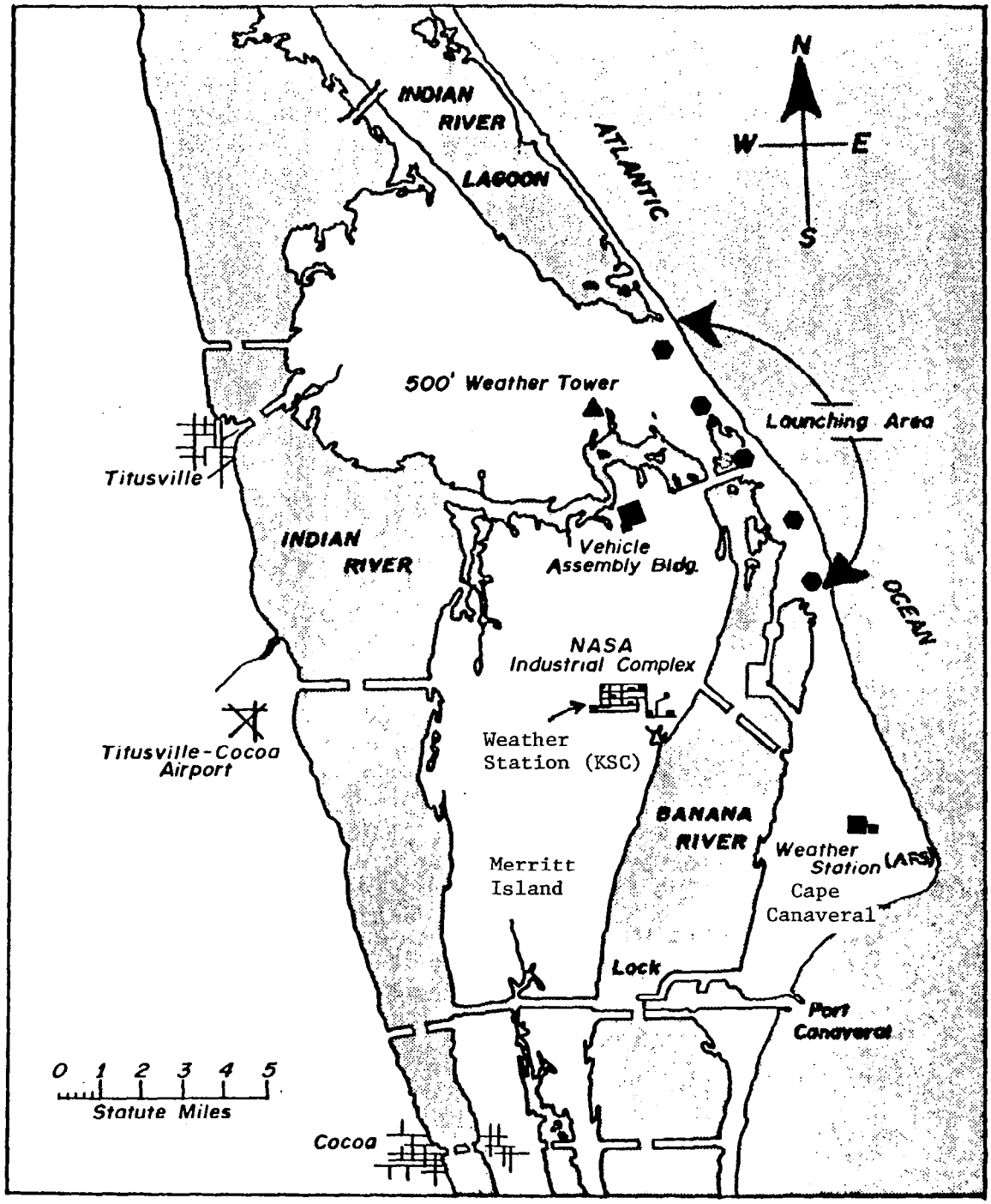

After Neumann (1970)

Fig. 44. Cape Canaveral area map

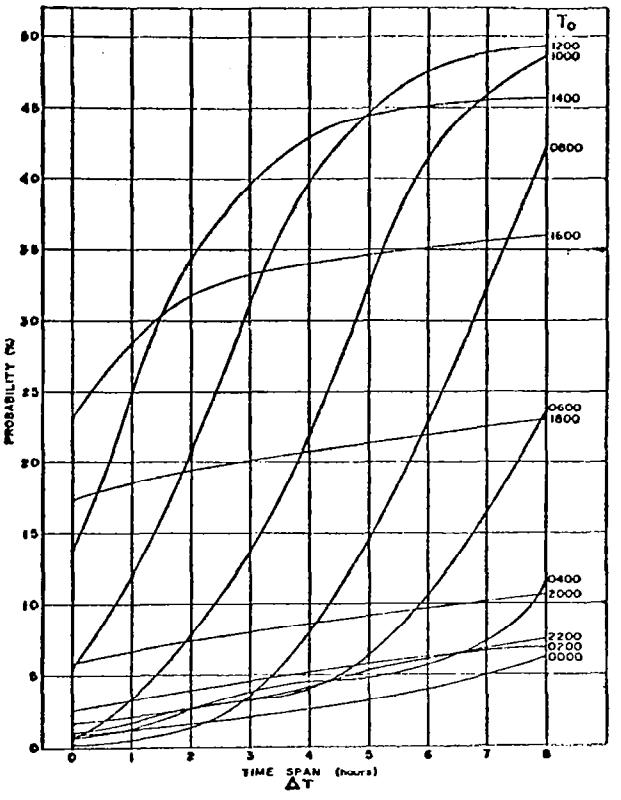

Probability (%) of at least one thunderstorm on August 1 (EST) between time T_o and time T_o + Δ T. (data derived from Part I).

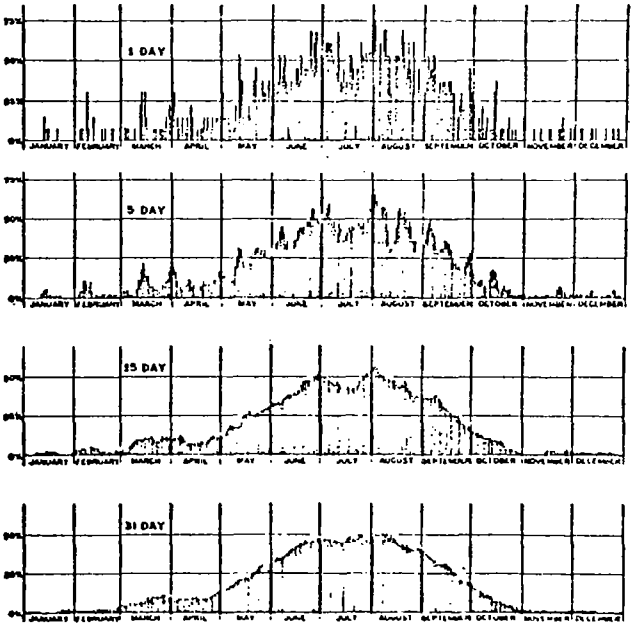

Daily thunderstorm frequencies (top panel) smoothed over periods of 5, 15, and 31 days (data derived from Part I).

After Neumann (1970)

Figure VI -45: Smoothed Cape Canaveral Daily Thunderstorm Frequencies (lower Panel)

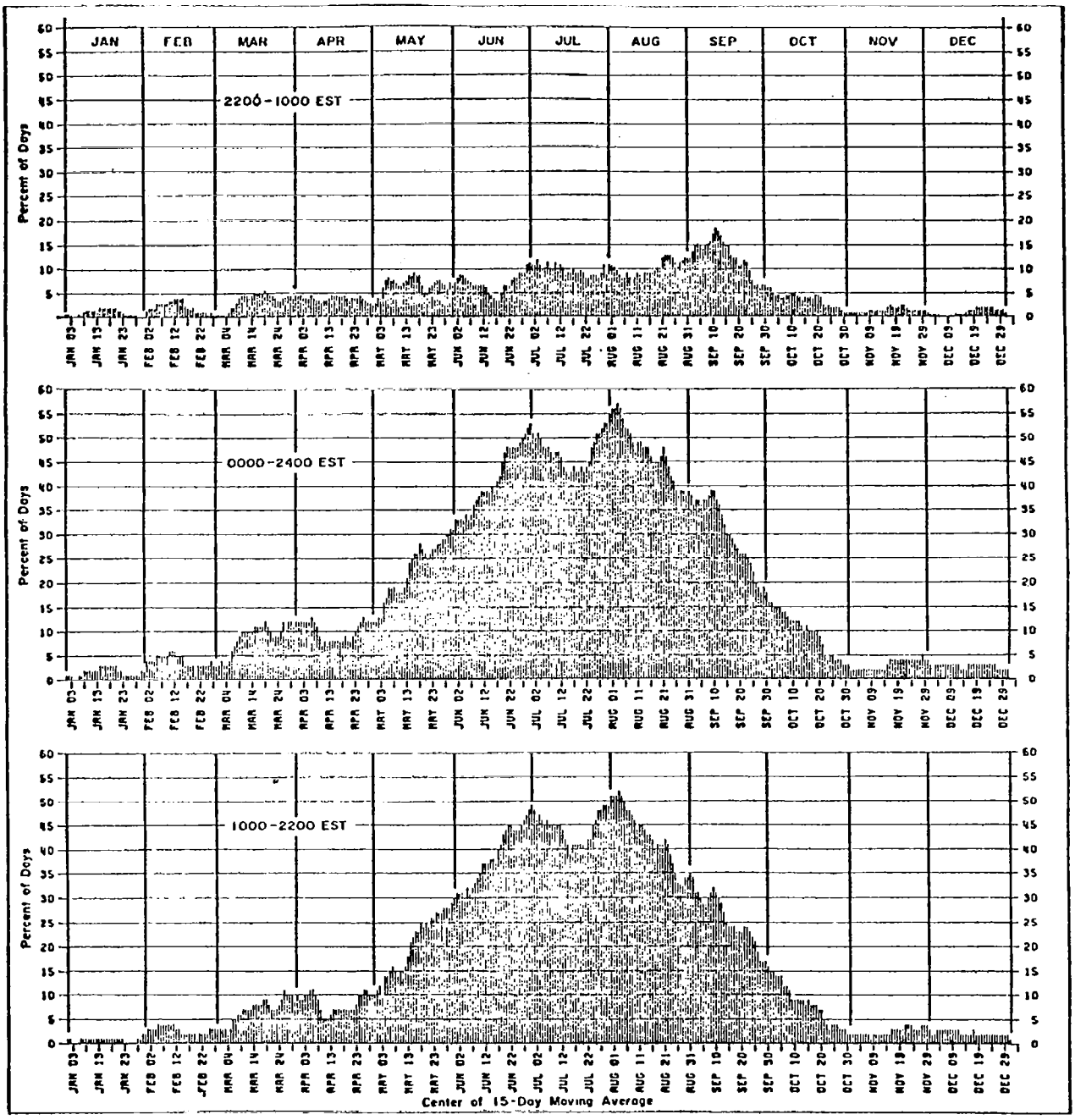

After Neumann (1970)

Probability of thunderstorms at or in the immediate vicinity of the Kennedy Space Center over specified time intervals (data derived from Part I).

Figure VI -46: Thunderstorm Probability at Cape Canaveral as a Function of Time

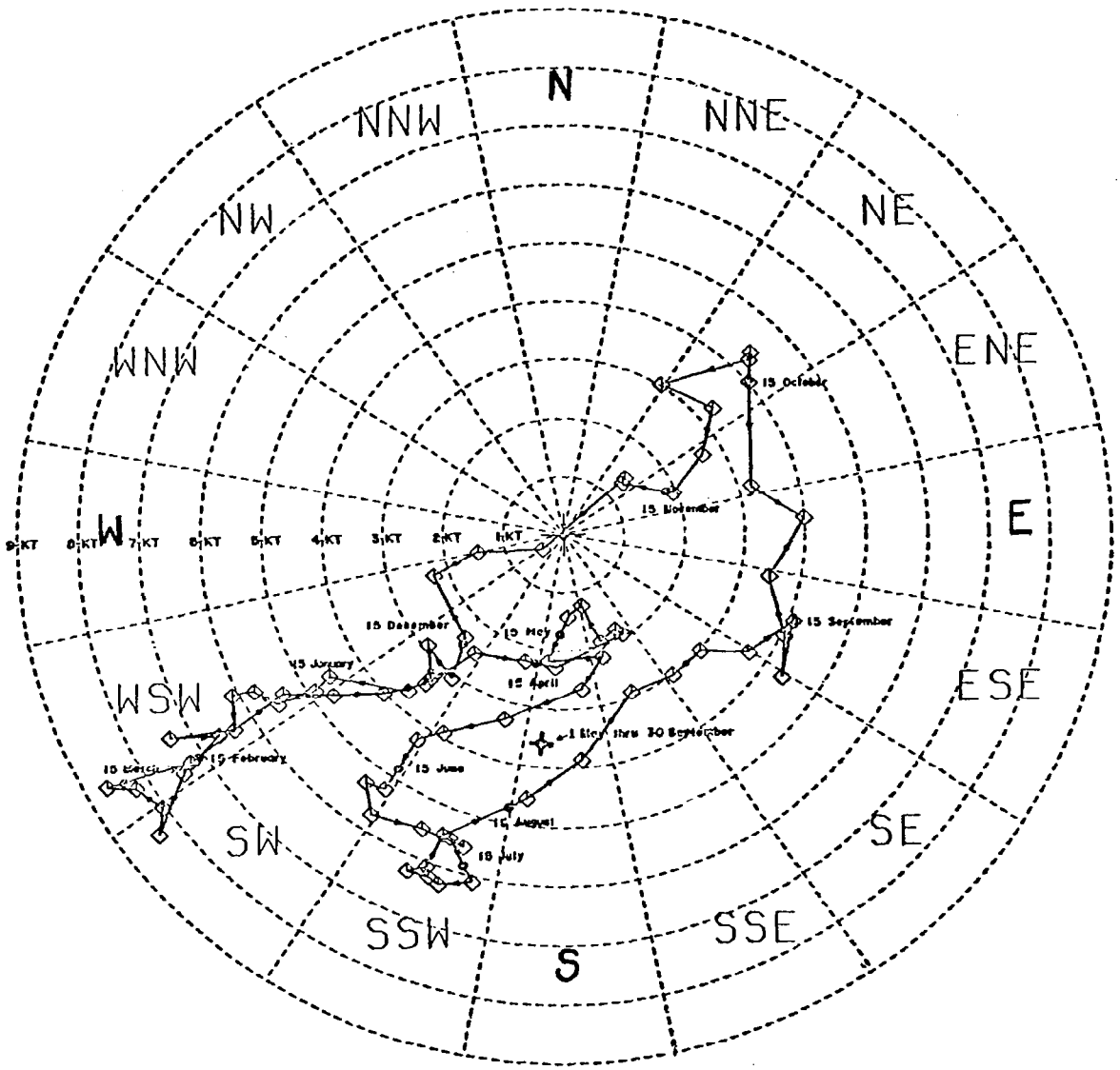

After Neumann (1970)

Location (◇) of the 1200 GMT 3000-foot resultant wind at the Kennedy Space Center for each of the 73 dates referred to in figure 3. The location (○) of the resultant wind for the 15th day of each month is interpolated from the location of the adjacent 5-day positions. The location (✛) of the resultant wind for the entire thunderstorm season is 187 degrees at 3.6 knots.

Figure VI-47: Cape Canaveral 1200 GMT 1000-Meter Resultant Winds During the Thunderstorm Season.

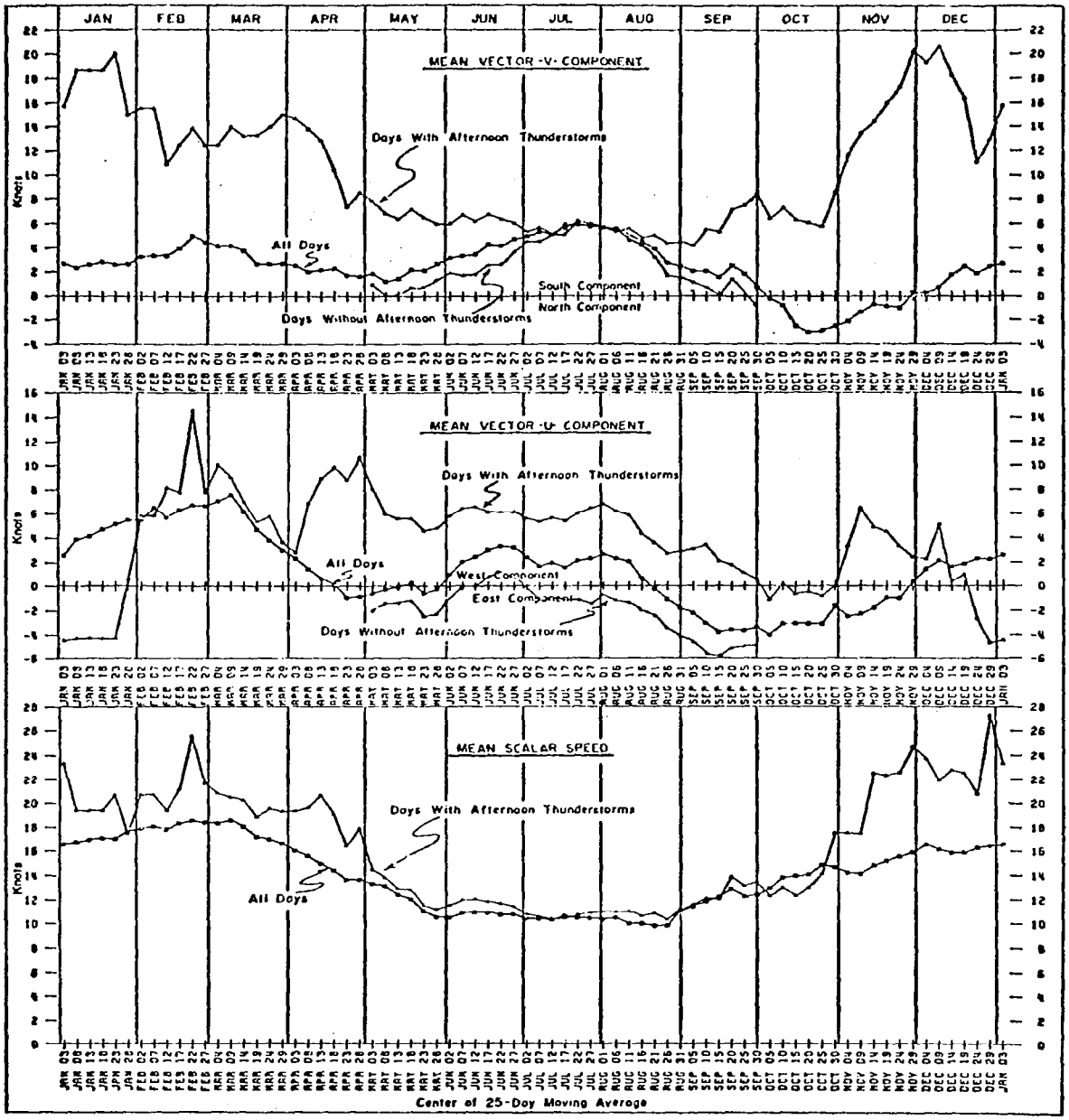

After Neumann (1970)

Annual variation in the 1200 GMT 3000-foot vector and scalar winds under conditions with and conditions with and without afternoon thunderstorms. The vector locations of the wind components under conditions without afternoon thunderstorms are given for the period May through September only.

Figure VI -48: Cape Canaveral 1200 GMT 1000-m Vector and Scalar Wind Variations During the Summer Season.

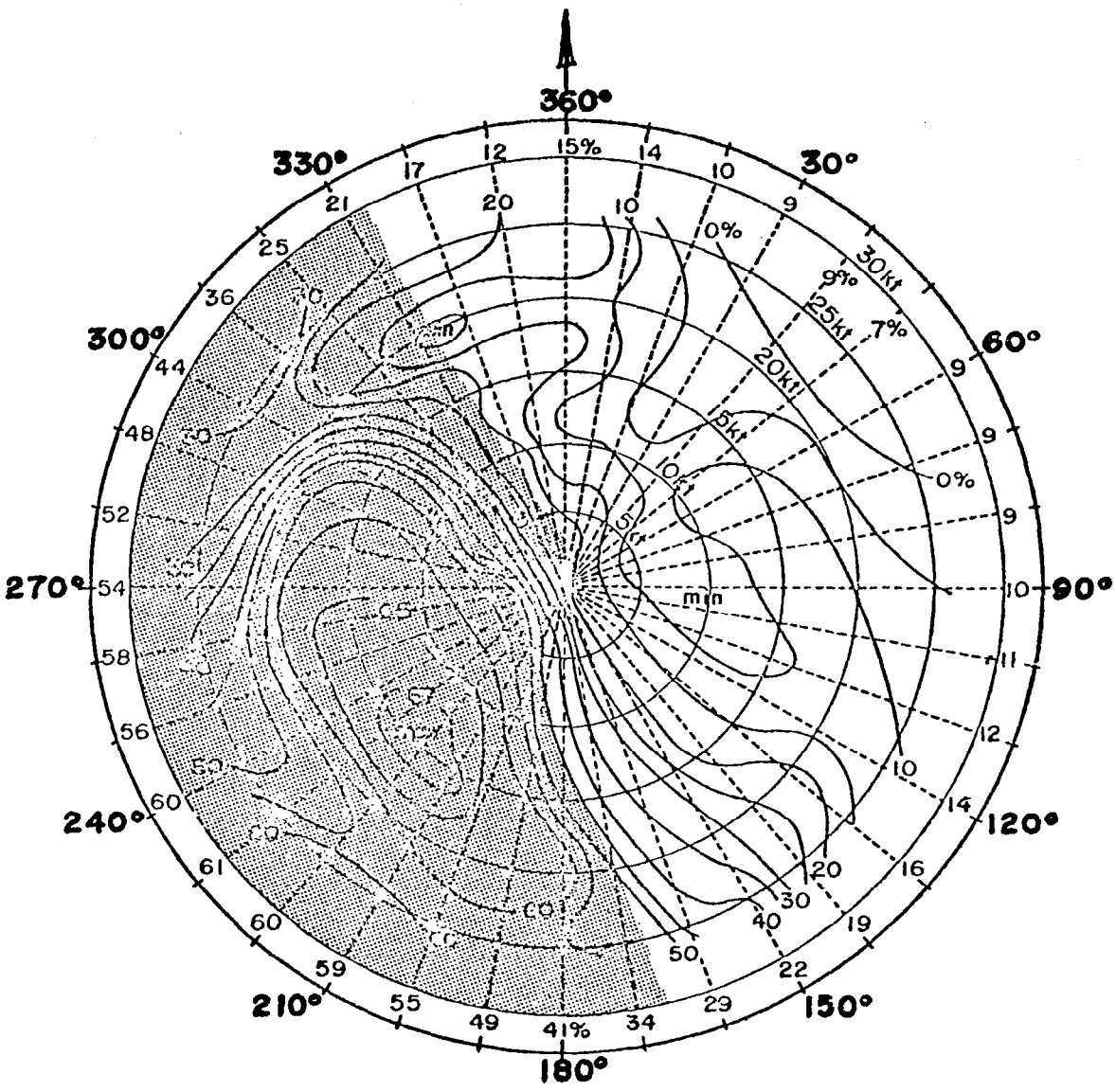

After Neumann (1970)

Probability of afternoon thunderstorms over the entire May through September thunderstorm season as a function of the 1200 GMT 3000-foot wind speed and direction. Values entered perimetrically in outer circle are the probabilities (%) for this direction without regard to the speed. This chart not to be used operationally since it applies to the season as a whole. Shading shows relative location of the Florida eastern coast.

Figure VI-49: Cape Canaveral Thunderstorm (DM) Probability Over May-September Period Based on 1200 GMT 1000-m Wind Speed and Direction.

APPENDIX II

Climatography of Cape Canaveral-Merritt Island, Florida

by

Richard Siler
Kennedy Space Center Weather Office

Climatography
of Cape Canaveral-Merritt Island, Florida
December 1966

Richard K. Siler

Physiography

Cape Canaveral, Florida is located on the Atlantic Ocean side of the Florida Peninsula at approximately 28.5 degrees north latitude. The Cape is separated from the Florida mainland by the Banana River, Merritt Island, and the Indian River--a total distance of about fifteen miles. At its widest part, Cape Canaveral is only about five miles wide. Cape Canaveral, like Merritt Island, is flat with elevations ranging from sea level to twelve feet or so. The vegetation on Cape Kennedy consists mainly of coarse grasses, scrub, and palmetto, though much of the natural vegetation has been cleared during the past few years. On that portion of Merritt Island where Kennedy Space Center is located, there are a number of citrus groves and pine covered areas in addition to the vegetation found on Cape Canaveral.

General Climatology

The climate of the Cape Canaveral-Merritt Island area is subtropical with short, mild winters and hot, humid summers. The rainy season occurs from June through October due initially to the beginning of the thunderstorm season and then later in connection with the peak of tropical storm activity. Winter time rains, generally caused by frontal activity, occur on the average of once every three to five days and amounts are generally light.

From April through the middle of October weather in the Cape Canaveral area is dominated by east or southeast winds traveling around the Bermuda Anticyclone. In October the prevailing winds shift abruptly to the north or northwest.

During the winter months, polar air masses move through the Central Florida area giving a distinct continental flavor to the climate during those months.

The Seasons

The climate of Cape Canaveral-Merritt Island has many of the characteristics of subtropical areas. Summer and winter are well-defined and may begin or end abruptly. Spring and fall are short, transitional periods possessing characteristics of both summer and winter.

Summer ordinarily begins around the middle of May and ends abruptly in the middle of October. The highest mean temperatures occur in July and August but the extreme highest temperatures are more likely to occur in June. Due to the east and southeast trade winds there is an inexhaustible supply of moisture and humidities are quite high during the entire summer.

A combination of this moisture, daytime heating of the land mass, and convergence of the sea breeze from each side of Florida results in extensive thunderstorm activity in this area. The thunderstorm season coincides almost exactly with the summer season, i.e., thunderstorm frequency increases sharply in mid-May, reaching a peak in August then sharply subsiding after mid-September. Thunderstorms in this area can be violent with frequent cloud to ground lightning, heavy rain and strong, gusty winds. Hail has not been recorded during these air mass thunderstorms.

Even though thunderstorms do not occur every day, they are a threat just about every day during the summer months. Likewise, hurricane activity, or tropical storm activity, constitutes a threat to the Cape Canaveral area, though without the immediacy of thunderstorms. The hurricane season begins in June and ends in December with the highest frequency of occurrence in August, September, and October. Actual direct "hits" of hurricanes on Cape Canaveral are rare. This fortuitous event is thought to be a result of the location of the Gulf Stream and the mean location of the Bermuda Anticyclone. In any event, hurricane centers have not been known to pass over this area during modern times.

Winter is generally characterized by mild temperature, comfortable relative humidity, and clear to partly cloudy skies. These near ideal conditions are interrupted by occasional frontal passages that are accompanied by cloudy skies and rain and then colder, drier air. Although temperatures are generally mild, on at least one occasion during the course of the winter temperatures below freezing should be expected. It is also noteworthy that 80° temperatures are likely to occur during each winter month. This general condition persists from November through March when spring-like storms may occur. Except for those winds associated with hurricanes, these storms, usually associated with cold fronts, produce highest peak winds found in this area. These winds are the results of thunderstorms in rapidly moving squall lines and can be tornadic in their force. Tornadoes do in fact occur occasionally in connection with these squall lines. The occurrence of hail has never been recorded at the weather station, but in association with storms of this type hail has fallen on nearby areas and so should be considered as a possibility during this time of year.

Though the winter season begins rather abruptly, it departs on a more gradual note. Starting in April, warm days are more numerous and cold air intrusions become less frequent until finally, by the middle of May, the last significant cold front has passed.

a rating of 4 and thus seemed worthy of further consideration. The remaining 80 percent of the atmospheric weather situations were not likely to be affected by the cloud plume.

Our evaluation also shows that summer launches compared to those in winter have twice the chance of producing some modification effect. This is due primarily to the increased moisture, convection, cloud depth, and storminess that tends to occur in the summertime. The same yearly pattern exists for modifying the cold and warm precipitation processes.

While the very large local concentration of highly effective cloud condensation nuclei contained in the exhaust cloud could have an important modifying effect on the persistence of fogs and/or haziness at ground level, the large amount of heat released by the rocket exhaust effectively lifts the plume aloft until it encounters a stable layer of air at several hundred meters to a kilometer above ground level. It is quite unlikely that the later diffusion of the rocket exhaust plume particles toward ground level will occur soon enough for any substantial effect to be noticeable. If fog or visibility is affected, it is more likely to occur in the wintertime than in the summer. If the cloud remains as a coherent plume and then encounters a downdraft near the edge of a large thunderstorm, it could be carried back to ground level. This is possible although unlikely since fog would hardly be present under the unstable conditions that exist when convective clouds develop.

There is a possibility that a coherent exhaust plume might be drawn into the convective plume of a large developing thunderstorm. If this were to occur, it could significantly modify such a storm.

The large concentration of cloud condensation nuclei entrained in the plume could delay the coalescence of the droplets in the cloud because of the high number of small drop sizes which would then develop. With a

delay in coalescence, the cloud would tend to grow larger and colder. The ice nuclei also present in the plume could then lead to the release of heat of crystallization, further adding to the size and intensity of the cloud system. This could be one of the most effective modifying effects of the rocket exhaust cloud if weather conditions were favorable for it to occur. It would most likely happen in the summer period as is indicated by the table.

While the summer period has more weather systems likely to be affected by the plume than in the wintertime because the plume is more likely to remain over the land and to encounter convective clouds, we believe that modification effects causing coalescence rain could be nearly as frequent in the wintertime.

In summary, it appears from our preliminary analysis of the year-round climatic patterns of eastern Florida centered about Cape Canaveral that about a fifth of them might in some manner be modified by the rocket exhaust plume during the time interval between 3 to 24 hours following launch time. For longer intervals, the possibility of modification falls off rapidly since the plume becomes effectively mixed with the surrounding air.

As indicated previously, we have based our conclusions on the best physical and visual (photographic) data available at this time. The lack of satisfactory and extended time data must be recognized in this evaluation. We hope that the procedures (and problems) encountered as have sought better information will establish adequate goals so that as the launch time for the Shuttle flights approaches, there will be accurate and pertinent information available to permit a more objective analysis and forecast of the effects likely to occur.

With these qualifications, the following risk situations for inadvertent weather modification due to the space shuttle exhaust were identified (see Table VII-1 and main text for detailed information).

1. Exhaust cloud encountering active convective precipitation cells with consequent vertical transport to the upper troposphere and potential for storm modification

(a) sea breeze convergence during the warm season with attendant afternoon thunderstorms. Effects include possible localized hail, altered rainfall amounts and brief wind gusts in excess of 20 ms^{-1}. Affected area is less than 100 km^2 with a maximum time scale of approximately T + 1 day.

(b) frontal and prefrontal activity including squall lines with attendant thunderstorms. Effects include possible localized hail, altered rainfall amounts and wind gusts. Affected area is 100-500 km^2 with a time scale of less than T + 2 days.

(c) general air mass thunderstorms not associated with (a) and (b) above but responding to different summer synoptic flow patterns. Effects include possible localized hail, altered rainfall amounts and brief wind gusts in excess of 20 ms^{-1}. Affected area is less than 100 km^2 with a time scale of less than T + 1 day.

(d) tropical storms in the vicinity of the Florida Peninsula within 24 hours of launch time. Potential effect of shuttle exhaust cloud caught up in the circulation of a tropical storm is unknown in terms of inadvertent weather modification.

2. In the months November-April, when advective and radiative fogs maximize, very significant worsening of visibility conditions in foggy situations could occur within the area affected by the dissipating S.G.C. up to T + 1 day (area affected up to 10^4 km^2) and particularly under wind flow conditions from the SE quadrant.

3. Minor risk associated with easterly flow in lower troposphere (unless tropical disturbances are present), particularly in those situations where atmosphere is stable and clouds do not reach the level where ice phase processes are operative. However, overseeding of warm clouds with CCN could result in a very significant reduction of precipitation over the entire area affected by the dispersing cloud. Effect diminishes after T + 1 day. (Criteria: shallow warm cloud system and no ice phase.)

4. Stagnating anticyclonic conditions with reduced dispersion of S.G.C. Little cloudiness is normally associated with conditions of this type. The impact is therefore restricted only in the area of visibility deterioration and solar energy reduction. This therefore constitutes a nuisance and conceivably might violate EPA standards. On rare occasions, air mass thunderstorms may develop, particularly along the sea breeze convergence zone, under stagnant anticyclonic conditions during the warm season. The risk would then be equivalent to 1(c) above.

5. Minimal risk and impact: strong westerly winds system extending through the lower troposphere

6. Risk of cumulative modification effects for the projected 40 launches per year, assuming several days spacing between launches: considered negligible

In terms of precipitation modification indicated above, the measurement of precipitation can often present major problems, not only in regard to the accuracy of an individual measurement, but also in regard to how

well the available measurements represent the precipitation over the whole area of interest. The position paper* prepared by the World Meteorological Organization-Weather Modification Programme, has addressed this problem:

> "Through the use of co-located gauges it has been found that rainfall can always be measured to better than 10%, with errors reducing to only a few percent when the rainfall exceeds 10-20 mm. Normally sited gauges for the measurement of snow are subject to much greater errors, conventionally averaging 50% and under extreme conditions errors approaching an order of magnitude may occur. Some investigations have been made by Woodley et al (J. Appl. Meteor. 1975, 14, 909-928) of the accuracy with which a network of gauges can measure the areal mean rainfall in Florida. Similar studies have been made by Huff in Illinois (Advances in Geophys. 1971, 15, 59-134). The results of these studies indicate that, largely due to differences in the rainfall regimes in the two areas, errors of assessing areal rainfall were greater in Florida than in Illinois for a given network density. The area studied in Florida was only 570 km^2 but, through comparisons with radar measurements of precipitation, the results of the study were extended to apply to an area of 1.3×10^4 km^2. For the latter area it was concluded that one gauge per 143 km^2 was necessary to ensure that the measured areal rainfall was within a factor of two of its true value 99% of the time. The same density would ensure that the measured areal rainfall was within $\pm$20% of its true value 75% of the time. It must be remarked that these figures apply to a specific area and to convective air-mass showers, and different network densities would be required to obtain similar accuracy of measurement of areal rainfall in other areas having different orography and/or different rainfall regimes. Nevertheless, it is very clear from these experiments that if a proper measure of areal rainfall is to be provided by precipitation gauges, a relatively dense network is essential."

It is therefore the opinion of the assessment team that even with a rain gauge network of the density stated above, it would be difficult to establish with acceptable statistical significance within a reasonable time frame that the shuttle launches modify the Florida Peninsula precipitation regimes. However, a comprehensive field program incorporating advanced observational techniques and numerical modelling likely could detect, on a case study approach, local and regional effects related directly to the impact of the S.G.C. on the atmosphere.

*Precipitation Enhancement Project, Report No. 2, WMO-Weather Modification Program, Geneva, Nov. 1976.

In conclusion, an assessment of the weather risks relating to the potential for inadvertent weather modification has been made for the Kennedy Space Center area in association with the shuttle exhaust cloud. The presence of convective elements and associated precipitation cells is the biggest source of concern.

Thus synoptic weather regimes which favor near surface onshore flow in the absence of strong westerlies above the planetary boundary layer and in the presence of active convective elements should especially be avoided in terms of the space shuttle launch. Characteristic synoptic regimes that would fall into this category include

(1) hurricanes

(2) easterly waves of summer

(3) stagnating frontal zones

(4) cool season squall lines

(5) cool season low latitude mid tropospheric troughs

(6) warm season weak mid tropospheric troughs

(7) coastal sea breeze convergence regimes

Disturbed conditions over land and water accompanying hurricanes or tropical storms may encompass the Cape Canaveral region one year out of three or four years (storm center may be as far as 500-1000 km away). These relatively disturbed conditions (cumulonimbus coverage 20-50%) may persist from 24 to 72 hours. Easterly waves with disturbed conditions (50% Cb average) may reach Florida every four or five days from mid July through September with the disturbed conditions persisting 12-24 hours.

Stagnating fronts across central Florida (Morgan 1975) carry risk factors of five to six days in March and December (less in January and February) and two to three days in early June and late September. Extensive precipitation may occur, particularly in September, in the low level easterly flow just to the north of the frontal zone. Disturbed conditions and accompanying rainfall may persist for 12 to 24 hours. Such events can be predicted with some skill relative to climatology 12 to 36 hours in advance. Occasional squall lines in advance of strong cold fronts may sweep across central Florida in winter (especially in December and March). The strong westerly flow accompanying such fronts results in precipitation duration of an hour or less--predictability is usually restricted to a general statement of likelihood 12 to 24 hours in advance of the event.

Cool season extensive precipitation (24-48 hours) may occur in the presence of very rare low latitude extratropical cyclogenesis accompanying deep, cold troughs aloft one year out of three. A recent example is the storm of 10-13 February 1973. Predictability can be poor because of the rarity of the event although antecedent conditions may provide useful clues to the experienced forecaster.

Finally, warm season weak mid-tropospheric troughs can interact with the sea breeze convergence regime to produce highly disturbed conditions several days each month. This leads to a general rule. With southwesterly flow at 850 mb at 1200 GMT a morning launch as opposed to afternoon launch is preferred. The reverse is usually true with morning southeasterly flow.

Regarding the concept of cloud neutralization, this may be desirable to minimize a potential acid-rain problem. However, the resultant particles (nuclei) so produced appear more likely to compound rather than lessen

inadvertent cloud modification probabilities. While some cloud microphysics modification is inevitable with either type of S.G.C., subsequent and significant modification of weather (rainfall, thunderstorms, winds, fog, etc.) is far more difficult to establish. Even carefully planned seeding programs under optimum circumstances often fail to detect unequivocal changes at an acceptable level of statistical significance. The cumulative effects of 40 launches per year (appropriately spaced) at Cape Kennedy producing significant inadvertent weather modification is considered to be remote. Localized short-term weather modification events could well occur and careful launch scheduling to minimize such possibilities have been enumerated.

Table VII-1

SYNOPTIC FLOW REGIME AND ESTIMATE OF POTENTIAL FOR INADVERTENT WEATHER MODIFICATION

	COOL SEASON					WARM SEASON				
	Frontal (E-W Slow Moving)		Squall Line in Advance of	Cold			Sea-Breeze Regimes		Weak Cold	
	North of KSC	South of KSC	Fast Moving Cold Fronts	Trough in Mid Trop.	Anticyclone	Easterly Wave	Dist. Day	Undist. Day	Mid Trop. Trough	Tropical Disturbances
Length Scale(km)	100	100	100	500-1000	1000	500	10-20	10-20	100-500	500
Time Scale(days)	1-2	1-2	0.2	1-3	1-5	1-2	.5	.5	1-2	1-3
Monthly Episodes	2-4	2-4	1-3	1-2	4-6	3-5	4-6	Near daily	1	<1
Atmospheric Stability*	Neutral	Stable	Unstable	Neutral to unstable	Stable	Unstable	Unstable	Neutral	Unstable	Unstable
Wind										
Surface	S-W	NE-SE	SE-SW	Var.	Var.(W-N)	E	E-S	E-S	SE-SW	Var.
850 mb(1.5 km)	S-W	S-W	S-W	S-W	Var.(W-N)	E	S-W	Var.	S-W	Var.
Shear $ms^{-1}(100\ m)^{-1}$	0.2-1.0	0.5-1.5	1.0-3.0	0.5-1.5	0.1-0.5	0.2-0.5	0.1-0.5	0.1-0.3	0.2-0.5	Var.
Diurnal Variation	Small	Small	Small	Small	Small(except near ground)	Small	Large	Large	Small	Small
Cloud										
Type**	Ci,As,Ac,Cb	As,Ac,Ns,St	All types	All types	Cu	All types	Cb(numerous), Cu	Cb(isolated), Cu	Cb(numerous), some middle types (As)	All types
Coverage(%)***	10-40	40-100	50-90	20-80	10-30	30-80	40-60	10-30	40-60	50-90
Diurnal Variation	Small except for Cb	Small	Small except for Cb	Afternoon max. over land		Small	- Afternoon max. over land -			Small
Precipitation										
R(mmh-1)****	1-10	1-5	10-100	1-10	1	10-50	10-100	10-50	10-100	10-100
Areal Coverage(%)	10-30	10-90	40-80	20-70	<10	30-80	30-60	10-30	30-60	50-90
Point Prob.	5-70	10-90	20-80	10-70	<10	30-80	20-50	10-30	20-50	50-90
Diurnal variation	Afternoon max.over land	Small	Afternoon max.over land		Small	Light afternoon max.	- Early afternoon max. -			Small

Table VII-1 (contd)

	COOL SEASON					WARM SEASON				
	Frontal (E-W Slow Moving)		Squall Line in Advance of	Cold			Sea-Breeze Regimes		Weak Cold	
	North of KSC	South of KSC	Fast Moving Cold Fronts	Trough in Mid Trop.	Anticyclone	Easterly Wave	Dist. Day	Undist. Day	Mid Trop. Trough	Tropical Disturbances
Predictability	High 24-48h	High 24-48H	Low 6-12h	Modest 24h	High 24-48h	Modest 24-36h	Modest 24h	Modest 12-24h	Low 12-24h	Modest 24-36h
Preferred Launch Window	Forecast	Forecast	Night, early morning	Forecast	Mostly open	Forecast	Night	Night	Night, early morning	Forecast (potentially none)
Estimate of Potential† of Exhaust Cloud Encountering:										
a.Precipitation Cell										
t + 3 hours	2	4	5	3	1	5	5	4	4	5
t + 1 day	4	4	2	4	2	4	5	3	4	5
t + 2 days	5	3	1	3	2	3	4	3	3	4
t + 3 days	5	3	1	2	3	3	3	3	3	3
b.Land										
t + 3 hours	2	5	3	3	4	5	5	5	3	4
t + 1 day	2	5	2	2	3	5	5	3	2	4
t + 2 days	1	4	1	1	3	4	4	3	2	3
t + 3 days	1	3	1	1	3	2	2	3	2	3
Estimate of Potential† for Inadvertent Weather Modification:										
a.Cold Rain Processes										
t + 3 hours	3	2	3	3	1	4	5	4	4	4
t + 1 day	2	1	2	2	1	3	4	2	3	3
t + 2 days	1	1	1	1	1	2	2	1	2	2
t + 3 days	1	1	1	1	1	1	1	1	1	1
b.Warm Rain Processes										
t + 3 hours	3	5	5	5	1	5	5	4	4	3
t + 1 day	3	4	2	4	1	5	5	3	3	1
t + 2 days	2	2	1	1	1	2	2	2	2	1
t + 3 days	1	1	1	1	1	1	1	1	1	1
c.Haze and Fog										
t + 3 hours	2	3	1	2	4	1	1	2	1	1
t + 1 day	1	1	1	1	3	1	1	1	1	1
t + 2 days	1	1	1	1	3	1	1	1	1	1
t + 3 days	1	1	1	1	2	1	1	1	1	1

Table VII-1 (contd)

	COOL SEASON					WARM SEASON				
	Frontal (E-W Slow Moving)		Squall Line in Advance of	Cold			Sea-Breeze Regimes		Weak Cold	
	North of KSC	South of KSC	Fast Moving Cold Fronts	Trough in Mid Trop.	Anticyclone	Easterly Wave	Dist. Day	Undist. Day	Mid Trop. Trough	Tropical Disturbances
d.Thunderstorms(hail, severe winds, lightning, etc.)										
t + 3 hours	1	2	3	2	1	4	5	3	3	3
t + 1 day	1	2	2	2	1	1	1	1	1	1
t + 2 days	1	1	1	1	1	1	1	1	1	1
t + 3 days	1	1	1	1	1	1	1	1	1	1

* $\delta\theta_e/\delta z > 0, = 0, < 0$ for stable, neutral, unstable, where θ_e refers to equivalent potential temperature

** World Meteorological Organization cloud definitions

*** Coverage within 100 km radius

**** Rainfall rates within 100 km radius

† Estimate of Potential Scale. 1 (unlikely) thru 5 (likely)

Detectability criteria: Microphysics (see text)

1. Report No.	2. Government Accession No.	3. Recipient's Catalog No.
NASA CR-3091		

4. Title and Subtitle	5. Report Date
Position Paper on the Potential of Inadvertent Weather Modification of the Florida Peninsula Resulting From Neutralization of Space Shuttle Solid Rocket Booster Exhaust Clouds	November 1979
	6. Performing Organization Code

7. Author(s)	8. Performing Organization Report No.
Eugene Bollay*, Lance Bosart**, Earl Droessler†, James Jiusto**, G. Garland Lala**, Volker Mohnen**, Vincent Schaefer**, and Patrick Squires††	
	10. Work Unit No.

9. Performing Organization Name and Address	11. Contract or Grant No.
Institute on Man and Science Rensselaerville, NY 12147	NAS1-14965
	13. Type of Report and Period Covered
12. Sponsoring Agency Name and Address	Final, Apr. 1977 - Feb. 1978
National Aeronautics and Space Administration Washington, DC 20546	14. Sponsoring Agency Code

15. Supplementary Notes Langley Technical Monitor: Gerald L. Pellett Final Report
*Bollay Associates, Santa Barbara, CA; **State University of New York at Albany, Albany, NY; †North Carolina State University, Raleigh, NC; ††National Center for Atmospheric Research, Boulder, CO Appendix II by Richard Siler

16. Abstract

NASA plans regular Space Shuttle launches (1980's) employing solid propellant rockets that liberate primarily HCl and Al_2O_3. To neutralize the acidic nature of the low-level stabilized ground cloud (SGC), a concept of injecting compounds into the exhaust cloud was proposed. This position paper deals with potential Inadvertent Weather Modification caused by exhaust cloud characteristics from three hours to seven days after launch. Possible effects of the neutralized S.G.C. in warm and cold cloud precipitation processes are discussed. Based on a detailed climatology of the Florida Peninsula, the risk for weather modification under a variety of weather situations is assessed.

The effect of cloud neutralization, while minimizing the possibility of acid rain, may well generate more nuclei conducive to cloud modification. In any event, some degree of microphysical changes to natural clouds would appear inevitable and careful launch scheduling to minimize such possibilities are enumerated. Cloud microphysics changes leading to significant and/or statistically detectable weather modification are considerably more difficult to establish - as is generally the case on planned weather modification programs even under "selected" circumstances. While some degree of weather modification might occur in individual cases, the cumulative effects of 40 projected launches per year (appropriately spaced) at Cape Kennedy capable of producing significant and deleterious inadvertent weather modification is estimated to be of low probability. Needed experiments and research to test this conclusion are enumerated.

17. Key Words (Suggested by Author(s))	18. Distribution Statement
Inadvertent weather modification Climatology of Florida Peninsula Cloud physics Light scattering by aerosols	Unclassified - Unlimited Subject Category 47

19. Security Classif. (of this report)	20. Security Classif. (of this page)	21. No. of Pages	22. Price*
Unclassified	Unclassified	202	$9.25

* For sale by the National Technical Information Service, Springfield, Virginia 22161

NASA-Langley, 1979